6.15 Alkenone Paleotemperature Determinations

T. D. Herbert

Brown University, Providence, RI, USA

6.15.1 INTRODUCTION

The organic biomarker proxy for past sea surface temperatures ("U^{k}_{37}") came to paleoceanography from an unexpected direction. Nearly all paleoceanographic tools rely on some aspect of the fossilized hard parts of marine organisms. Thus, assemblages of calcareous microplankton such as foraminifera and coccoliths, or of siliceous plankton such as radiolaria and diatoms, provided the basis for the CLIMAP reconstruction of the Ice Age ocean (CLIMAP, 1976, 1981). Additionally, a host of chemical methods relies on the same hard parts to furnish isotopic and trace element signatures, and generally requires that skeletal material be well preserved. The alkenone method differs in several important ways. Individual molecules, extracted and separated from a matrix of hundreds to thousands of other organic compounds, are the targets. In most cases, the remnant alkenones and alkenoates that are the subject of this review constitute no more, and often considerably less, than a few percent of their initial flux that left the surface layer of the ocean and fell toward the sediments. Good preservation is thus not a major issue for use of the proxy. In addition, while many geochemical techniques assume that skeletal material is a passive recorder

of isotopic and trace element composition of seawater, and that incorporation of paleoenvironmental signals follows thermodynamic laws that can be modeled using nonbiogenic phases in the laboratory, the alkenone method assumes that the ratios of biomarkers measured were actively regulated by the producing organisms in life according to the temperature of the water in which they grew.

Alkenone paleothermometry promises a direct estimate of near-surface ocean temperatures. Alkenones and the related alkenoates come exclusively from a few species of haptophyte algae. These organisms require sunlight, and they generally prefer the upper photic zone. The environmental information contained in their molecular fossils therefore is quite specific, although, as will be discussed at length in a later section, ambiguities still exist on the depth and seasonal variations of alkenone-producing species in the ocean. In contrast, many assemblages of planktonic organisms such as foraminifera and radiolaria contain many species known to live well below the surface mixed layer. The link between microfossil assemblages and sea surface temperature and salinity is therefore indirect and statistical, rather than mechanistic.

As originally defined by the Bristol organic geochemistry group (Brassell, 1986a,b), the U^{k}_{37} index reflected the proportions of the di-($C_{37:2}$), tri-($C_{37:3}$), and tetra-($C_{37:4}$) unsaturated ketones. Subsequent work showed that there was no empirical benefit to including the $C_{37:4}$ ketone in a paleotemperature equation. The currently accepted $U^{k'}_{37}$ index (Prahl and Wakeham, 1987) varies positively with temperature, and is defined as $C_{37:2}/(C_{37:2} + C_{37:3})$, where $C_{37:2}$ represents the quantity of the di-unsaturated ketone and $C_{37:3}$ the quantity of the tri-unsaturated form. The alkenone paleotemperature proxy thus depends only on the relative proportions of the common C_{37} ketones and not on their absolute amounts. Furthermore, although the alkenones are produced by calcareous algae, they survive in sediments where carbonate has dissolved, as first recognized by Marlowe *et al.* (1984a,b) and Brassell *et al.* (1986a). The above expression for the index shows that it can vary between 0 and 1.0; thus, it may saturate at either extremely cold or warm temperatures.

Alkenones appear recalcitrant to diagenesis in the water column and within sediments relative to other large macromolecules. Indeed, the first reported occurrence of alkenones came not from recent material, but from Miocene age sediments of the Walvis Ridge (Boon *et al.*, 1978). Shortly thereafter, these compounds were linked to modern haptophyte algae, principally *Emiliania huxleyi* (de Leeuw *et al.*, 1980; Volkman *et al.*, 1980a,b; Marlowe *et al.*, 1984a,b). Reviews of lipid analyses of Deep Sea Drilling Project sediments revealed that most sediments of Pleistocene through mid-Eocene age appeared to contain measurable quantities of alkenones and alkenoates (Marlowe *et al.*, 1984a, 1990; Brassell, 1993). Brassell *et al.* (1986a) provided the seminal study linking alkenone unsaturation to paleotemperature fluctuations in the Late Pleistocene. After noting that modern surface sediments differed in their unsaturation ratios depending on latitude, Brassell *et al.* (1986a,b) reconstructed alkenone unsaturation in conjunction with benthic and planktonic foraminiferal $\delta^{18}O$ over the last 8×10^5 yr in a core from the subtropical North Atlantic. The unsaturation index declined during glacial periods, suggesting cooler surface ocean temperatures during ice age conditions. The authors further demonstrated that the alkenone index gave a continuous paleoclimatic curve, even in intervals barren of foraminifera due to dissolution. Prahl and Wakeham (1987) and Prahl *et al.* (1988) proposed the first quantitative calibration of alkenone unsaturation to growth temperature. Unsaturation parameters measured on a strain of *E. huxleyi* grown in the laboratory at known temperatures were compared to the unsaturation index on particulate material collected from the near-surface ocean in the northeast Pacific. Prahl and Wakeham (1987) showed that the laboratory calibration appeared to apply well to the field observations of unsaturation and the water temperature in which the alkenones apparently were synthesized. The calibration of alkenone unsaturation to temperatures expanded with the first systematic study of core-top sediments by Sikes *et al.* (1991). That study produced two important results: (i) the unsaturation index in recent sediments followed a relation to overlying sea surface temperatures (SSTs) very similar to the Prahl *et al.* (1988) calibration, and (ii) there appeared to be no ill effects on the unsaturation index over the time of core storage. Pristine or frozen samples were therefore not needed to produce good estimates of the $U^{k'}_{37}$ index for paleoceanographic studies.

As with any paleoceanographic proxy, a number of uncertainties must be evaluated that could affect the accuracy measurement as an estimate of past SSTs. The principal caveats raised can be broadly categorized as ecological, physiological, genetic, and diagenetic. All describe factors, which could cause the $U^{k'}_{37}$ index to deviate from a unique relation to SSTs. Ecological concerns come from observations that alkenone-producing species do not inhabit precisely the same depth throughout the ocean, and that they vary in abundance seasonally. The alkenone unsaturation parameter recorded by sediments could therefore measure past temperatures very precisely, but at which depths, and with what

seasonal bias? It is also possible that the proportions of alkenones synthesized by haptophyte algae vary with growth rate, independent of temperature. Our present state of ignorance dictates that we do not know the growth phase of haptophyte material exported out of the photic zone—whether the products represent the initial exponential growth phase observed in culture or stationary growth. Natural populations also differ in their genetic composition. Alkenone-producing species are notable for their wide range of environmental tolerances. The consequences for the $U^{k'}_{37}$ index of genetic variations within strains of the same producing species and between the different alkenone-synthesizing species are still debated. In addition, alkenones measured in sediments represent the surviving molecules of a series of degradational pathways that begin in the water column, proceed to the sediment/water interface, and may continue into the sediment. Should there be a bias in the relative lability of the $C_{37:2}$ and $C_{37:3}$ ketones, this would be imparted to paleoceanographic reconstructions of temperature.

As should become clear, the $U^{k'}_{37}$ index appears nevertheless to provide a remarkably faithful estimate of paleotemperatures near the sea surface. At the same time, difficulties in matching the space and timescales of modern process studies to the information contained in sediments mean that the caveats raised above remain significant. Field studies provide only snapshots of haptophyte abundance and alkenone unsaturation parameters, sediment traps provide only a few years of data at only a few locations in the global ocean, and it is unclear how well laboratory cultures replicate the natural environment. I have endeavored to treat different lines of evidence systematically, but I have found it difficult to discuss each aspect in a purely serial way. The reader will therefore be asked to digest a review in which very diverse measurements and paradigms are woven together to answer the central question of how to reconstruct past ocean surface temperatures with the $U^{k'}_{37}$ proxy.

6.15.2 SYSTEMATICS AND DETECTION

Alkenones occur as a typical suite of 37-, 38-, and 39-carbon chained (C_{37}, C_{38}, C_{39}) ketones in marine particles and sediments. This set of compounds (Figure 1) constitutes a "fingerprint" for alkenones extracted from sediments. Their existence went undetected until chromatographic columns capable of sustaining the high temperatures at which long-chained alkenones elute came into existence in the late 1970s (Volkman *et al.*, 1980b). Although all alkenones are straight-chain hydrocarbons, they may differ in the number of double bonds (unsaturation) in the chain, and in the structure of the terminal ketone group (terminal carbon in the chain bonded to either a methyl or ethyl group). The C_{37} alkenones used in the $U^{k'}_{37}$ index are methyl ketones. 38-carbon chained molecules include not only tri- and di-unsaturated methyl ketone forms, but also $C_{38:3}$ and $C_{38:2}$ ethyl ketones (de Leeuw *et al.*, 1980; Volkman *et al.*, 1980a). A $C_{38:4}$ ethyl ketone has been reported from sediments underlying cold waters (Marlowe *et al.*, 1984b). As discussed at greater length in a later section, the total concentration of the four common C_{38} ketones is generally nearly the same as the sum of the two common C_{37} ketones in marine particulates and sediments (Conte *et al.*, 2001). Di- and tri-unsaturated C_{39} ethyl ketones (Figure 1) are also commonly observed at ~10–20% of the concentration of C_{37} ketones in analyses of alkenone-containing materials (Prahl *et al.*, 2001). Novel C_{35} and C_{36} methyl ketones have been reported recently from Black Sea sediments (Xu *et al.*, 2001); these apparently come from precursor organisms not commonly found in normal marine waters.

C_{36} and C_{37} fatty acid methyl esters (alkenoates) and C_{37} and C_{38} alkenes also accompany alkenones in alkenone-producing species (Volkman *et al.*, 1980b; Marlowe *et al.*, 1984b; Conte and Eglinton, 1993; Rosell-Mele *et al.*, 1994; Grossi *et al.*, 2000; Mouzdahir *et al.*, 2001). The relative proportions of alkenones, alkenoates, and alkenes vary greatly between different strains of alkenone-containing species grown in culture (Conte *et al.*, 1994a, 1995). The chain length and degree of unsaturation of alkenoates and alkenes follows the pattern of the long-chained alkenones (Marlowe *et al.*, 1984b; Conte and Eglinton, 1993; Grossi 2000). Unfortunately, alkenoates and alkenes rarely reach more than 10% of the concentrations of the C_{37} ketones in sediment extracts (the author has never observed significant quantities of C_{37} or C_{38} alkenes), and thus have limited utility for paleoceanographic reconstructions.

Our laboratory has found few marine sediment locations where alkenones cannot be extracted in enough quantity for quantification. Exceptions to the rule include very oligotrophic oceanic gyre locations, such as the Ontong-Java Plateau, and the red clay province of the North Pacific, where alkenone determinations are exceedingly difficult. Typical quantities of C_{37} ketones in marine sediments range from 100 ppb to 10 ppm of total sediment (dry weight). Alkenones can be extracted from sediments and particulates as part of a total lipid extract. From 1 g to 5 g of dry sediment is extracted with organic solvent (typically 9 : 1 methanol : methylene chloride) by Soxhlet apparatus, by repeated sonication at room temperature, or by an Accelerated Solvent

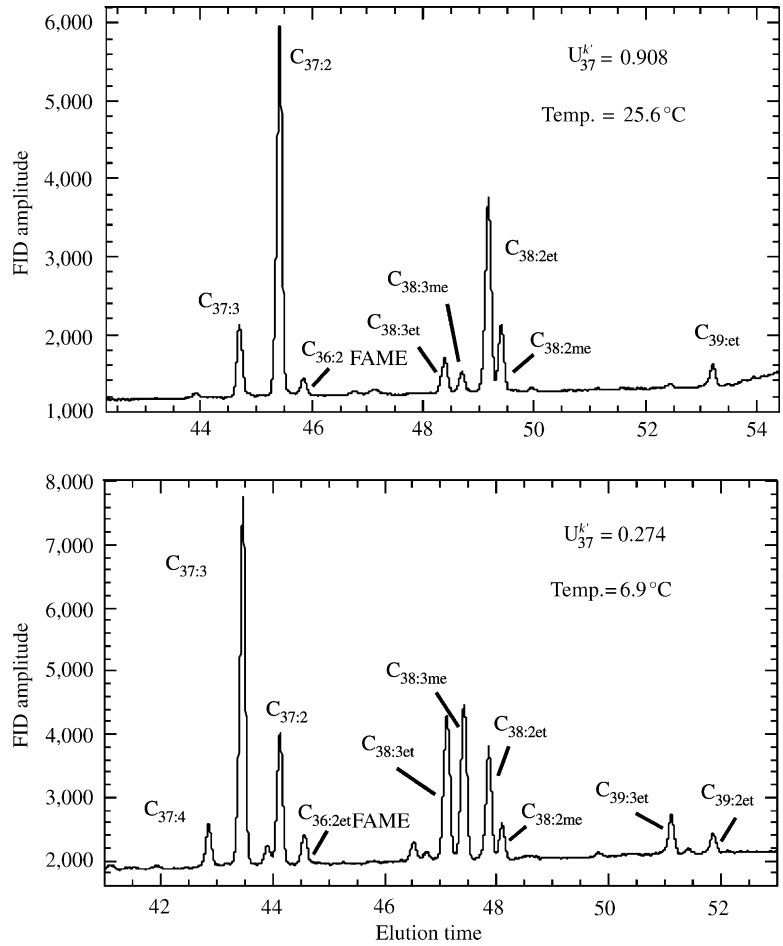

Figure 1 Typical GC-FID chromatograms of alkenone-containing sediment extracts.

Extraction system such as that offered by Dionex Corp. Some laboratories analyze alkenones as part of the total lipid extract; others prefer to run "cleaner" fractions following one of a number of schemes of fraction purification using silica gel columns or thin-layer chromatography (Villanueva *et al.*, 1997). Most open-ocean sediment extracts do not contain appreciable amounts of interfering lipids; however, some samples with more complex matrices may benefit from cleanup procedures.

Gas chromatography coupled to one of several detectors separates alkenones from their lipid matrix and permits their quantification. Relative to most lipid compounds in sediments, alkenones have high molecular weights and high boiling points. Elution through a nonpolar chromatographic column separates alkenones largely through boiling point, and subordinately by chemical interactions with the column film. Boiling point is largely determined by the molecular weight of the lipid. Because the mass differences between $C_{37:4}$, $C_{37:3}$, and $C_{37:2}$ ketones are small (molecular weights of 526 amu, 528 amu, and 530 amu, respectively), long chromatographic columns and/or slow temperature programs are required to completely resolve the component alkenones. In analogy with the $U^{k'}_{37}$ index, unsaturation ratios can be defined by the proportions of di- and tri-unsaturated C_{38} ketones (Conte *et al.*, 1998a). These relate linearly to the $U^{k'}_{37}$ index in culture (Conte *et al.*, 1998a; Yamamoto *et al.*, 2000), water-column (Conte and Eglinton, 1993; Conte *et al.*, 2001) and sediment studies (Figure 2). However, analytical challenges are greater for the four C_{38} ketones, whose pairs of ethyl and methyl di- and tri-unsaturated ketones prove very difficult to separate completely (Figure 1). Unsaturation ratios based on the C_{38} ketones therefore rarely appear in the alkenone literature. C_{39} ketones make up only a minor component of an alkenone-containing extract, and are rarely quantified.

Most alkenone determinations are made with a flame ionization detector (FID). This detector is simple, reliable, and highly sensitive. However, the FID functions essentially as a carbon detector, and does not give diagnostic information on the structure of the compounds detected. Alkenones are identified by FID by their elution times and by

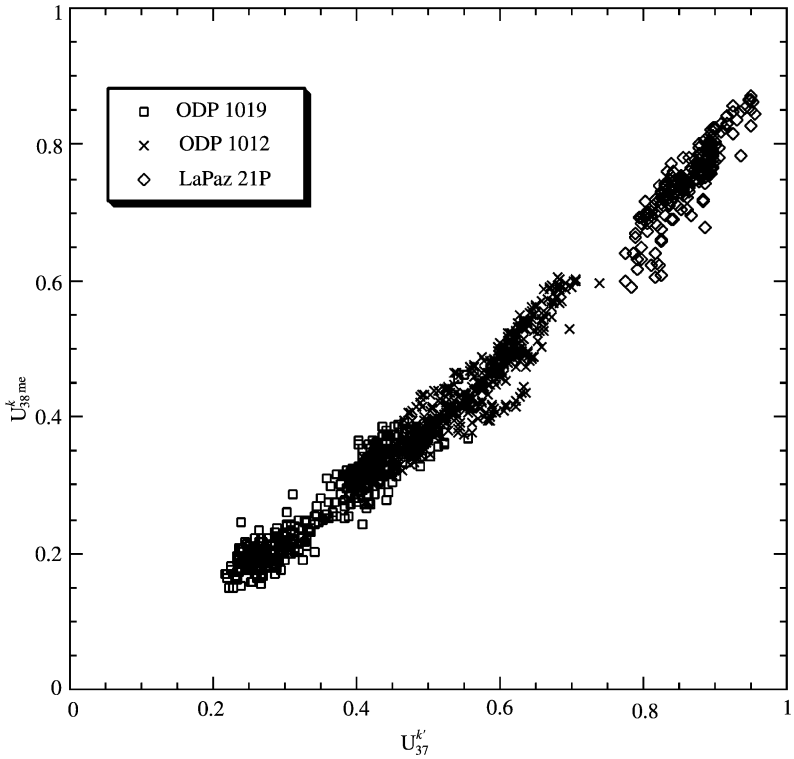

Figure 2 Relationship observed between the $U^{k'}_{37}$ index and the U^{k}_{38me} index [$C_{38:2me}/(C_{38:2me} + C_{38:3me})$] in a set of cores along the California margin (Herbert, unpublished). See Figure 1 for identification of the alkenone peaks. Note that the two indices are closely related, although the U^{k}_{38me} index has a slope and intercept offset from the $U^{k'}_{37}$ index. Scatter in the relationship primarily comes from analytical difficulties in quantifying the C_{38me} peaks accurately.

reference to external standards added to the injected solvent. Should other compounds share a common elution time (co-elution) with the alkenone chromatographic peaks, they cannot be separated from the signals of interest. The accuracy of gas chromatography (GC)-FID analysis therefore depends on the quality of chromatographic separations in the GC column, and on the presence or absence of interfering compounds. Fortunately, experience shows that interfering high molecular weight compounds are very rare in extracts of marine particulates in sediments. The stability of alkenones during microbial degradation, relative to other high molecular weight lipids, apparently enhances the alkenone signal in sediment extracts. Alkenones stand out not only as some of the most abundant compounds detected in typical lipid extracts, but also as one of the few sets of chromatographic peaks to elute late in the separation. Indeed, the virtual isolation of the alkenone "fingerprint" from the majority of chromatographic peaks almost certainly led to the initial recognition of their paleotemperature significance.

Other detection techniques offer more specificity, but require more analytical time and effort. Alkenones can be determined by GC-mass spectrometry (GC-MS) (Boon *et al.*, 1978; de Leeuw *et al.*, 1980), which identifies each compound by the molecular ion and characteristic fragmentation patterns. However, because the ionization efficiency for alkenones is low, GC-MS generally has lower sensitivity than GC-FID. Chemical ionization coupled to mass spectrometry can improve detection limits for alkenones (Rosell-Mele *et al.*, 1995a; Chaler *et al.*, 2000), but few laboratories employ this technique. GC-MS is therefore used primarily to confirm compound identification by GC-FID, and to detect the presence of co-eluting peaks in the region of alkenone elution if such contamination is suspected. Recently developed variants of GC-FID, such as multidimensional gas chromatography (Thomsen *et al.*, 1998) and comprehensive GC × GC (Xu *et al.*, 2001), promise to improve the specificity of alkenone detection, while maintaining the high throughput and sensitivity of GC-FID. This GC × GC method introduces "slices" of a separation by a first chromatographic column via thermal modulation into a second column of different polarity. The two-dimensional separations achieved appear to enhance the discrimination between potentially interfering compounds (Xu *et al.*, 2001).

In the absence of agreed-upon alkenone reference standards, the results of a recent interlaboratory comparison (Rosell-Mele *et al.*, 2001) offered a largely pleasant surprise. The intercomparison produced a greater consistency in the alkenone unsaturation parameter between laboratories than might have been anticipated. Splits of homogenized unidentified sediment samples were sent to each participating laboratory. Bristol University also prepared mixtures of synthetic $C_{37:3}$ and $C_{37:2}$ ketones. Laboratories were asked to perform replicate extractions and chromatographic determinations following their standard procedures. Interlaboratory variability for the $U^{k'}_{37}$ index, the most commonly measured alkenone unsaturation parameter, translated to a maximum of 2.1 °C between laboratories (95% confidence limit). Individual laboratories routinely obtain precision on replicate measurements on the order of 0.005 $U^{k'}_{37}$ units, or ~0.15 °C. The interlaboratory comparison also found no difference between the mean values determined by laboratories that put lipid extracts through cleanup procedures and those that analyzed total lipid extracts. This result indicates that reliable alkenone determinations can be made for most marine sediments with minimal sample preparation. Care should, however, be used to make sure that compounds are correctly identified and resolved in samples with unusually large amounts of labile compounds, such as found in shallow continental margin sediments. Early diagenesis generally removes interfering compounds in more slowly accumulating pelagic sediments.

Analytical challenges most likely occur at the extreme ends of the unsaturation index, where either the $C_{37:3}$ or $C_{37:2}$ alkenone abundances become very small, and in coastal sediments, where one encounters a more complex matrix of lipids than true for open-ocean sediments. Ternois *et al.* (1997) showed that a short (30 m) column on Norwegian Fjord samples ($U^{k'}_{37}$ ~0.2) did not resolve $C_{37:2}$ ketones from $C_{36:3}$ FAMEs, and hence produced erroneous estimates of sea-surface temperature. Using a 50 m column on the same samples obviated these problems. A more subtle error may come from irreversible adsorbtion of alkenones on the chromatographic column (Villanueva and Grimalt, 1996; Grimalt *et al.*, 2001). The effect is negligible for most samples, but can become significant when one is analyzing either the $C_{37:2}$ or $C_{37:3}$ alkenone near its limit of detection. Grimalt *et al.* (2001) recommend determining the irreversible adsorbtion for a GC system by varying the concentrations of extracts and determining the intercepts of a plot of $C_{37:3}$ and $C_{37:2}$ peak area versus concentration. Their modeling demonstrates that temperature errors can arise at both the high and low ends of the $U^{k'}_{37}$ scale, but will more likely affect results at the warm end of the $U^{k'}_{37}$ range (Grimalt *et al.*, 2001). Chromatographic biases will be toward warmer apparent temperatures at high $U^{k'}_{37}$ values and lower apparent temperatures at low values. Villanueva and Grimalt (1996) recommend introducing at least 5–10 ng of alkenones into the GC to avoid the bias of irreversible adsorbtion, corresponding to a threshold of 50 ng g^{-1} alkenone concentration in the sediments if 1 g is extracted. Our laboratory has also found that buildup of nonvolatile compounds on either a guard or chromatographic column will lead to preferential absorbtion of the $C_{37:3}$ alkenone, or a bias toward warmer temperature estimates, even in samples with large quantities of both ketones (see also Villanueva and Grimalt, 1996). The solution is to trim the column at the injection point by 20–30 cm daily, and to monitor the deterioration of the column by running known material frequently to detect drifts.

6.15.3 OCCURRENCE OF ALKENONES IN MARINE WATERS AND SEDIMENTS

Long-chained alkenones were first identified in Miocene through Pleistocene age marine sediments on the Walvis Ridge (Boon *et al.*, 1978). A group led by de Leeuw (de Leeuw *et al.*, 1980) in the Netherlands subsequently identified C_{37} and C_{38} alkenones in recent sediments of the Black Sea, where *E. huxleyi* dominates the coccolithophorid flora. Simultaneously, work at Bristol University established the connection between alkenone synthesis and certain species of extant haptophyte (coccolithophorid) algae (Volkman *et al.*, 1980a,b; Marlowe *et al.*, 1984a,b, 1990). Researchers at Bristol began to culture the producing species in the lab and to examine modern sediments for the presence of long-chained alkenones. It is now clear that two widely distributed species of coccolithophorid algae, *E. huxleyi* and *Gephyrocapsa oceanica*, are the principal alkenone synthesizers in the modern ocean (Conte *et al.*, 1994a; Volkman *et al.*, 1995). Other coccolithophorid species tested to date do not yield alkenones. In addition, alkenone production has been reported from some, but not all, species of the noncalcifying haptophyte genera *Isochrysis* and *Chrysotila* (Conte *et al.*, 1994a; Marlowe *et al.*, 1984b; Versteegh *et al.*, 2001; Volkman *et al.*, 1989). Cruises along the California margin and the equatorial Pacific suggest that noncalcifying haptophyte algae often dominate over coccolithophorid forms (Thomsen *et al.*, 1994). The possibility therefore exists that other noncalcifying haptophyte species that synthesize long-chained alkenones may well have gone undetected (Brassell *et al.*, 1987).

As far as is known, no marine algal groups other than the haptophytes synthesize long-chained alkenones.

The coccolithophorid algae, of which the principal alkenone producers represent a subset, play an important role in the cycles of both organic and inorganic carbon in the ocean (Balch *et al.*, 1992; Sikes and Fabry, 1994; Thomsen *et al.*, 1994). Coccolithophorids surround their cell with a number (in the case of *E. huxleyi*, ~23) of minute (micron-sized) calcite platelets. The intact aggregate is referred to as a coccosphere; after death the coccosphere may disintegrate into its component coccoliths. The biogeography of coccolithophorids is quite well understood, thanks to the distinctive liths produced by different species (Winter *et al.*, 1994). *E. huxleyi* is the most abundant and ubiquitous extant coccolithophore (Okada and Honjo, 1973; Winter *et al.*, 1994). In many plankton studies, it may compose 60–80% of the coccolithophorid assemblage. *E. huxleyi* appears to tolerate a large range of temperatures, salinities, nutrient levels, and light availability (Winter *et al.*, 1994). It therefore occurs in waters of nearly all temperatures, excluding those of the truy polar oceans, and in waters ranging from the highly saline (41‰) Red Sea to the brackish Sea of Azov and Black Sea (Bukry, 1974). Unlike many coccolithophorids, which thrive in the oligotrophic central gyre regions of the ocean, *E. huxleyi* can flourish in more eutrophic environments. *E. huxleyi* blooms appear to be triggered under conditions of a highly stratified upper water column, a shallow (10–20 m deep) mixed layer, and high light intensities (Nanninga and Tyrell, 1996). *E. huxleyi* may have a competitive advantage over other phytoplankton under conditions of high light intensity and low inorganic phosphate ability, as concluded by modeling work on mesocosm experiments in Norwegian fjords (Aksnes *et al.*, 1994). Doubling rates can be as fast as 2.8 d^{-1} (Brand and Guillard, 1981). Under bloom conditions, *E. huxleyi* occurs in large enough quantities in the surface ocean that scattering of light by the platelets can modify the optical properties of the water observed by satellite (Balch *et al.*, 1992). Indeed, dense milky patches of *E. huxleyi* blooms as large as 10^5 km^2 have been observed from space in the high latitude (40–60° N) North Atlantic and North Pacific oceans, off the Falklands in the South Atlantic, and on the north Australian margin (Brown and Yoder, 1994).

G. oceanica, the other known alkenone-synthesizing species of importance, has a more limited oceanic distribution. *G. oceanica* apparently does not occur in waters colder than ~12 °C (Okada and McIntyre, 1979). It commonly occurs in tropical and subtropical waters, in particular, the high fertility regions of the eastern Pacific and the Arabian Sea (Houghton and Guptha, 1991; Roth, 1994). This preference is consistent with a pulse of *G. oceanica* observed along the California margin during spring upwelling conditions (Ziveri *et al.*, 1995). However, the abundance of *G. oceanica* in the western equatorial Pacific warm pool demonstrates that the species does not require high nutrient concentrations. It reportedly tolerates very high salinities (45–51‰) (Winter, 1982), but cannot grow in water of low (15‰) salinity (Brand, 1984). As with *E. huxleyi*, *G. oceanica* can often dominate coccolithophorid assemblages, where it thrives (Roth, 1994).

The alkenone-producing species are typically reduced in abundance or excluded in oceanic provinces that favor diatom growth (Brand, 1994). Thus, they do not occur in the truly polar Arctic waters, and in the much broader siliceous province in the Southern Ocean, where they taper to zero abundance poleward of ~60° S (Nishida, 1986; Sikes and Volkman, 1993). The abundance of *E. huxleyi* and *G. oceanica* is also reduced in regions of high silicate availability, such as in many coastal zones and upwelling regions. Where nutrients such as nitrate and phosphate, or trace metals, such as iron, are low, the competitive advantage reverses to favor coccolithophores over the siliceous phytoplankton (Brand, 1991).

A series of reports of alkenone occurrences in sediments from brackish and freshwaters indicates that haptophytes other than the recognized marine producers may generate inputs of long-chained ketones in these environments. In some cases, the alkenone unsaturation ratio is consistent with open-marine settings, and may point to the extreme tolerance of *E. huxleyi* to low salinities. For example, Ficken and Farrimond (1995) studied a Norwegian Fjord recently opened to the open ocean by human activity. The sediments recorded the transition from fresh to brackish (10‰) conditions by an abrupt increase in C_{37} alkenones in the marine section. The $U^{k'}_{37}$ temperatures recorded in the recent interval lie between 7 °C and 10 °C using the standard marine temperature calibration, suggesting to the authors that *E. huxleyi* was likely the producing organism. The earlier lacustrine sediment sequence also contained alkenones, although at low levels. These differed from the marine sequence in their high abundance of the $C_{37:4}$ ketone (Ficken and Farrimond, 1995). Indeed, unusually high concentrations of the tetraunsaturated ketone seem to signal a "brackish" component to the haptophyte flora in environments such as the Baltic Sea (Schulz *et al.*, 2000) and Chesapeake Bay (Mercer *et al.*, 1999), and also to characterize lacustrine sediments (Cranwell, 1985; Volkman *et al.*, 1988; Li *et al.*, 1996; Thiel *et al.*, 1997; Mayer and Schwark, 1999; Zink *et al.*, 2001). No study has

yet confidently connected particular producing organisms to these "freshwater" alkenones.

6.15.3.1 Genetic and Evolutionary Aspects of Alkenone Production

Given that the synthesis of various alkenones and alkenoates is evidently regulated closely by the haptophyte producers, the question arises as to whether a universal response of parameters such as the $U^{k'}_{37}$ unsaturation index would be expected in the face of genetic diversity. Genetic variations could affect the use of alkenone paleothermometry in at least three different scales. In wide-ranging organisms such as *E. huxleyi* and *Gephyrocapsa*, strains evolve with physiologies attuned to the local environment (Paasche, 2002). The extent of genetic exchange between strains is unknown. If as a result of genetic isolation, the relations between alkenone unsaturation and growth temperature differ from strain to strain, then one would somehow have to account for this variation in paleoceanographic studies, or at least attempt to estimate how much uncertainty should be added to paleotemperature determinations due to strain effects. At a larger biogeographic scale, where the relative abundance of *E. huxleyi* and *G. oceanica* varies widely, one needs to decide whether each species has a significantly different $U^{k'}_{37}$–temperature relation, and, if so, then how to proceed to quantify the proportions of alkenone flux due to the two species. A temporal scale problem exists as well. The stratigraphic range of alkenones in sediments far exceeds the paleontological range of the extant alkenone-producing species (Marlowe *et al.*, 1990; Brassell, 1993). Does one assume that the $U^{k'}_{37}$ measured before the appearance of *E. huxleyi* or *G. oceanica* denotes the same temperature as a calibration derived from the modern organisms?

Genetic differences between strains of *E. huxleyi* and *G. oceanica* undoubtedly exist. Growing isolates in cultures is one way to establish which features might show genetic variation. Among the characters whose variation appears genetic are growth rate, temperature preference, salinity tolerance, calcite production rate, chloroplast pigment composition, and long-chained lipid composition (Fisher and Honjo, 1989; Paasche, 2002). As examples, Brand (1982) found that clones isolated from the cold water Gulf of Maine are genetically adapted to lower temperatures than those from the warm Sargasso Sea. Brand also determined that the oceanic genotypes from the Sargasso Sea cannot grow in 15‰ salinity, while coastal genotypes can (Brand, 1984). The relative success of the strains reversed when the strains were grown in saline conditions. Reproductive rates of *G. oceanica* clones from open ocean and neritic strains also differed in cultures (Brand, 1982). However, genetic variation does not always correspond to geographical separation. Young and Westbroek (1991) studied several genetically different morphological forms of *E. huxleyi,* whose populations were only partially separated by temperature preferences. Brand (1982) discovered that while strains of *G. oceanica* from the coastal waters might differ genetically, strains of *E. huxleyi* from the same regions did not.

At the same time, molecular and paleontological evidence is growing to support the strong genetic similarity of all marine alkenone producers. Two dominant morphotypes (A and B) of *E. huxleyi* are recognized. Yet Medlin *et al.* (1996) found little genetic variation when they compared ssu rRNA from three geographically isolated type A clones and a type B clone. In their judgment, the degree of separation did not warrant separating the A and B morphotypes at the species level. Two studies that sequenced portions of the genome of a number of coccolithophorid species were also revealing. Fujiwara *et al.* (2001) recognized four clades within the coccolithophores based on the gene for the subunit of the Rubisco enzyme *rbc* L. They recognized *Emiliania–Gephyrocapsa* as one clade, with identical nucleotide sequences for the *rbc* L subunit. By sequencing the spacer region of the Rubisco operon, Fujiwara *et al.* (2001) found that the noncalcifying alkenone-producing genus *Isochrysis* is an ingroup of the *Emiliania–Gephyrocapsa* clade. The authors suggest that *Isochrysis* may have secondarily lost the ability to form coccoliths. Ultrastructural similarities in the endoplasmic reticulum of *Emiliania*, *Isochrysis*, *Gephyrocapsa*, and *Chrysotila* also link the known alkenone-producing species (Fujiwara *et al.*, 2001). An independent study of the sequence of 18S rDNA by Edvardsen *et al.* (2000) confirmed the genetic clustering of the *Emiliania–Gephyrocapsa* clade within the coccolithophores.

A recent morphometric study of the distribution of *Gephyrocapsid* coccoliths hints that the previously recognized species may all belong to one biological species with strong morphological variations along environmental gradients. Bollman (1997) looked at a set of 70 globally distributed Holocene sediment assemblages to make quantitative determinations of *Gephyrocapsid* coccolith morphometric parameters such as size, bridge angle, ellipticity, and the width of the central collar. Bollman found strong environmental controls on the occurrence of morphotypes. Temperature and chlorophyll abundance (inferred from satellite data) proved to be the strongest predictors, although there was also a weak influence of salinity on the occurrence of some morphotypes. The largest morphological differences between

samples corresponded to the greatest environmental differences. Furthermore, within assemblages, Bollman found gradations in morphotypes between the end-members he recognized. Bollman proposed that six major morphotypes would be conventionally associated with different *Gephyrocapsid* species (his *Gephyrocapsa* Equatorial = *G. oceanica*; *Gephyrocapsa* Oligotrophic = *G. carribbeanica*; *Gephyrocapsa* Transitional = *G. margerli*; *Gephyrocapsa* Cold = *G. muellerae*; *Gephyrocapsa* Large = *G. oceanica rodela*; *Gephyrocapsa* Minute = *G. aperta*). Although Bollman admitted that paleontological examination cannot answer the question of whether his six morphotypes represent six biological species or only one species with strong morphological plasticity, he clearly leans toward the latter. This result is in accord with what many nannofossil authors see as difficulty in *Gephyrocapsid* species concepts (Ziveri *et al.*, 1995; W. Wei, personal communication). For example, Wei's (1993) stratigraphic study of the evolution of Plio-Pleistocene nannofossils distinguishes the first appearance of several "species" of *Gephyrocapsids* that would include most definitions of *G. oceanica*, at ~0.9 Ma. However, Wei labels these as *Gephyrocapsa* sp. C–D to denote the state of taxonomic uncertainty.

Results suggesting the close evolutionary relationship between alkenone-producing species are encouraging as paleoceanographers apply the alkenone method to sediments that predate the appearance of modern taxa. *E. huxleyi* first appeared during marine oxygen isotope stage 8 (Thierstein *et al.*, 1977), at ~280 ka. Its appearance can be shown to be globally synchronous to within 5–10 kyr by comparing its first appearance datum to oxygen isotope data measured in foraminifera in the same sediments. How sharply the evolutionary first occurrence of *E. huxleyi* appears depends on sediment location and sample interval; in some cases its coccoliths rapidly become abundant, while in others its arrival is less dramatic (Thierstein *et al.*, 1977). *Emiliania* almost certainly descended from a *Gephyrocapsid* ancestor (McIntyre, 1970). The species apparently reached its modern levels of abundance earlier in the tropics (ca. 85 ka) than at higher latitudes (Jordan *et al.*, 1996). Before the advent of *E. huxleyi*, *G. oceanica* was globally dominant during some intervals of the Pleistocene (Thierstein *et al.*, 1977; Bollman, 1997). The genus *Gephyrocapsa* has been reported in sediments as old as Middle Miocene (South Atlantic: Jiang and Gartner, 1984; Equatorial Pacific: Pujos, 1987), although its first frequent occurrence is in the mid-Pliocene (~3.5 Ma, Bollman, 1997). All morphological variations of *Gephyrocapsa* have existed since at least 620 ka, with the exception of Bollman's (1997) *Gephyrocapsa Cold* and *Gephyrocapsa Oligotrophic*.

Marlowe *et al.* (1990) produced an important review that compared the occurrence of alkenones in sediments with micropaleontological data on the coccoliths of the same material. Their synthesis indicated that a number of morphologically related species in the family *Gephyrocapsaceae* were potential sources of alkenones and alkenoates (genera *Crenalithus*, *Dictyococcites*, *Emiliania*, *Gephyrocapsa*, *Pseudoemiliania*, and *Reticulofenestrata*). The *Gephyrocapsaceae* were the only nannofossil family uniformly associated with alkenone-bearing sediments. The extinct genus *Reticulofenestra* evolved early in the Eocene and continued through the Pliocene, where it most likely left the genus *Gephyrocapsa* as its descendant (Rio, 1982). *Reticulofenestra* is the only genus of *Gephyrocapsids* to accompany alkenones in Miocene, Oligocene, and Eocene samples (Marlowe *et al.*, 1990). In the Pleistocene, *Gephyrocapsa* coccoliths always appear where alkenones have been detected (Marlowe *et al.*, 1990).

Cretaceous precursor alkenones have been reported; their evolutionary relationship with the modern clade of alkenone-producing organisms is unknown. Cretaceous alkenones (Farrimond *et al.*, 1986; Yamamoto *et al.*, 1996) differ from the modern suite in that C_{41} and C_{42} ketones dominate, and these consist (to date) only of di-unsaturated forms.

In sum, genetic and micropaleontological data suggest very close evolutionary relationships between the alkenone-producing species. Alkenone production occurs (and occurred) in species or variants already known to be closely related by micropaleontologists. Critical questions such as the degree of genetic exchange between species variants, and the degree of genetic variability within living populations, remain to be determined. Ignorance of the role of alkenones in the cells of haptophyte algae, and of genetic versus environmental controls on alkenone parameters, means that genetic effects in both space and time remain important unknowns in alkenone paleotemperature research.

6.15.4 FUNCTION

Alkenones occur in both motile and coccolith-bearing forms of *E. huxleyi* (Volkman *et al.*, 1980b; Conte *et al.*, 1995; Bell and Pond, 1996). The role that alkenones play in the producing organisms is not understood. That they play some critical role in *E. huxleyi* and related species is suggested by the large fraction of cellular investment accounted for by alkenones and alkenoates (Prahl *et al.*, 1988; Conte *et al.*, 1994b; Epstein *et al.*, 2001; Versteegh *et al.*, 2001)—generally

5–10% of cell carbon. Marlowe *et al.* (1984a) and Brassell *et al.* (1986b) proposed that alkenone unsaturation helps to regulate membrane fluidity at different temperatures, in analogy with the known function of membrane lipids in many plants. This model clearly associates the unsaturation index with a physiological response to growth temperature. However, alkenones have not been conclusively associated with the membranes of haptophyte algae. Conte and Eglinton (1993) did not detect alkenones in fragmented membranes of *E. huxleyi*. Mouzdahir *et al.* (2001) interpreted the rapid light-dependent degradation of C_{31} and C_{33} alkenones in contrast to the recalcitrance of C_{37} and C_{38} alkenones as an indication that the shorter-chained alkenes resided in membranes, while the longer-chained ketones resided elsewhere in the cell. Epstein *et al.* (2001) noted that cell quotas of alkenones increase with decreasing growth rate in cultures grown from an initial stock of nutrients. In analogy with triacylglycerides in cultures of other marine plankton, they proposed that alkenones may serve as storage molecules for the producing organisms. If this view is correct, then we have no clear reason why the unsaturation should relate to growth temperature.

6.15.5 ECOLOGICAL CONTROLS ON ALKENONE PRODUCTION AND DOWNWARD FLUX

Since alkenone-producing haptophytes can live in a range of depths in the photic zone, and vary greatly in their productivity over the course of an annual cycle, there is much to be learned about how the ecology of these organisms can affect the $U^{k'}_{37}$ signal eventually encoded in the sediments. Depending on the depth of maximum production relative to the mixed layer, alkenone producers may synthesize biolipids in temperatures representative of SST, or offset to colder temperatures by several degrees. Phytoplankton production is also quite seasonal in most ocean locations. If alkenone production follows a strong annual cycle, then again the $U^{k'}_{37}$ temperature could contain a bias relative to mean annual conditions (in the latter case, the bias could be toward either colder or warmer than average temperatures, depending on the season of maximum production). Profiles of coccolith and alkenone abundance through the photic zone, and over the yearly cycle, give indications of how ecological biases may vary between different oceanic provinces. Sediment traps intercept falling coccoliths and lipids to give windows into how the annual cycle in the near-surface is exported downward to the seafloor. A number of such studies will be reviewed below for their implications for the $U^{k'}_{37}$ thermometer. Many are micropaleontological, assessing both the absolute vertical fluxes of the alkenone producers *E. huxleyi* and *G. oceanica,* and the proportions of these species relative to the entire coccolithophorid assemblage. Lipid analyses also are available to measure the abundance of alkenones in the upper water column, and their flux into sediment traps. Unfortunately, very few studies combine both micropaleontological and geochemical approaches.

Nearly all micropaleontological time-series data collected on near-surface samples and sediment traps found either *E. huxleyi* or *G. oceanica* to dominate the coccolith flora on an annual basis. The density of living coccolithophorids is best measured by counting the number of intact coccospheres per unit volume of water sampled (e.g., Haidar and Thierstein, 2001). *E. huxleyi* accounts for the majority of the coccolithophorids surveyed in time series acquired off Bermuda (Haidar and Thierstein, 2001; 64% on an annual basis), the San Pedro Basin off Southern California (Ziveri *et al.*, 1995; 30–80% during the annual cycle), the Northeast Atlantic (Broerse *et al.*, 2000b; 69% and 72% at two sites surveyed), and off the coast of Northwest Africa (Sprengel *et al.*, 2000). *G. oceanica* was the most important taxon in year-long sediment trap studies of the Arabian Sea upwelling area, followed by *E. huxleyi* (Andruleit *et al.*, 2000; Broerse *et al.*, 2000c).

Depth profiles of cell densities in the photic zone generally show *E. huxleyi* to live within the mixed layer. Cortés *et al.* (2001) studied the seasonal depth distribution of coccolithophorid species off Hawaii. Sampling showed that the main production occurred in the middle photic zone (50–100 m), which lay within the mixed layer for most of the year. While the depth of maximum *E. huxleyi* density varied during the annual cycle, it generally lay between the shallowest sampling level (10 m) and 100 m. Depth profiles off Bermuda (Haidar and Thierstein, 2001) found that maximum densities of *E. huxleyi* were nearly always shallower than 100 m, and more commonly within the upper 50 m. The highest cell densities for *E. huxleyi* recorded were at 1 m depth in March, after the seasonal advection of nitrate into the mixed layer. Seven years of water-column particulate data off Bermuda confirm that alkenone concentrations in the surface mixed layer are 2–4 times higher than in the deep fluorescence maximum at 75–110 m (Conte *et al.*, 2001).

Hamanaka *et al.* (2000) conducted the only published study that directly estimated alkenone production as a function of depth habit. These authors incubated phytoplankton at 0 m, 5 m, 10 m, 25 m, 40 m, and 60 m depth, and measured

growth rates by spiking the water with $\delta^{13}C$. Maximum incorporation into alkenones occurred at 5 m depth, which coincided with the peak in alkenone concentration in particulates. Production rates at the surface and below 5 m were very low (from 269 ng l^{-1} d^{-1} at 5 m to 1.4 ng l^{-1} d^{-1} at 25 m). The depth of maximum alkenone synthesis lay well above the depth of the chlorophyll maximum at 25 m, indicating that the alkenone-producing species were offset vertically from the majority of the phytoplankton community. An array of shallow sediment traps intercepted the largest alkenone flux at 15 m, just below the layer most productive of alkenones.

There is, however, indirect evidence to suggest that alkenone synthesis may occur at depths below the mixed layer in some environments. $U^{k'}_{37}$ values in particulates often correspond to temperatures colder than the mixed layer. For example, Prahl *et al*. (2001) found that the alkenone flux to sediment traps in the Wilkinson Basin (coastal northeastern United States) peaked during summer time when surface waters stratified and a subsurface chlorophyll maximum was established in the upper seasonal thermocline. The $U^{k'}_{37}$ temperatures of the summer particulates corresponded to temperatures at the base of the upper thermocline, 6–7 °C colder than the ~5 m thick summer mixed layer. Similarly, Ternois *et al*. (1996) used the $U^{k'}_{37}$ of sediment trap material to time series of upper water-column temperatures in the western Mediterranean to deduce that the depth of maximum alkenone production varies over the annual cycle. The $U^{k'}_{37}$ temperature during the spring season corresponded to a maximum production depth of 50 m, while that depth apparently shallowed to 30 m during the second phase of high production in the fall months. Both Ohkouchi *et al*. (1999) and Prahl *et al*. (1993) have further argued that $U^{k'}_{37}$ values should be systematically offset to colder temperatures than the mixed layer in gyre regions, where the deep nutricline tends to produce subsurface chlorophyll maxima. It should be noted that in order to use the $U^{k'}_{37}$ value to estimate the depth of alkenone synthesis, one has to assume a temperature calibration. The suggestion of subsurface production is not purely circular, however, as one can compare the qualitative features of the $U^{k'}_{37}$ values over the annual cycle with the temperature time series. Thus, the $U^{k'}_{37}$ of falling particles actually decreased from spring into the onset of summer water-column stratification in the Wilkinson Basin study (Prahl *et al*., 2001), in direct contrast to the warming of the surface layer.

Alkenone production also occurs in the context of the annual cycle of upper water-column temperatures. Standing stocks of alkenone-producing species and their falling products display strong changes over the course of the year in all studies to date. In most cases, the time of maximum abundance of *E. huxleyi* and/or *G. oceanica*, and the maximum flux of alkenones into sediment traps, coincides with the dominant period for phytoplankton blooming. Thus, production peaks in spring months in most subtropical and mid-latitude locations (Prahl *et al*., 1993; Sprengel *et al*., 2000, 2002; Broerse *et al*., 2000b; Antia *et al*., 2001; Cortés *et al*., 2001; Harada *et al*., 2001; Haidar and Thierstein, 2001). In the typical cycle, cell densities of *E. huxleyi* increase in the upper photic zone after the seasonal advection of nitrate that occurs with winter and early spring mixing (Haidar and Thierstein, 2001). The abundance of *E. huxleyi* may increase by an order of magnitude (Cortés *et al*., 2001) or more (Haidar and Thierstein, 2001) in the upper water column during the spring bloom, as does its flux to sediment traps in locations such as the Northeast Atlantic (Broerse *et al*., 2000b). A sediment trap sample obtained in May in the Norwegian Sea intercepted a nearly monospecific bloom of *E. huxleyi* (Cadee, 1985). Flux maxima are, however, more commonly diffuse, occupying 2–3 months of time (Broerse *et al*., 2000b). Alkenone fluxes in sediment traps generally show a spring peak, indicating that surface ecological signals are exported to depth (Ternois *et al*., 1997; Sicre *et al*., 1999).

Maximum alkenone production may be shifted to the summer months in some regions. For example, Prahl *et al*. found that alkenone flux to sediment traps peaked during the early summer months at the Wilkinson Basin location (43° N), after the water column had stratified. At higher-latitude locations such as the Norwegian Sea and the Barents Sea in the northern hemisphere (Samtleben and Bickert, 1990; Thomsen *et al*., 1998), and in the Indian Ocean sector of the Southern Ocean (Ternois *et al*., 1998), the flux of *E. huxleyi* and alkenones is phased even more strictly to the summer months. Winter production can reach vanishingly small amounts during winter months in such harsh environments (Ternois *et al*., 1998; Broerse *et al*., 2000a). While such a pattern follows the classic seasonal progression of maximum production with latitude, exceptions to the rule occur. Goni *et al*. (2001) recorded a two- to threefold increase in the organic-carbon normalized fluxes of alkenones in the Gulf of California from June to October, well past the expected spring bloom. The latter authors speculated that maximal alkenone production could be separated from that of other phytoplankton groups by competition. Groups such as diatoms that often dominate peak bloom periods (Giraudeau *et al*., 1993; Broerse *et al*., 2000a,c) also generally show higher seasonal variability than does *E. huxleyi* (Beaufort and Heussner, 1999, 2001; Harada *et al*., 2001).

A competitive interaction apparently was observed by Ziveri *et al.* (1995), who found that the highest coccolith and coccosphere flux occurred in winter in the San Pedro basin off Southern California. This peak preceded the spring upwelling season favored by diatoms. Further evidence of *E. huxleyi* and/or alkenone production offset from that of other phytoplankton groups can be found in the studies of Ziveri *et al.* (2000), Harada *et al.* (2001), and Muller and Fischer (2001).

A number of oceanic regimes also produce twice-yearly flux maxima of alkenone production. In the Mediterranean, a fall bloom of alkenone production occurs (Ternois *et al.*, 1996; Sicre *et al.*, 1999). This is also true off Hawaii (Cortés *et al.*, 2001), in the central equatorial Pacific (Harada *et al.*, 2001), in the Sea of Okhotsk (Broerse *et al.*, 2000a), and in the Norwegian Sea (Thomsen *et al.*, 1998). A lack of dissolved silica may inhibit diatom growth and promote haptophyte production during the fall months in such locations (Broerse *et al.*, 2000a).

The monsoonally driven upwelling system of the Arabian Sea offers a special occasion to study the seasonality of alkenone production. In this environment, *G. oceanica* dominates, although *E. huxleyi* still occupies the second position in the coccolith flora (Andruleit *et al.*, 2000; Broerse *et al.*, 2000c). Winds favorable to upwelling occur twice per year. The Southwest monsoon in late spring/early summer sees the peak in upwelling conditions (Prahl *et al.*, 2000), while a secondary maximum occurs when the winds shift direction during the northeast monsoon (Andruleit *et al.*, 2000; Prahl *et al.*, 2000). Coccolithophore fluxes, comprised of 60–70% *G. oceanica* and *E. huxleyi*, increase during the southwest monsoon, at the same time as the maximum in silica flux (Broerse *et al.*, 2000c). Flux maxima lasted for nearly three months in this sediment trap study. In another sediment trap experiment conducted in the Arabian Sea, Prahl *et al.* (2000) determined that distinct alkenone flux maxima occur at the start and stop of the northeast and southwest monsoons. A lag in alkenone flux relative to other phytoplankton biomarkers suggested a successional delay in haptophyte production during the more dramatic southwest monsoon (Prahl *et al.*, 2000). No observable offset in production occurred during the less distinctive northeast monsoon, or at the close of the southwest monsoon. During peak monsoonal upwelling, alkenone fluxes reached ~25 times those of the unproductive months of the year.

Because only a few sediment trap experiments report data for much more than one year's duration, we have only a glimpse at the importance of interannual variability in the productivity of alkenone-synthesizing species. Reports do suggest large changes in the downward flux of either *E. huxleyi* or alkenones between years. Three years of sediment trap data from the northwestern Mediterranean Sea revealed, in addition to the bi-annual flux maxima mentioned earlier, considerable interannual variability (Sicre *et al.*, 1999). In general, Sicre *et al.* (1999) found that maximum alkenone fluxes coincided with maximum total organic carbon (TOC) fluxes. In the year 1994, however, there were comparable TOC fluxes to other bloom periods without correspondingly large C_{37} ketone fluxes. This study also reported large variability in the amplitudes of the spring and fall blooms in alkenones. For example, the spring and fall blooms produced fluxes of C_{37} ketones of 8 $\mu g^{-1}\, m^{-2}\, d^{-1}$and 16 $\mu g^{-1}\, m^{-2}\, d^{-1}$, respectively, in 1989–1990, but in 1994, the fall bloom amounted to a flux of only 0.1 $\mu g^{-1}\, m^{-2}\, d^{-1}$ to the 200 m trap. Muller and Fischer's (2001) four-year sediment trap study in the upwelling region of North Africa also documented approximately sevenfold variations in the annual flux of alkenones to sediment traps. These authors found no repeatable seasonal cycle in alkenone fluxes at their study location. Strong year-to-year variations in coccolith and coccosphere fluxes have also been identified in sediment trap data from the North Atlantic (Ziveri *et al.*, 2000) and in water-column censuses off Bermuda (Haidar and Thierstein, 2001). Conte *et al.* (1998b) report a particularly interesting short-lived alkenone flux peak in a Sargasso Sea sediment trap experiment. This region produces a classic spring bloom following the winter deepening of the mixed layer. The pulses of alkenone production detected by Conte *et al.* (1998b) preceded this predictable part of the annual cycle. Several short-lived flux events occurred, usually during December to January, but not for every year studied. During the flux events, falling organic matter was enriched in labile, phytoplankton-derived debris, including alkenones. For unknown reasons, a transient event in the surface water was inefficiently degraded and sent rapidly to depth (Conte *et al.*, 1998b).

Tiered sediment trap arrays present a picture of how seasonal and episodic production works its way toward the seafloor. Nearly all such arrays show that the near-surface temporal variability is attenuated with depth. The seasonal variability, so evident in many shallow sediment trap time series, is reduced by factors of 2 (Broerse *et al.* (2000a), Sea of Okhotsk; Ziveri *et al.* (2000), Northwest Atlantic; Muller and Fischer (2001), northwest African margin), to 3 (Harada *et al.* (2001), central equatorial Pacific; Thomsen *et al.* (1998), Norwegian Sea). This attenuation presumably comes both from the selective biological degradation of more labile lipids at shallow depths,

and a diffuse supply of fine-grained sediment particles at depth that partially masks the variability of surface production (see more below).

These observations raise the question of exactly what factors control the downward transport of alkenones. Clearly, as molecules associated with organisms only 10–20 μm size (before decomposition and disaggregation of coccoliths), they must have vanishingly low settling rates without the aid of processes that cause aggregation. The majority of sediment trap studies find that the coccolith and/or alkenone flux is highly correlated with the total mass flux over the yearly cycle (Beaufort and Heussner, 1999; Andruleit *et al*., 2000; Broerse *et al*., 2000a,b). This may signal the general synchronization of *E. huxleyi* and/or *G. oceanica* production with the total biogenic flux, which then sweeps smaller particles out of the photic zone (Thomsen *et al*., 1998; Ziveri and Thunell, 2000). To support this idea, shallower sediment trap collections find that the intact coccosphere flux, which must represent the most recently produced and least remineralized component of the haptophyte flux, coincides with the time of highest detached coccolith flux, and that these peak the same time as the highest total mass flux (Broerse *et al*., 2000a). Broerse *et al*. (2000a) note the role of marine snow in entangling coccospheres in the autumn bloom in the Sea of Okhotsk, and a complementary role played by large diatoms in the spring. Coccospheres represent only a tiny portion of the coccolith carbonate flux (Broerse *et al*., 2000a; Ziveri *et al*., 2000; Ziveri and Thunell, 2000); most of the coccolith flux must undergo multiple cycles of release and reaggregation (Ziveri *et al*., 2000).

Studies that report alkenone fluxes relative to total organic carbon (normalized to TOC in typical units of 100–1,000 $\mu g\ g^{-1}$ TOC) also provide evidence that much of the alkenone flux from the photic zone comes from bloom episodes. Such normalized alkenone concentrations in sediment traps ranged from lows of 29 $\mu g\ g^{-1}$ C during unproductive winter months in the Wilkinson Basin (northeast margin of the US) to highs of 1,054 $\mu g\ g^{-1}$ C during the early summer bloom period (Conte *et al*., 1998b; Prahl *et al*., 2001). Similar results were reported in the Southern Ocean (Ternois *et al*., 1997), Mediterranean Sea (Sicre *et al*., 1999), and Norwegian Sea (Thomsen *et al*., 1998). Alkenone accumulations during times of very low flux may indeed represent the sedimentation of "relict" material synthesized during more productive seasons (Conte *et al*., 1998b; Sicre *et al*., 1999; Prahl *et al*., 2001). There are, however, several sediment trap studies that do not report significant correlations between the alkenone flux and the total organic flux (Ternois *et al*., 1996; Muller and Fischer, 2001).

Evidence has recently emerged that some benthic environments may also receive a diffuse supply of fine-grained particles with associated alkenones. Processes such as resuspension of continental margin and slope sediments during major storms, and benthic currents may thus contribute lateral supplies of alkenones to the sediments. Fluxes of coccoliths in a deep-sea canyon setting in the Bay of Biscay increased significantly during the fall and winter stormy months (Beaufort and Heussner, 1999), as did coccolith and alkenone fluxes during summer resuspension months in the Norwegian Sea (Andruleit, 1997; Thomsen *et al*., 1998). Core-top $U^{k'}_{37}$ estimates can apparently be affected by the input of fossil alkenones in the Norwegian and Barents Sea. Thomsen *et al*. (1998) determined $U^{k'}_{37}$ values in shallow sediment traps consistent with production in (cold) surface temperatures, but showed that deeper traps and surface sediments had $U^{k'}_{37}$ indices 5–10 °C too warm for the locations. The presence of pre-Quaternary coccoliths in floral assemblages unequivocally indicates that some portion of the flux comes from the erosion of older slope and shelf sediments (Beaufort and Heussner, 1999, 2001; Weaver *et al*., 1999). A number of other sediment traps have found higher coccolith fluxes at depth than in shallow traps, indicating a lateral source of material (Sprengel *et al*., 2000, 2002; Ziveri *et al*., 2000; Antia *et al*., 2001).

The effect of lateral transport on $U^{k'}_{37}$ temperature estimates will depend on the age of the transported material (e.g., contemporary or fossil), the location from which it comes (e.g., from similar latitude and surface temperature, or from long distance), and the ratio of the advected flux to the alkenones sedimented in the vertical sense. Deep equatorward benthic currents are apparently responsible for transporting alkenones, along with the fine fraction, a great distance from their source in at least two instances. In the southwestern Atlantic, recent age sediments under the Brazil–Malvinas Confluence and Malvinas Current produce anomalously cold (by 2–6 °C) $U^{k'}_{37}$ temperature values (Benthien and Müller, 2000). The remainder of the 87 core tops that these authors analyzed in a large region from 5° N to 50° S had $U^{k'}_{37}$ values in good agreement with global core-top calibrations to local mean annual SST. Benthien and Müller (2000) argue that sediments in these specific regions were transported northward and offshore by benthic currents, and hence contain $U^{k'}_{37}$ signals of their origin in cold waters. Benthic boundary current advection of alkenones has been documented in a different way by Ohkouchi *et al*. (2002) in Bermuda Rise drift sediments. Compound-specific AMS ^{14}C dating of alkenones shows that they may be significantly older than foraminifera in the same

layers. The authors attribute this to southward advection of the fossil fine fraction material from the Nova Scotia margin. However, there may also be environments with significant lateral transport in which the effect of allocthonous material does not swamp primary coccolithophorid ecological signals. For example, Beaufort and Heussner (1999) found that the seasonal cycle of succession in coccolithophorid species was preserved in the Bay of Biscay sediment trap time series, despite the input from resuspended margin sediments. The primary $U^{k'}_{37}$ signal would presumably be preserved as well in such a case.

6.15.5.1 Effects of Water-column Recycling and Sediment Diagenesis on the Alkenone Unsaturation Index

As they descend through the water column and are incorporated into sediments, alkenone and other lipid biomarkers encounter different degradational conditions (Prahl *et al*., 1989a; McCaffrey *et al*., 1990; Sun and Wakeham, 1994; Koopmans *et al*., 1997; Rontani *et al*., 1997; Teece *et al*., 1998; Sinninghe-Damsté *et al*., 2002). The amount of time that lipids spend exposed to these metabolic pathways varies substantially, as does the degradational efficiency of each pathway. Rapid transit under oxic conditions generally occurs through the water column. Slow passage, often under suboxic to anoxic conditions, characterizes the entrance of alkenones into the sedimentary record. The key question for paleoceanographers is whether these steps produce measurable changes in the alkenone unsaturation index.

The fraction of alkenones buried in sediments represents less than 1% of the initial flux from the photic zone in most cases. This attenuation can be measured by comparing tiered sediment trap fluxes to surficial sediment fluxes. The synchronization of alkenone flux peaks between shallow and deep traps shows that the time required for alkenone-containing particles to reach the seafloor is only one to two weeks (Conte *et al*., 1998b; Muller and Fischer, 2001). Somewhat slower average sinking velocities pertain to periods of low alkenone and total mass flux (Muller and Fischer, 2001). During their descent, alkenones are strongly recycled, both relative to their initial flux, and relative to bulk organic matter (Sicre *et al*., 1999; Muller and Fischer, 2001). Alkenones do appear more resistant to degradation than most other lipids of planktonic origin (Prahl *et al*., 2000; Volkman *et al*., 1980a). Recycling in the sediments adds further attenuation to the roughly one order of magnitude loss in the water column. In the slow deposition rate of most marine environments, alkenones will be exposed to degradation under oxic conditions for thousands of years. However, where sediment accumulates more rapidly, as along continental margins, and where oxygen levels in either the bottom water or sediment pore waters plummet, alkenones will be exposed to nonoxic bacterial metabolic pathways. Comparison of sediment trap fluxes to surface sediments in pelagic regions suggests alkenone preservation factors of 0.2% (relative to the deep trap flux) (Muller and Fischer, 2001), 0.6% (Prahl *et al*., 1989b), and 1% (Prahl *et al*., 2000). In pelagic environments, degradation of alkenones in surface sediments appears approximately an order of magnitude more efficient than the reduction in bulk organic carbon (Prahl and Muelhausen, 1989; Prahl *et al*., 2000; Muller and Fischer, 2001). However, much better preservation occurs in high sediment flux settings. The highest preservation efficiency of alkenones reported is 44% in the shallow (~300 m) and high deposition rate setting of the Wilkinson Basin (Prahl *et al*., 2001) and nearly 100% in the anoxic bottom sediments of the Guaymas Basin (Goni *et al*., 2001). Prahl *et al*. (1993) used an onshore–offshore sediment trap and sediment transect to demonstrate that the preservation efficiency of alkenones and total organic carbon was high, and similar (~25%) at their near-shore site (water depth 2,717 m), but fell systematically in the direction of the open ocean to only 0.25% in the most distal site. The deepest water site clearly displayed preferential loss of alkenones relative to bulk organic carbon (Prahl *et al*., 1993). Preservation efficiency in sediments thus seems to depend strongly on exposure time to oxic degradation (Madureira *et al*., 1995; Prahl *et al*., 2001).

None of the sediment trap studies reports significant shifts in the alkenone unsaturation index as a consequence of degradation. A sediment trap deployment in the northwestern Mediterranean Sea found that despite a fivefold loss in alkenones between shallow and deep traps, there was no apparent offset in the $U^{k'}_{37}$ ratio of the biomarkers. Sawada *et al*. (1998) similarly found no shift in the unsaturation index through the enormous vertical path length of the northwest Pacific (traps arrayed at 1,674 m, 4,180 m, 5,687 m, and 8,688 m). Furthermore, the $U^{k'}_{37}$ composition of underlying sediments agreed with sediment trap estimates, indicating that early diagenesis in the sediments did not modify the unsaturation index relative to the incoming composition. Other comparisons of the $U^{k'}_{37}$ index between sediment traps and core tops find very good agreement as well (Muller and Fischer, 2001; Prahl *et al*., 1989b, 2001).

Several investigators have conducted laboratory studies of the effects of degradation on the alkenone unsaturation index. In the early history of the development of the $U^{k'}_{37}$ index,

Volkman *et al.* (1980a) compared the unsaturation index in fecal pellets of the copepod *Calanus helgolandicus* with that of the *E. huxleyi* used to feed them. No change in the index was observed after passage through the guts of these zooplankton. Grice *et al.* (1998) obtained similar results by feeding the alkenone-synthesizing haptophyte *I. Galbana* to the copepod *Temora*. The best study of sedimentary processes comes from Teece *et al.* (1998), who exposed alkenones to microbial degradation under different conditions for almost 800 days. Oxic, sulfate-reducing, and methanogenic experiments produced time series of the degradation rates of alkenones and other lipids. After rapid initial degradation of lipids, the fate of alkenones varied significantly. About 85% of the initial alkenone inventory had been degraded under oxic conditions by the end of the experiment. The two anoxic pathways yielded different results. Under sulfate-reducing conditions, degradation essentially ceased with ~60% of the alkenones remaining. Methanogenic conditions led to preservation not much better than for oxic conditions (~80% degradation). Teece *et al.* (1998) conclude that the different apparent alkenone degradation rate constants under different anoxic conditions lead to subtleties in understanding the preservation of alkenones under varying redox states. A very important finding, however, was that the $U^{k'}_{37}$ index did not shift beyond a very modest increase (0.03 units, equivalent to less than 1 °C apparent temperature change) reported for the oxic experiment (Teece *et al.*, 1998).

Two sediment studies present the dissenting view that the alkenone unsaturation index may shift to higher $U^{k'}_{37}$ values (higher apparent temperature) during diagenesis. Gong and Hollander (1999) compared near $U^{k'}_{37}$ sediment data acquired down-core at two sites in the Santa Monica Basin that differed in bottom-water oxygenation. They attribute a positive $U^{k'}_{37}$ offset at the oxic site to indicated preferential degradation of the $C_{37:3}$ ketone. In order to estimate the offset, Gong and Hollander had to match samples of the same age between the cores. Thus, some of the apparent temperature offsets of up to 2.5 °C depend on the quality of the age models. Nevertheless, Gong and Hollander (1999) present evidence over the last two centuries of deposition for an average $U^{k'}_{37}$ offset equal to 0.9 °C at the oxic site. Another way to study the possibility of diagenetic alteration of the $U^{k'}_{37}$ index is to look for gradients in the index with preservation of initially homogeneous material. Fine-grained turbidites, the sedimentary product of near-instantaneous emplacement of well-mixed sediment on the seafloor, offer this opportunity. After the emplacement of the turbidite layer (often 10–100 cm thick), a well-developed redox front moves downward from the sediment–water interface. The top of the turbidite layer will experience significant oxidation, while the base may suffer none at all. Hoefs *et al.* (1998) studied $U^{k'}_{37}$ indices through oxidation fronts in a number of fossil turbidite layers cored on the Madeira abyssal plain. They reversed the conclusion of Prahl *et al.* (1989b), who had earlier found negligible shift in the $U^{k'}_{37}$ index in a relatively young turbidite sequence in the same region. Hoefs *et al.* reported that alkenones were degraded to a far greater degree (factors of 50–1,000) in the oxidized zones of the turbidites relative to total organic carbon. The samples with the lowest alkenone concentrations produced $U^{k'}_{37}$ estimates 2.5–3.5 °C warmer than samples in the unaltered bases of the turbidites. Hoefs *et al.* (1998) conclude that diagenesis may indeed selectively degrade the $C_{37:3}$ ketone and produce significant artifacts for paleoceanography.

Grimalt *et al.* (2000) mounted a serious criticism of the evidence for differential diagenesis based on the turbidite studies. They noted that the amount of apparent temperature change depended strongly on the reported alkenone concentrations. The strongest evidence for differential diagenesis (Hoefs *et al.*, 1998) comes from samples with extraordinarily low alkenone concentrations. Grimalt *et al.* conclude that the shift to higher $U^{k'}_{37}$ values could well be an analytical artifact of attempting to analyze the $C_{37:3}$ ketone at its limit of detection. As noted earlier, irreversible chromatographic column adsorbtions become significant at very low concentrations of either ketone. In Madeira Abyssal Plain sediments, the initial (unoxidized) $C_{37:3}$ ketone concentration is quite low relative to the di-unsaturated ketone, and it could well reach its limit of detection under the concentrations analyzed by Hoefs *et al.* (1998).

What is the long-term fate of the alkenone unsaturation index in sediments? The time available for alteration in sediments dwarfs the few thousand years of near-surface exposure. It is difficult to completely answer the question, since without knowing *a priori* what correct SST estimates would be for ancient sediments, we cannot get a direct estimate of diagenetic offsets or lack thereof. Nevertheless, some qualitative lines of reasoning suggest that the alkenone index probably remains quite stable on geological timescales. The signature of differential diagenesis on the $U^{k'}_{37}$ index would include long-term trends toward reduced concentrations of alkenones with greater time and burial depth. Most authors would expect that a diagenetic overprint, if there is one, would be at the expense of the $C_{37:3}$ ketone. If one models the degradation as first-order with concentration of the C_{37} ketones, then one can imagine that slightly different rate constants could be

involved. The available evidence suggests that, once the alkenones have survived the relatively high metabolic activity of the upper few centimeters to tens of centimeters of the sediment column, these rate constants must be very small. That is because the time alkenones and other lipids spend below the surficial layer is one order of magnitude longer at 10^4 yr, and three orders of magnitude greater at 1 Myr than the time spent during early diagenesis. Over these long timescales, decay rate constants of perceptible size should produce nearly monotonic trends in alkenone loss as a function of sediment age, even if there were primary variations in the initial alkenone concentration of the sediment, because the sediment age would be many e-folding times of the inverse rate constant. Our laboratory has found that, to the contrary, alkenone concentrations are frequently higher in sediments hundreds of thousands to millions of years old than they are in the core-top material of the same sites (Figure 3). The implication we draw is that variations in initial near-surface alkenone concentration persist for very long durations in the deeper sediment column without diagenetic attenuation. Furthermore, alkenones appear stable when normalized to other products of photosynthesis. Figure 4 displays the alkenone content of sediments from the Oman Margin (ODP Site 723) normalized to total organic nitrogen and chlorins, an early diagenetic transformation product of chlorophylls, as a function of age. Considered individually, all three data sets show high-amplitude variations with time that are related to changes in their production and preservation in this dynamic upwelling zone. This variability disappears into near-monotonic

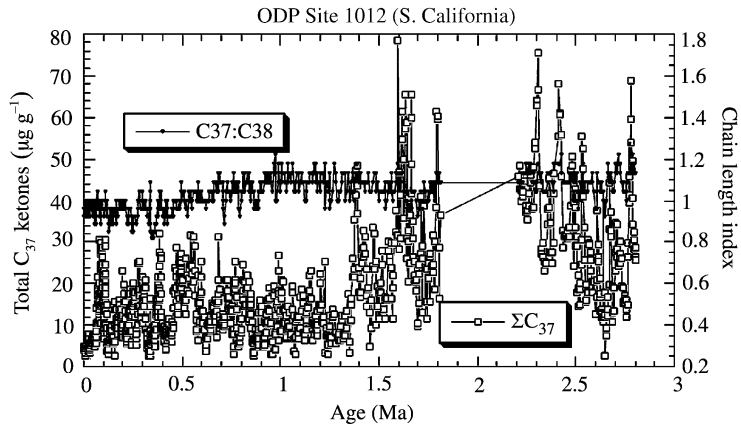

Figure 3 Alkenone concentrations (μg g^{-1} dry sediment weight) determined over a 2.8 Ma record from ODP Site 1012 off the southern California coast. Note the absence of a down-core decrease in alkenone concentrations that would suggest progressive diagenetic loss of alkenones in older sediments. Evolutionary conservatism in alkenone synthesis is suggested by the stability of the chain length index $\left(\sum C_{37}/(\sum C_{37} + \sum C_{38})\right)$ over the record.

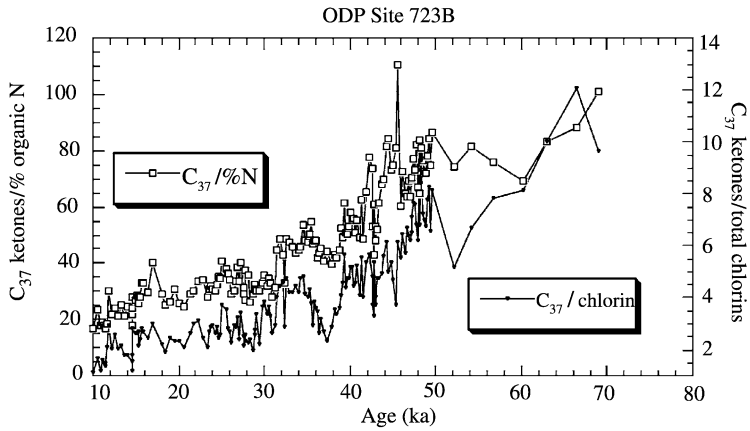

Figure 4 Down core trends in alkenone-normalized organic Nitrogen and total chlorins from ODP Site 723 (Oman Margin). The records extend from the late Holocene at the core top to ~70 ka. Note the monotonic decrease of the two organic classes relative to alkenones. This behavior is consistent with the progressive degradation of these more labile components and the diagenetic stability of the C_{37} alkenones.

trends of increasing normalized alkenone concentration with greater age (Figure 4), which are best explained as preferential degradation of organic nitrogen and chlorophyll relative to alkenones.

Sediments with elevated pore-water temperatures provide at least one exception to this general rule of the diagenetic stability of alkenones. Simoneit *et al*. (1994) measured alkenone abundances in sediments of the Middle Valley of the Juan de Fuca spreading center. Hydrothermal alteration of the sediments resulted in the loss of alkenones at temperatures greater than 200 °C. The Simoneit *et al*. (1994) study thus suggests caution in using the alkenone unsaturation index in other regions of unusually high geothermal gradients, or in very deeply buried sediments.

6.15.6 CALIBRATION OF $U^{k'}_{37}$ INDEX TO TEMPERATURE

The calibration of the alkenone unsaturation index actually resolves into two questions for paleoceanographers to address. The first concerns defining an equation, or sets of equations if one should not prove globally applicable, which relate the unsaturation index to the water temperature in which the producing organisms grew. The second involves understanding how the unsaturation index recorded in sediments, which represents an enormous integration of growth–temperature histories of individual organisms, and relates to a consistent measure of sea-surface temperature (e.g., SST versus subsurface depth, and annual versus seasonal temperature). These are not one and the same question, because *E. huxleyi* and related species may not always live in the mixed layer, and because their production may vary seasonally. For this reason, I evaluate evidence in the following section for how the influences of water-column habitat, seasonality, and particle transport through the ocean may affect the interpretation of the sedimentary $U^{k'}_{37}$ index.

One can approach the question of the quantitative relation of the $U^{k'}_{37}$ index to growth temperature at considerably different scales of time, genetic, and environmental variability. Culture studies allow the experimentalist to eliminate many confounding variables in the natural environment (genetically mixed populations, varying nutrient availability, different depth habitats, etc.) to isolate the influence of factors such as growth temperature, physiological state (exponential versus late-log, versus stationary growth), and nutrient availability on alkenone and alkenoate systematics. Despite the elegance of the experimental approach, results from such studies must be viewed as models for what may exist under natural conditions, not necessarily as calibrations. By collecting particulate material in the water column, either by filtering material in the euphotic zone, or collecting falling particles in sediment traps and relating their alkenone composition to time series of near-ocean temperatures, we move closer to relating the growth environment of the alkenone-producing algae to the signals sent to the sediment. This comes at the cost of unknown genetic variability in the natural populations, and some ambiguity in the actual time and depth of alkenone synthesis and, hence, the appropriate growth temperature versus alkenone/alkenoate relations. Near-surface sediments now provide a global database to examine the paleo-environmental information contained in the preserved record of alkenones and alkenoates. The time averaging inherent in sedimentation means that one is integrating temporal, physiological, and genetic influences on scales not approached in the laboratory or in field studies. However, correlations from the sediments to environmental variables in the water column rely on statistical relations, since one cannot directly link the sediment $U^{k'}_{37}$ index to particular ecological controls on the unsaturation–temperature relation.

6.15.6.1 Culture Calibrations

Prahl and co-workers (Prahl and Wakeham, 1987; Prahl *et al*., 1988) conducted seminal studies that still provide the widely accepted calibration of the $U^{k'}_{37}$ index to growth temperature. These papers report the $U^{k'}_{37}$ values of one strain of *E. huxleyi* grown at different temperatures. Prahl and his collaborators argued that the good comparison of their laboratory results to the results of $U^{k'}_{37}$ analyses of water-column particulates collected at known temperatures in the eastern Pacific suggested that they had arrived at a valid calibration between 5 °C and 25 °C. It may well be that linking laboratory to field data helped ensure the robustness of their calibration. The relationship derived by Prahl and Wakeham (1987 and amended slightly by Prahl *et al*. (1988)) followed a linear relationship with temperature. Extrapolated to the limits of the $U^{k'}_{37}$ index of 0 and 1, it suggests a lower temperature limit of ~1 °C, and an upper limit of ~28 °C. Both the very coldest and warmest surface temperatures of the ocean would therefore lie outside the range of the $U^{k'}_{37}$ index.

Numerous culture studies of alkenone-producing species and strains have followed Prahl's initial studies, under the theory that cultures uniquely allow the experimentalist to isolate factors that may influence alkenone and alkenoate distributions. Experience shows that differences can exist between results obtained from using batch

or continuous culture methods on the same strain of alkenone-producing algae (Popp *et al*., 1998), from the phase of growth from which alkenones are harvested (Conte *et al*., 1998a; Epstein *et al*., 1998, unpublished; Yamamoto *et al*., 2000), and from different laboratories culturing the same strain (see results of culturing *E. huxleyi* strain VAN556 by Conte *et al*. (1998), compared to Prahl *et al*. (1988), or to data presented by Sawada *et al*. (1996) showing differences between two laboratories). Furthermore, replicate cultures grown in the same laboratory under ostensibly similar conditions can yield a spread of $U^{k'}_{37}$ values (Conte *et al*., 1995; Versteegh *et al*., 2001). In batch culture, a nutrient medium is provided to a strain inoculate. After a period of rapid (exponential) growth, the cell density approaches a limit, and may even decline. The investigator can harvest cells at various times during the sequence to determine alkenone and alkenoate concentrations. Continuous cultures maintain the organisms in the exponential growth phase by supplying nutrients. Growth of alkenone-producing haptophyte algae in chemostats (Popp *et al*., 1998) represents a particularly sophisticated manipulation, as these cultures grow in a medium of constant (low) nutrient availability. It is not clear whether batch or continuous growth models better represent natural conditions, or whether the sinking flux of alkenones and alkenoates in the ocean comes from populations in exponential, late logarithmic, or stationary growth state.

All culture studies confirm the first-order dependence of $U^{k'}_{37}$ and other alkenone (Conte *et al*., 1998a) unsaturation parameters on growth temperature, but produce results that conflict in many ways. The study of Prahl *et al*. (1988) demonstrated that haptophytes grown in the laboratory adjust their unsaturation to temperature changes on a timescale of days; culture work by Conte *et al*. (1998a) suggested rapid adjustment of alkenoate/alkenone ratios to changes in growth temperature as well. However, culture calibration studies suggest very large variations in the relation of unsaturation to growth temperature that may depend on genetic and physiological factors (Conte *et al*., 1995, 1998a; Epstein *et al*., 1998). Twenty-four strains of alkenone-producing species cultured by Conte *et al*. (1995) at 15 °C gave $U^{k'}_{37}$ values that ranged from 0.3 to 0.55. Only one of these approached the value of ~0.56 appropriate for the Prahl *et al*. (1988) temperature calibration and, indeed, Conte *et al*. (1995) obtained a $U^{k'}_{37}$ value of ~0.4 at 15 °C for VAN55, the strain used by Prahl and Wakeham (1987) and Prahl *et al*. (1988). Volkman *et al*. (1995) suggested that cultures of *G. oceanica* produce a significantly different relation of unsaturation to growth temperature; however, their experimental results do not agree with *G. oceanica* cultures grown by Sawada *et al*. (1996) or Conte *et al*. (1998a).

It also seems clear that factors such as growth phase, light, and nutrient levels can significantly influence the unsaturation index of haptophytes grown in the laboratory (see summary in tables 4 and 5 of Versteegh *et al*., 2001). Both Conte *et al*. (1998a) and Epstein *et al*. (1998) found changes in the unsaturation index between log, late-log, and stationary phases of growth. Epstein *et al*. (1998) proposed that nutrient availability, which would control growth rates of cultured and natural populations, could significantly affect the calibration of unsaturation to growth temperature. Both investigations found increasing alkenone concentrations (pg cell^{-1}) in late logarithmic and stationary phase growth. Conte *et al*. (1998a) also documented very large ranges in the ratios of alkenoates to C_{37} and C_{38} ketones (0–2.8), and in the $\sum C_{37} : \sum C_{38}$ ketone ratio depending on growth phase. Comparison of these parameters to field data led Conte *et al*. to conclude that natural populations most closely resemble late-log of stationary populations grown in the laboratory. In contrast to the batch culture experiments discussed above, Popp *et al*. (1998) used chemostats to control steady-state growth rates, which they argue may be a better model for natural systems. The latter study found no significant dependence of $U^{k'}_{37}$ on growth rate at constant temperature.

A number of studies have investigated whether genetic and/or physiological differences create "fingerprints" in other aspects of alkenone/alkenoate systematics that might allow investigators to distinguish past variations in species/strain production in sediments. Volkman *et al*. (1995) and Sawada *et al*. (1996) suggested that the proportions of C_{37} to C_{38} ketones ("chain length index"), or alkenoate/alkenone ratios, might relate to the proportions of *E. huxleyi* to *G. oceanica* at the time of production (see also Yamamoto *et al*., 2000). Further culture work by Conte *et al*. (1998a) does not support either suggestion (see also Section 6.15.4).

Nearly all culture calibration studies predict higher growth temperatures for the same unsaturation index than postulated by the Prahl *et al*. (1988) regression, although several (Conte *et al*. (1998a) and *G. oceanica* cultures of Sawada *et al*. (1996)) fall very close to the Prahl relation. If this ensemble of culture data is correct, field and sediment studies applying the Prahl *et al*. (1988) calibration might frequently overestimate temperatures. As we evaluate water-column, sediment-trap, and core-top data, we should assess whether the large range of possible $U^{k'}_{37}$–temperature relations suggested by culture studies, whether of genetic or physiological origin, demonstrably affect the accuracy of a unified calibration

relation. One would expect to find that different haptophyte biogeographic regions produce distinct calibrations of unsaturation to temperature, and to see the influence of nutrient availability in offsets between upwelling and nonupwelling regions.

6.15.6.2 Particulates

By studying alkenone parameters in particulate matter collected in the photic zone, we lose the ability to manipulate potential genetic or physiological influences, but we gain the ability to compare alkenone systematics to temperatures in the natural setting. Calibration equations can be generated and tested by comparing the alkenone unsaturation index in suspended particles with ambient water temperatures. One generally assumes that the measured water temperature is the same as the temperature in which the alkenones and alkenoates were synthesized. This may not always be correct for particles sinking or mixing through a temperature-stratified water column. In fact, given a general tendency for particles to sink, the temperature of alkenone synthesis might be higher than the temperature in which the particles are collected, but almost certainly not be lower (Sicre *et al.*, 2002). A potential temporal offset also exists between the time of alkenone synthesis and the measurement. Thus, the alkenone temperatures could be set to the temperature of previous "bloom" conditions, rather than the currently measured water-column temperature.

In contrast to culture studies, relationships between $U^{k'}_{37}$ and temperature in suspended particulate organic carbon show much more agreement with the Prahl *et al.* (1988) calibration equation. Several large-scale compilations of water-column unsaturation ratios have been presented (Brassell, 1993; Sikes *et al.*, 1997; Conte *et al.*, in press), as well as regional studies in the North Atlantic and Mediterranean (Conte *et al.*, 1992; Conte and Eglinton, 1993; Sikes and Volkman, 1993; Ternois *et al.*, 1997; Sicre *et al.*, 2002). Data have been variously interpreted as requiring regional calibrations of growth temperature (Conte and Eglinton, 1993; Ternois *et al.*, 1997), or as requiring modifications of the original Prahl *et al.* (1988) culture-based $U^{k'}_{37}$ equation to a more appropriate relation based on water-column particulates equation (Brassell, 1993; Sikes and Volkman, 1993; Conte *et al.*, in press). The arguments favoring regional calibrations are based on regression estimates of a small number of samples, and are not yet compelling. In the case of the Black Sea, however, Freeman and Wakeham (1992) determined a water-column $U^{k'}_{37}$ that would underestimate SST by more than 5 °C. It now appears that the Black Sea represents a special case of mixing of brackish water haptophyte alkenone-producing algae with open-ocean varieties. In other cases, a regional particulate $U^{k'}_{37}$ calibration does not accurately predict surficial sediment values in the western Mediterranean Sea (Ternois *et al.*, 1998; Cacho *et al.*, 1999). This discrepancy points out the dangers of using calibrations based on limited temperature ranges and short space- and timescales to derive accurate $U^{k'}_{37}$ paleotemperature equations.

The most extensive synthesis of water-column $U^{k'}_{37}$–temperature relations argues for the global applicability of a single calibration equation (Conte *et al.*, in press; Figure 5). This study examines 392 samples from all major ocean basins, gathered in the mixed layer (0–30 m) to prevent including samples acquired in the seasonal thermocline, which might be falling from the warmer layer above. Although the data set is weighted heavily to the North Atlantic, it includes provinces dominated by *G. oceanica* as well as *E. huxleyi* (see also the recent study by Bentaleb *et al.* (2002) for additional water-column data in the *G. oceanica* province of the western equatorial Pacific), upwelling zones and gyres. Regional data sets fall nicely along a global relation, contradicting earlier interpretations (e.g., Conte and Eglinton, 1993; Ternois *et al.*, 1998), which proposed that regional $U^{k'}_{37}$–temperature equations were needed for accurate temperature estimates. The similarity of the regional data sets is striking enough for Conte *et al.* (in press) to conclude that differences in the genetic makeup of natural alkenone-synthesizing populations, and

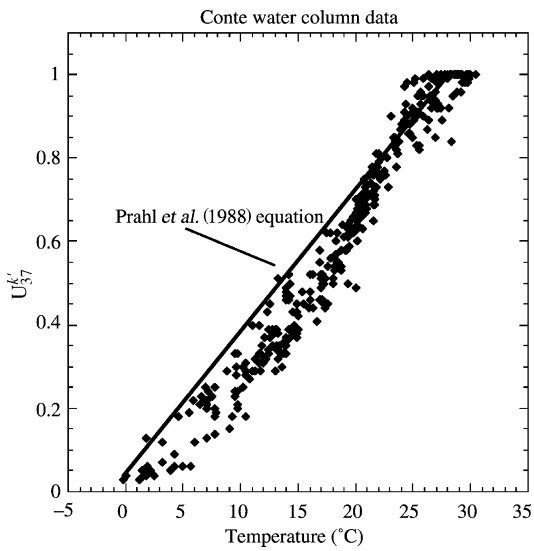

Figure 5 Compilation of the $U^{k'}_{37}$ index of mixed-layer particulates in relation to *in situ* temperature (Conte *et al.*, in press). The heavy solid line indicates the linear Prahl *et al.* (1988) paleotemperature relation used for sediment estimates.

differences in their growth environment (differing nutrient fluxes and/or water-column stability) do not significantly detract from the use of a global calibration equation for paleotemperature estimation.

In my judgment, however, Conte *et al.* (in press) overstep their data by arguing that the correct form of a global equation must be nonlinear, and that water-column calibrations conflict with sediment-based $U^{k'}_{37}$–temperature regressions. Conte *et al.* propose a third-order polynomial equation to describe the flattening of the $U^{k'}_{37}$–temperature relation near the cold and warm ends of the data set. As they note, the data suggest more variability of the index in relation to temperature at the warm and cold extremes of the surface ocean. The scatter may reflect some combination of the importance of nonthermal factors on alkenone synthesis near the extremes of temperature encountered by haptophyte algae (Conte *et al.*, in press), but it may also include analytical errors, as $C_{37:3}$ and $C_{37:2}$ alkenones approach their detection limits in warm and cold waters, respectively (cf. Grimalt *et al.*, 2001; Pelejero and Calvo, in press). In any event, the third-order polynomial fit of water-column $U^{k'}_{37}$ to *in situ* temperatures improves the r^2 value to 0.97 as compared to the r^2 value of 0.96 for a linear fit, and reduces the standard error of estimate from 1.4 °C to 1.2 °C. The slope (0.038) and intercept (−0.104) of a linear fit of water-column particulate $U^{k'}_{37}$ to *in situ* temperature may not be statistically different from the canonical Prahl *et al.* (1988) equation or its nearly identical core-top version (Muller *et al.*, 1998). If the Conte *et al.* (in press) calibration is accurate, then the authors find offsets between the temperatures derived from $U^{k'}_{37}$ analysis of core-top sediments and the mean annual temperature of the surface waters overlying the core sites. $U^{k'}_{37}$ sediment values at mid-latitudes would be systematically high compared to mean annual growth temperatures. Whether the sediment bias of 2–3 °C at mid-latitudes inferred by Conte *et al.* (in press) exists depends critically on the choice of the third-order polynomial description of the $U^{k'}_{37}$–temperature relationship, and may be premature. As discussed below, sediment-up calibrations do not favor the polynomial formulation preferred by Conte and colleagues.

6.15.6.3 Sediment Traps

Sediment trap material provides a valuable view of the $U^{k'}_{37}$ and quantity of alkenones transiting to the seafloor. Few time-series experiments have been reported to date, although data from the Gulf of California (Goni *et al.*, 2001) and off the coast of Angola (Muller and Fischer, 2001) offer reasonable resolution for 1.5 yr and 4 yr

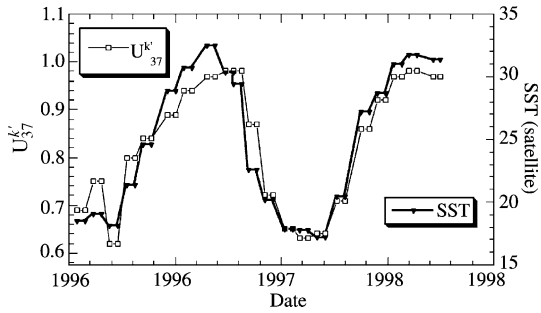

Figure 6 Comparison of Gulf of California sediment trap $U^{k'}_{37}$ time-series versus SST estimated from satellite measurements (Goni *et al.*, 2001). Note the rapid response of the $U^{k'}_{37}$index to changes in SST. The $U^{k'}_{37}$ index may not record the warmest temperatures accurately; see text for discussion.

periods, respectively. Goni *et al.* (2001) compared the $U^{k'}_{37}$ of monthly sediment collections in the Gulf of California to sea surface temperatures taken from satellite (AVHRR). Their results (Figure 6) show that the $U^{k'}_{37}$ index closely tracks changes in the satellite-derived SST, with little or no time offset. For most of the year, the temperatures estimated from the Prahl *et al.* (1988) calibration agree with SST. Somewhat lower than predicted $U^{k'}_{37}$ values were obtained during the warmest summer months (inferred SST >28 °C). These results could be rationalized by some combination of subsurface alkenone production during the summer thermal stratification, errors in the satellite SST measurements, and nonlinearity in the $U^{k'}_{37}$ index at the warm extreme of growth conditions. Muller and Fischer's time-series data from the Cap Blanc upwelling center off the coast of southwest Africa also show a strong seasonal cycle in $U^{k'}_{37}$ that is consistent with changes in SST. After removing a small temporal offset due to the sinking time of particles from the surface ocean to their sediment traps, the authors conclude that both the amplitude and absolute values of the $U^{k'}_{37}$ temperature estimates are in good agreement with weekly sea surface temperature estimates.

6.15.6.4 Core Tops

Surficial sediments should reflect the weighting function of alkenone production at all seasons and depths throughout the annual cycle—the integrated production temperature (IPT) concept of Conte *et al.* (1992). Core-top material also provides the benefit of temporal and spatial averaging of other factors, such as genetic variability and variations in growth rate that may influence alkenone systematics. This comes at costs: the time averaging varies with sedimentation rate and bioturbation, and much information

that relates to the original production of alkenones in the surface ocean is lost. Furthermore, a sediment-based regression compares surficial material, representing centuries to millennia of ocean history to the short period of instrumental temperature data used by ocean atlases such as the Levitus (1994) global climatology.

Large data sets (Herbert *et al*., 1998; Rosell-Mele *et al*., 1995b; Sonzogni *et al*., 1997) of core-top $U^{k'}_{37}$ show strong convergence with the original Prahl *et al*. (1988) temperature calibration, using mean annual surface temperature (MAST) (0–10 m) as the reference (Figure 7). A recent compilation by Muller *et al*. (1998) synthesized results of over 300 core-top analyses from the different ocean basins, determined by various laboratories. The Muller *et al*. (1998) data set encompasses the entire range of temperatures and biogeographic provinces of alkenone producers, but is biased toward continental margin sediments. Muller *et al*. noted that $U^{k'}_{37}$ in core tops also correlated highly to seasonal temperatures in the upper water column, as these covary with mean annual temperature. The correlation decreased significantly, however, if alkenone unsaturation was regressed against temperatures at 20 m and below. Sediments thus provide strong empirical evidence that alkenones synthesis occurs in the mixed layer in most areas of the ocean. Updated recently to 490 samples by P. Muller (P. Muller, personal communication), the core-top calibration of $U^{k'}_{37}$ to mean annual sea surface temperature does not differ statistically from the original Prahl *et al*. (1988) culture and water-column line. A single global, linear regression of $U^{k'}_{37}$ to MAST produces a standard error of estimate of 1.4 °C, of the same size as the Conte *et al*. (submitted) linear fit of particulate matter $U^{k'}_{37}$ to water-column measurements. A careful statistical comparison now needs to be performed to determine whether core-top and water-column regressions to temperature differ beyond the uncertainties of regression parameters.

The reproducibility of the $U^{k'}_{37}$ values in surface sediments from the same region can be quite extraordinary. Figure 8 displays two regions where our laboratory was able to obtain recent sediments from a number of box cores off the coast of California. The temperature estimates derived from $U^{k'}_{37}$ analysis not only agree closely with MAST using the Prahl/Muller equation, but they agree with each other to very nearly the analytical error.

Little support for the large range in alkenone parameters (ratios of C_{37} to C_{38} ketones, alkenones to alkenoates, etc.) observed in culture experiments comes from the sediment realm. As one example, I compared (Herbert, 2000) the frequency distribution of the ratio of total C_{37}

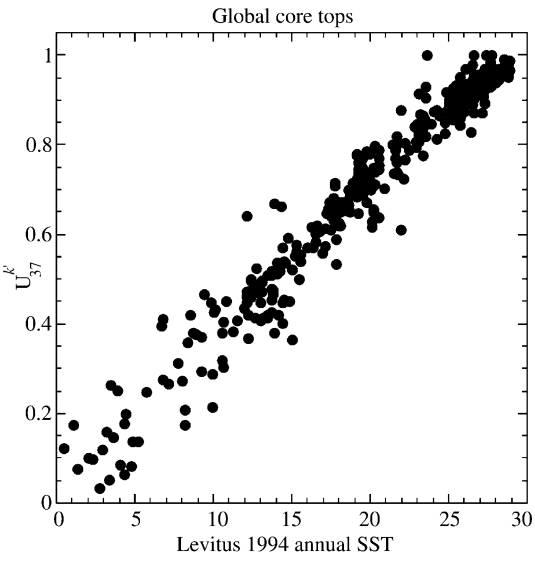

Figure 7 Global compilation of near-surface sediment $U^{k'}_{37}$ values (Muller *et al*., 1998; Muller *et al*., unpublished; Herbert, unpublished) plotted versus mean annual SST from the closest grid point of the Levitus (1994) World Ocean Atlas.

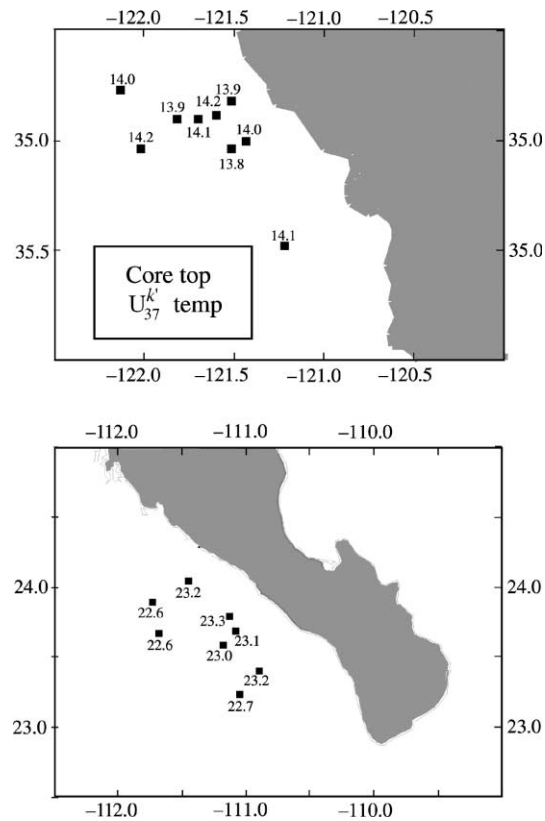

Figure 8 $U^{k'}_{37}$ temperature estimates taken from the top cm of box cores off the California Coast (Herbert *et al*., 1998). Note that the temperature estimates are consistent to nearly the analytical error of the gas chromatographic technique.

ketones ($\sum C_{37}$) to total C_{38} ketones ($\sum C_{38}$) in a core-top data set generated by our laboratory. The data set is weighted to samples along the California margin, but also includes samples from the North Atlantic, equatorial Pacific, central Pacific gyre, Peru margin, and western Pacific. The tight cluster of core-top values around a mean of just over 1.0 contrasts with the extreme heterogeneity of culture results, but is in very good agreement with the average ratio of 1.04 from a large upper water-column data set off Bermuda (Conte *et al*., 2001). The values we found are similar to the mean of ~1.2 determined by Rosell-Mele *et al*. (1994) in North Atlantic core top and by Sonzogni *et al*. (1997, 1998) in Indian Ocean sediments, and the average of ~1.15 reported by Sawada *et al*. (1996) from the Sea of Japan. Core-top data do not therefore encourage the idea that alkenone systematics can "fingerprint" regional variations in the fraction of production due to *E. huxleyi* and *G. oceanica* (cf. Volkman *et al*., 1995; Sawada *et al*., 1996).

The success of core-top temperature calibrations indicates that physiological state, genetic variability, and depth and seasonality of production play secondary roles to the control on the sedimentary $U^{k'}_{37}$ index exerted by mean annual near-surface temperature. In most cases, these factors produce errors at the level of 1.5 °C or less in the global core-top calibration. To this observer's opinion, core-top data cannot be reconciled with the large variations in the $U^{k'}_{37}$ index attributed to genetic or physiological factors by some culture studies. This does not indicate that the culture data are wrong in a technical sense, but that their results cannot always be extrapolated to the natural environment (Popp *et al*., 1998).

Core-top data sets still leave significant room for improvement in several important regards. The important question of nonlinearity at the high and low ends of the $U^{k'}_{37}$–temperature relation remains unsettled. In particular, several studies suggest that the $U^{k'}_{37}$–temperature relationship flattens at temperatures above 26 °C or 27 °C (Sikes *et al*., 1997; Sonzogni *et al*., 1997; Bentaleb *et al*., 2002). However, other studies of sediments underlying tropical waters find that the linear Prahl relationship seems to hold throughout the calibration range (Pelejero and Grimalt, 1997; Pelejero and Calvo, in press), and the global sediment compilation of Muller *et al*. (1998) provides no support for a nonlinear relationship. One would expect that calibrations on the extreme ends of the temperature range become difficult. Analytical difficulties grow as the di-unsaturated ketone becomes a minor peak at the low end of the index; similar difficulties pertain to the detection of the $C_{37:3}$ ketone in the face of chromatographic interferences in sediments under very warm ocean surface waters. In addition, it is also likely that seasonal production biases become large in high-latitude waters, emphasizing the need to combine modern-day ecological information with core-top data to better calibrate the $U^{k'}_{37}$ signal in cold waters. We also have little consensus on the temperature significance of the tetra-unsaturated C_{37} ketone. Originally included in the original $U^{k'}_{37}$ index by Brassell *et al*. (1986a), the $C_{37:4}$ ketone appears only in cold waters and in sediments underlying cold waters. Prahl *et al*. (1988) found that including the tetra-unsaturated ketone in a temperature equation did not improve the fit, and therefore omitted it from their $U^{k'}_{37}$ index. It remains to be explained why the $C_{37:4}$ ketone should be common in the high-latitude North Atlantic, where surface temperatures fall below 10 °C (Conte *et al*., 1994a; Rosell-Mele *et al*., 1994, 1995a; Rossell-Mele, 1998; Calvo *et al*., 2002; Sicre *et al*., 2002), but rare to absent in water-column particulates and sediments of the very cold waters of the Southern Ocean (Sikes and Volkman, 1993; Sikes *et al*., 1997; Ternois *et al*., 1998). Rosell-Mele and co-workers (Rosell-Mele, 1998; Rosell-Mele *et al*., 2002) propose that the presence of large amounts of the $C_{37:4}$ ketone in lipid extracts may signal low salinity waters, at least in the North Atlantic.

6.15.7 SYNTHESIS OF CALIBRATION

The resemblance of core-top alkenone unsaturation data to both mean annual SST and the original Prahl *et al*. (1988) culture calibration is a quite remarkable result that is not completely understood. As the review above suggests, the calibration of a temperature proxy for paleoenvironmental analysis involves a host of steps, ranging from the physiology and genotype of the producing organisms, their ecology, and eventually the transport and degradation of particles in the water column and sediments. In the case of the alkenone thermometer, it is comforting to note that water-column and sediment calibrations come quite close. The consistency of the sediment regression to the original Prahl *et al*. (1988) linear relation is in some sense fortuitous. Other culture studies produce results that differ as much as 5 °C from the standard Prahl *et al*. (1988) calibration, and there is no inherent reason to prefer a linear calibration of unsaturation to growth temperature to a nonlinear one. Further, we know that alkenone producers do not operate at constant rates throughout the year in most regions of the ocean, and that they do not always live in the mixed layer. One should therefore keep in mind that the Prahl *et al*. (1988) and the identical Muller *et al*. (1998) relation of $U^{k'}_{37}$ with the mean annual SST are idealizations. We can note, however, that

at least some of the caveats raised in the application of alkenone thermometry do not seem born out by sedimentary evidence. The hypothesis of Epstein *et al.* (1998) predicts that physiological factors would lead to a large offset in the $U^{k'}_{37}$ temperatures estimated from alkenones synthesized in upwelling and nonupwelling regions. Core-top data cover the oceans well enough to state that such an upwelling/nutrient bias must be no larger than the mean standard error of the entire regression (±1.4 °C), if it exists at all. Similarly, core-top data sets cover a large span in the proportions of strains of *E. huxleyi*, and in the contribution of *G. oceanica* to alkenone production, yet no statistical evidence emerges to treat the $U^{k'}_{37}$ of different oceanic biotic provinces differently.

The convergence of so much sedimentary data to a simple model must mean that an apparently fortuitous result (the good relation with mean annual SST) has an underlying predictability. One of the few efforts to quantify the consequences of seasonal variations in production and/or remineralization of alkenones is instructive. Conte *et al.* (in press) modeled the impact that such variations would have on the $U^{k'}_{37}$ in a time-averaged sediment. They found that seasonality produced only small offsets (<1 °C) from SST in the net (IPT) alkenone signal except at very high latitudes. Unless the season of the alkenone-producing bloom is restricted to the precise time of the coldest or warmest seasonal temperatures, it is not easy to cause the $U^{k'}_{37}$ delivered to sediments to depart much from the mean annual SST. This lesson was demonstrated by Sonzogni *et al.* (1997) and Muller *et al.* (1998), who used satellite chlorophyll estimates to make seasonally weighted flux estimates of alkenone production at core locations, assuming that alkenone fluxes correlate with bulk phytoplankton production. They found that the resulting flux-weighted temperature corrections to mean annual SST were negligible. It may also be that when subsurface production occurs, the temperature near the top of the seasonal thermocline is not colder by more than 1–2 °C from mean annual SST.

Alkenone production in oceanic gyres does appear to give evidence for a subsurface temperature bias. For example, Prahl *et al.* (1993), Doose *et al.* (1997), and Herbert *et al.* (1998) all report core-top $U^{k'}_{37}$ values lower than mean annual SST by 1–2 °C in gyre locations in the eastern North Pacific, consistent with subsurface fluorescence maxima (Prahl *et al.*, 1993), and maximal production during the late winter and early spring in the region. Ohkouchi *et al.* (1999) argued similarly for a subsurface gyre bias in a survey of core tops in the central North Pacific Ocean. One can therefore expect that a careful treatment of the core-top database may develop rules for how the $U^{k'}_{37}$ index will deviate systematically (~1 °C) according to distance from the nearest coastline, or some other simple proxy for gyre versus margin position. The influence of diagenesis on $U^{k'}_{37}$ values cannot be excluded, but its impact apparently ranges from negligible (most studies) to perhaps a warm bias ~1 °C (Hoefs *et al.*, 1998; Gong and Hollander, 1999).

Caution should probably be used in interpreting small down-core changes in $U^{k'}_{37}$ in high- and low-latitude regions. Here, one is in less reliable analytical territory (Grimalt *et al.*, 2001; Pelejero and Calvo, 2003), and the core-top and water-column $U^{k'}_{37}$ data can be modeled by either linear or polynomial fits (Sikes *et al.*, 1997; Sonzogni *et al.*, 1997). Even if evidence eventually conclusively supports nonlinear fits at the cold and/or warm extremes of the $U^{k'}_{37}$ range, interpreting small changes in these regions quantitatively is probably a losing game. Flattening of the $U^{k'}_{37}$ relationship with temperature would mean that the index loses sensitivity to temperature in very high and low latitudes. At the same time, the analytical error grows. One therefore needs to be wary of generating spuriously large temperature changes from $U^{k'}_{37}$ deviations of dubious reliability. As a practical limit, I suggest not interpreting $U^{k'}_{37}$ deviations quantitatively for paleotemperatures at values lower than ~0.20 or higher than ~0.96 (5 °C or 27 °C, respectively, according to the Prahl/Muller equations).

6.15.8 PALEOTEMPERATURE STUDIES USING THE ALKENONE METHOD

The rapidity and high precision of alkenone analysis makes the technique ideally suited to produce time series of past near-surface ocean temperatures. High signal-to-noise ratio can be demonstrated in a number of ways. The ocean-drilling program acquires offset holes at drilling sites to assure the continuity of the recovered sedimentary record. High-resolution analyses of offset holes that cover the same stratigraphic interval show that even small-scale changes in the $U^{k'}_{37}$ index are reproducible (Zhao *et al.*, 1993). Alkenone temperature estimates that cover the Late Holocene paint a picture of subdued SST changes, in accord with polar ice cores evidence that describes this period as quite stable in comparison to other recent intervals of Earth history. Alkenone-derived temperatures over the past 10 ka rarely deviate from modern values by more than 1–2 °C, even in very densely sampled records (e.g., Schulte *et al.*, 1999; Zhao *et al.*, 2000). In contrast to foraminiferal faunal and $\delta^{18}O$ estimates, the alkenone technique apparently has the reliability necessary to define Late Holocene cooling trends of only −0.27 °C kyr^{-1} to

$-0.15\,^{\circ}C\,kyr^{-1}$ in a coherent manner in the northeast Atlantic and Mediterranean sea (Marchal *et al*., 2002).

In the following sections, I divide alkenone paleotemperature studies roughly by the time span covered. While arbitrary to some degree, this should allow the reader to gauge the contributions of the alkenone technique to important paleoclimatic questions, which tend to be arrayed by the age and duration of Earth history studied. In addition, studies at different time resolutions will have different sets of supporting information, caveats, and questions to be addressed by future work. Nearly all of the studies cited rely on the standard Prahl *et al*. (1988) temperature scale. However, a few applications of nonstandard calibrations exist in the literature (Pelejero *et al*., 1999a; Wang *et al*., 1999; Calvo *et al*., 2002).

6.15.8.1 Holocene High-resolution Studies

Because instrumental records rarely date back more than a century, the alkenone technique may play an important role in characterizing past ocean surface temperature variability on timescales of a few years to centuries. Alkenone analyses may thus complement information derived from geochemical analyses of corals, whose usefulness in studying past El Nino cycles and other phenomena is now well established. Unlike corals, alkenone-producing organisms range over nearly the entire ocean. Only certain locations will be favorable, however, for preserving alkenone signals for high-resolution analysis. These generally occur along continental margins, where sediment flux is high. Areas along various coastlines where anoxic, or dysaerobic bottom water contacts sediments have the additional potential to resolve yearly or even seasonal variations, through the deposition of laminated sediments. Such highly productive, highly preserving settings have elevated alkenone concentrations in the sediments. Because so little material (perhaps only 100 mg) is required for a reliable $U^{k'}_{37}$ determination, very high resolution sampling becomes feasible.

Two regions of the eastern Pacific have been tested by the alkenone method for details of past El Nino (ENSO) variability. A set of early papers by Farrington *et al*. (1988) and McCaffrey *et al*. (1990) targeted the Peru upwelling zone, which experiences large surface warmings during El Nino conditions. The authors used ^{210}Pb-dated box cores to study the alkenone record of the past few centuries at three locations along the Peru margin. Samples were taken at estimated 5–10 yr intervals, with one long record extending back to ~1680 AD (McCaffrey *et al*., 1990). $U^{k'}_{37}$ temperature variations correlated in part with historical ENSO indices, but without one-to-one matches. McCaffrey *et al*. (1990) attributed the mismatches to a combination of dating uncertainties, the difficult in precisely resolving layers for sampling, and redistribution of the alkenone signal over a broader stratigraphic interval, so that ENSO anomalies are smoothed. They also noted that alkenone records may be biased away from ENSO warm events by the decline in phytoplankton production that accompanies El Nino anomalies.

Sediments from the Santa Barbara Basin off Southern California display layers that can be sampled at annual resolution. A pioneering study by Kennedy and Brassell (1992) produced annual-resolution data from the core top to an estimated basal age of 1915 AD, based on a varve chronology. The authors showed that SSTs varied by 1–2 °C on an annual basis in this time interval. Intervals of major historical El Nino-related warmings along the California Coast stood out in most cases as warm $U^{k'}_{37}$ anomalies. Our laboratory produced a slightly longer record that confirms most of the details of the Kennedy and Brassell (1992) record, although the absolute temperature estimates are offset due to interlaboratory differences. We found that the alkenone method detected 80–90% of the known El Nino warmings over the last century. We also found that most warm intervals had low alkenone abundances, which would be consistent with the historical association of decreased upwelling along the California margin during major El Nino events. Zhao *et al*. (2000) extended the Santa Barbara record to 1440 AD with approximately biannual sample resolution. They found that SST oscillated around its modern mean value of 15.5 °C with an amplitude of less than 3 °C. Their sampling recognized 5 of 12 very strong ENSO events over the period 1840–1920 for which ENSO anomalies in the equatorial Pacific have been defined. A significant trend to low SST around the turn of the twentieth century coincides with a known period of low SST along the California margin. Other approximately centennial-scale oscillations are evident in the time series as well (Zhao *et al*., 2000). Significantly, the ~500 yr record shows no linear temperature trend over time, and no dip in SST during the Little Ice Age period of the late 1500s to early 1600s. If Zhao *et al*. (2000) alkenone record accurately reflects regional SST, then the Little Ice Age cooling of the North Atlantic may not have been expressed along the west coast of North America.

It is still too early to assess how well the alkenone method will resolve variations on the ENSO timescale. Issues of chronology are significant, since a varve counting error of only a few years will produce miscorrelations between alkenone records and other historical indices of the ENSO phenomenon. It is also not clear

how reliable individual core records will be at recording SST at the annual scale. Patchiness of SST anomalies and surface productivity may impose noise on already small (1–3 °C) anomalies in mean annual SST. For ENSO-related alkenone work to progress, we will need more records gathered from the same basin, sampled with the best possible chronology. These will give us a more reliable sense of the success rate of the alkenone paleothermometer in resolving very short-lived SST variations in the late Holocene.

On somewhat longer timescales, several studies have used the alkenone index to resolve variations of SST within the Holocene (last 12 kyr). The Holocene represents an interesting mix of some of the factors that on longer timescales help to drive ice age cycles. Northern hemisphere summer insolation peaked at ~9 ka, and has declined continuously since that time as the Earth's orbital configuration shifted. The Holocene has not, however, seen any significant change in ice volume or atmospheric CO_2. A coherent long-term cooling of between 1 °C and 2 °C over the past 9–10 ka seems to have occurred in the Atlantic Ocean and the Mediterranean Sea, according to $U^{k'}_{37}$ time series (Zhao *et al.*, 1995; Bard *et al.*, 2000; Cacho *et al.*, 2001; Calvo *et al.*, 2002; Marchal *et al.*, 2002). The cooling appears amplified in some regions, such as the Mediterranean (Cacho *et al.*, 2002). In detail, the timing of peak Holocene temperatures progresses within the Mediterranean (Cacho *et al.*, 2002). Marchal *et al.* (2002) point out that the cooling trend exhibited by $U^{k'}_{37}$ in the North Atlantic is consistent with evidence for late Holocene glacial readvance in Iceland, with borehole temperature reconstructions from Greenland ice cores, and with pollen data in Europe and North America that indicate a southward migration of the cool spruce forest.

The cooling trend detected in the North Atlantic appears to be a regional, rather than global pattern. Alkenone data from the Indian Ocean (Bard *et al.*, 1997; Cayre and Bard, 1999), the South China Sea (Wang *et al.*, 1999; Kienast *et al.*, 2001; Steinke *et al.*, 2001), and the western tropical Atlantic (Ruhlemann *et al.*, 1999) in fact show very slight sea surface warming from the early Holocene toward the present. High-resolution sampling along the western margin of North America (Prahl *et al.*, 1995; Kienast and McKay, 2001; Herbert, unpublished data) shows no trend at all during the last 9 ka, although the alkenone data do suggest millennial oscillations of perhaps 1 °C amplitude. Variability within the Holocene also emerges from the Doose-Rolinski *et al.* (2001) high-resolution study of SST over the last 5 ka in the Arabian Sea. The authors sampled a high-deposition rate core at ~20 yr intervals, and measured the $\delta^{18}O$ of planktonic foraminifera in addition to alkenone unsaturation. Total variance within the 5 kyr period is ~0.6 °C (1σ), but temperature extremes of up to 3 °C are recorded (it should be noted that the authors used a nonstandard calibration whose slope would increase the estimated temperature changes by nearly 50% compared to the canonical (Prahl *et al.*, 1988 equation). Stronger than average northeast monsoon winds were inferred to result in cooler than average temperatures, with the reverse occurring when stronger south west monsoons dominated the system. Variance in SST apparently increased in the last 1,500 years, suggesting high variability of monsoonal winds during the latest Holocene in comparison to the mid-Holocene.

6.15.8.2 Millennial-scale Events of the Late Pleistocene and Last Glacial Termination

The discovery of very rapid climatic anomalies in the high-latitude North Atlantic region sparked the search for similar events in other regions. Among the prominent anomalies are the Younger Dryas event, Dansgaard–Oeschger (D/O) cycles, and Heinrich events. Pollen successions in northern Europe identified a brief interval during the last deglaciation when climate returned to very cold conditions. Spectacularly revealed in the isotopic record of Greenland ice cores (Dansgaard *et al.*, 1989; Johnsen *et al.*, 1992; Grootes *et al.*, 1993), the Younger Dryas interval lasted from ~11 ka to ~13 ka. Greenland ice cores also demonstrate a highly unstable climate during the last glacial interval (marine oxygen isotope stages 2 and 3). Isotopic changes equivalent to 6–8 °C changes in air temperature occur as rapid bursts known as the D/O cycles. These appear to be grouped in units of 3–4 cycles, which terminate in a longer period of unusually cold temperatures in Greenland. The D/O cycles can be recognized one-to-one in marine cores from the North Atlantic (Bond *et al.*, 1993). There, regionally coherent pulses of ice-rafted debris that originates from Canada, Iceland, and the Norwegian Sea, are termed Heinrich events. The most recent of these occurred during late glacial time at ~18 ka. Most authors correlate the Heinrich events with the terminations of bursts of D/O cycles (Bond and Lotti, 1995).

Regional amplitudes of the millennial-scale events, and their timing relative to the Greenland ice sheet template, constitute important pieces of the puzzle. Many theories propose that the millennial events originate from instabilities in the North Atlantic thermohaline circulation (Broecker, 1994) and propagate through the deep ocean "conveyor belt." It is also possible that the millennial-scale temperature changes originate outside the North Atlantic, and are merely well

expressed there. Millennial anomalies could also spread by means other than the thermohaline circulation. It seems likely that good regional coverage of SST anomalies may in the end provide the "fingerprints" necessary to decide which models of millennial-scale variability during glacial times are the most plausible.

Alkenone SST reconstructions in the North Atlantic and Mediterranean show the Younger Dryas, D/O cycles, and Heinrich events very clearly (Eglinton *et al*., 1992; Zhao *et al*., 1993; Rosell-Mele *et al*., 1997; Cacho *et al*., 1999, 2002; Bard *et al*., 2000; Calvo *et al*., 2001). Millennial-scale temperature changes apparently are exported from the North Atlantic by the Canary Current (Zhao *et al*., 1995; Bard *et al*., 2000) or through the atmosphere (Cacho *et al*., 2002). Recognizing that the Greenland anomalies propagate into the subtropical North Atlantic helps to explain initially puzzling features of high-resolution alkenone data taken during the glacial interval. Zhao *et al*. (1995) found that the time of maximum global ice volume (last glacial maximum (LGM), 21–23 ka) did not have the coldest SST of the glacial period off Northwest Africa. It has since become clearer that the interval of Heinrich event H2 (18 ka) produced the coldest temperatures of the late glacial period in the North Atlantic, and that this cooling is detected in numerous cores off northwest Africa (Zhao *et al*., 1995). While the LGM period saw cold SST in the subtropical North Atlantic relative to the Holocene, it was sandwiched between even colder periods paced by millennial climate instability.

The alkenone records from the Mediterranean Sea by Cacho *et al*. (1999, 2002) show some of the most spectacular evidence for how millennial events pervade the regional climate of the North Atlantic and Western Europe (Figure 9). All of the millennial features of the Greenland ice cores for the last 50 ka are immediately recognizable as large SST changes, some as rapid as 6 °C per century (Cacho *et al*., 2002). Intervals calibrated as colder than 12 °C by the $U^{k'}_{37}$ method also have pulses of the polar foraminifera *G. pachyderma* (left-coiling variety). The coldest events correspond in each case to the time of Heinrich periods of intense ice rafting in the high-latitude North Atlantic. Because the times of Heinrich events do not stand out as the coldest millennial periods in the Greenland ice core record, the SST data imply that these events may have a different spatial pattern and mode of propagation compared to the D/O anomalies. As found in cores off northwest Africa, the LGM in the Mediterranean did not have the coldest temperatures recorded during the last 50 ka. These occurred at ~16–18 ka, ~24 ka, ~30 ka, ~39 ka, and ~46 ka (Cacho *et al*., 2002).

Details of millennial variability away from the North Atlantic are still emerging. A Younger Dryas cooling occurred along the northwest margin of North America (Kienast and McKay, 2001; Seki *et al*., 2002). Its timing is identical to that of the Younger Dryas in the circum-North Atlantic region within the error of AMS ^{14}C dating. Off the coast of British Columbia, the Younger Dryas produced a cooling of ~4 °C from the Allerod–Bolling warm interval, and ended with a warming of almost 6 °C to peak Holocene temperatures at 10–11 ka (Kienast and McKay, 2001). The Younger Dryas event shows up along the central California coast in subdued form at

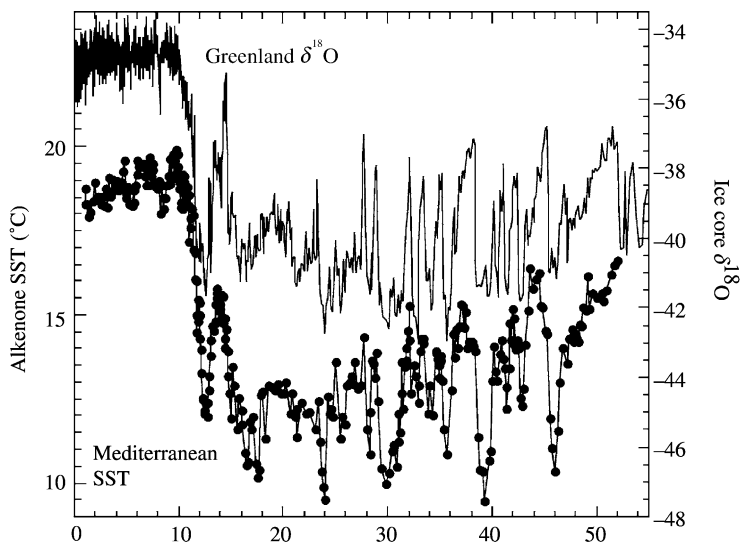

Figure 9 High resolution alkenone temperature estimates obtained by Cacho *et al*. (2002) from the Mediterranean Sea in relation to oscillations in temperature recorded by $\delta^{18}O$ in Greenland ice cores. Important millennial events (Younger Dryas = YD, H = Heinrich Event, D/O = Dansgaard/Oeschger Event) line up between the records to the precision of the independent chronologies.

ODP Site 1017 (Seki *et al*., 2002). There, the cooling appears to be ~12 °C according to $U^{k'}_{37}$ estimates. The Seki *et al*. work also demonstrates that this part of the California margin felt the effects of D/O and Heinrich perturbations on SST. Substantial (3–4 °C) temperature anomalies correlate to the Greenland D/O events. The coldest temperatures of the 80 kyr record correspond to the intervals of North Atlantic Heinrich events (Seki *et al*., 2002). In the tropics, the Younger Dryas period apparently led to small (0.5–1 °C) coolings in many locations in phase with the North Atlantic cooling. Well-dated alkenone evidence for a tropical expression of Younger Dryas cooling come from the South China Sea (Kienast *et al*., 2001; Steinke *et al*., 2001; Wang *et al*., 1999), the Indian Ocean (Bard *et al*., 1997; Cayre and Bard, 1999), and the South Atlantic (Kim *et al*., 2002). Evidence for millennial-scale variability matching the Greenland ice core record is weaker—the very highly sampled 40 kyr record of Wang *et al*. (1999) in the South China Sea does not reveal significant changes in SST corresponding to either D/O or Heinrich events, but Schulte and Müller (2001) found small SST anomalies in the Arabian Sea at the same time as the North Atlantic millennial events.

Rapid temperature changes detected by alkenone paleothermometry may actually be anti-correlated to the North Atlantic pattern in some places. This effect is in fact predicted by the conveyor belt theory for the origin of millennial variability. If the North Atlantic thermohaline circulation drives millennial cycles in temperature, then the excess or deficit of heat transported to the high-latitude North Atlantic is compensated by adjustments in the cross-equatorial heat transport from the southern hemisphere. Records from the western tropical Atlantic and from the southern hemisphere might thus show warming at the same time as the coolings observed in Greenland ice cores. Resolving this question puts a premium on good dating, since the events in question lasted only centuries to one to two millennia. Ruhlemann *et al*. (1999) produced a densely dated (by AMS 14C) record of SST from a high deposition rate core off Grenada in the western tropical Atlantic. Both $\delta^{18}O$ of the planktonic foraminifer *G. ruber* and the $U^{k'}_{37}$ index show modest warming during the Younger Dryas and Heinrich event H1 times. The authors conclude that the apparent antiphasing of western tropical and North Atlantic SST supports the thermohaline model of millennial-scale events. Mazaud *et al*. (2002) attempted a similar analysis in the Southern Indian Ocean. In their case, they used a geomagnetic intensity signal in the sediments to attempt to synchronize alkenone and paleontological estimates of SST to the Greenland ice core data over the interval 32–50 ka. Alkenone analyses suggested that oscillations of 1–2 °C did occur at millennial timescales in this region. While several cold pulses appear to coincide with North Atlantic Heinrich events, longer coolings that may correlate to clusters of D/O cycles appear anti-correlated to the North Atlantic. The evidence thus favors a model that allows for different modes of producing and/or propagating different styles of millennial change of the surface temperature field.

6.15.8.3 Marine Temperatures during the LGM

Alkenone paleothermometry arrived at a time of controversy on the spatial pattern of cooling at the LGM. New estimates of tropical cooling derived from the Sr/Ca of fossil corals challenged the results of the seminal CLIMAP effort to map surface ocean temperatures at the last Ice Age (CLIMAP, 1976, 1981) CLIMAP employed a variety of planktonic microfossil groups, principally foraminifera, to derive seasonal anomalies of LGM temperatures relative to present day. One of the most significant conclusions of the studies was the poleward amplification of glacial cooling. The tropical ocean temperatures remained very near their present values, while temperatures decreased by as much as 8–10 °C in the North Atlantic, and 4–6 °C in the high latitude Southern Ocean (CLIMAP, 1976, 1981). Coral Sr/Ca thermometry placed tropical cooling in some places at 4–6 °C (Beck *et al*., 1992; Guilderson *et al*., 1994). Noble gases in continental groundwaters also suggested more cooling at low latitudes than evident in the CLIMAP reconstruction (Stute *et al*., 1995).

The LGM is defined by the period during the last glacial cycle when ice volume reached its largest extent, at ~21–23 ka (EPILOG definition of Mix *et al*., 2001). Since the definition relates to ice volume and carries a specific chronostratigraphic value, it does not necessarily correspond to the time of coldest ocean temperatures, as demonstrated in the high-resolution studies mentioned in the previous section. As reviewed by Mix *et al*. (2001), the best criterion for defining the LGM comes from multiple bracketing AMS ^{14}C dates. Oxygen isotopic data provide the next best tool for recognizing the LGM interval. The temperatures and temperature differences I review here follow the chronostratigraphic definition of the LGM. In most cases, the LGM is defined by isotopic data, rather than radiocarbon dates. The reader should also keep in mind that the LGM temperature anomaly depends on the reference frame. One gets somewhat different numbers if one uses only the latest Holocene alkenone SST points to define the contrast to LGM temperatures, as opposed to peak Holocene temperatures, because regional cooling and/or warming has occurred in the Holocene in

many regions. All anomalies discussed here will be expressed as the differences between alkenone SST estimates at the stratigraphic level of the LGM and the latest Holocene samples, which I assume represent temperatures very close to modern day.

In this author's opinion, alkenone reconstructions favor rather decisively what might be termed a "modified CLIMAP" view of ocean surface cooling at 21 ka (Figure 10). Cases certainly occur where the $U^{k'}_{37}$ index indicates substantially more cooling at the LGM than the CLIMAP reconstruction (e.g., Jasper and Gagosian, 1989). The alkenone method typically favors more Ice Age tropical cooling than suggested by CLIMAP, but preserves the fundamental conclusion that the tropics cooled much less than did the high latitudes. In one particularly telling study, Bard and co-workers (Bard *et al.*, 1997; Sonzogni *et al.*, 1998) looked at an array of 20 cores in the Indian Ocean between 20° N and 20° S. $U^{k'}_{37}$ data showed more cooling (2–3 °C) away from the equator, but only ~1 °C cooling within 5° of the equator. Significantly, the alkenone temperature estimates weighed in with cooling in the northern Indian Ocean, where foraminiferal estimates had shown no cooling and even warming at the LGM (Bard *et al.*, 1997; Sonzogni *et al.*, 1998). The difference in results between faunal and alkenone techniques might be due to the superior signal-to-noise ratio of alkenone analysis, to the fact that foraminiferal faunas in the tropics respond to variables other than temperature, and to the observation that glacial faunas frequently have poor analogues in the modern ocean, making micropaleontological estimates more open to doubt. Other regions where the alkenone technique has been used to estimate tropical ocean temperatures at the LGM include the western equatorial Pacific (Ohkouchi *et al.*, 1994), the South China Sea (Wang *et al.*, 1999; Pelejero *et al.*, 1999a; Steinke *et al.*, 2001), and the tropical Atlantic (Zhao *et al.*, 1995; Schneider *et al.*, 1996; Sikes and Keigwin, 1994).

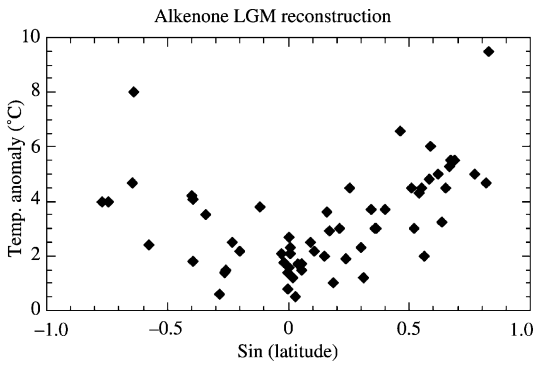

Figure 10 Compilation of all available alkenone estimates of cooling of ocean surface temperatures at the LGM relative to the late Holocene. The estimates have been projected onto the sine of latitude to approximately compensate for the distribution of ocean surface area from the equator to the poles. Note that the Ice Age anomalies are much stronger at mid and high latitudes than in the tropics. Scatter at any given latitude reflects variability in the quality of the chronological control used to assign the LGM level in alkenone time series, but also includes an important contribution from real heterogeneity of cooling at the LGM.

One should note that the impact of a few degrees of cooling in the tropical ocean is not climatically trivial. Since one-half of the Earth's surface lies between 30° of the equator, any cooling has a significant effect on the globally integrated surface cooling during the last Ice Age. It also seems likely that more $U^{k'}_{37}$ work will resolve spatial patterns of cooling that implicate dynamical adjustments of the tropical surface ocean to the changed sea level, orbital, and CO_2 boundary conditions at the LGM.

Evidence in hand already suggests that the ocean cooled differently according to region at the LGM. Although the details of how SST evolved during the last glaciation and through the glacial termination differ widely, one can distinguish two major patterns: those regions where the SST profile looks much like the oxygen isotope curve, and hence sea level and ice volume, and those in which SSTs depart significantly from the global pattern of ice volume. Many records show that SSTs ran in parallel with the ice volume cycle; e.g., in the high-latitude North Atlantic (Villanueva *et al.*, 1998; Calvo *et al.*, 2001), the South China Sea (Huang *et al.*, 1997; Pelejero *et al.*, 1999a; Steinke *et al.*, 2001), off Hawaii (Lee *et al.*, 2001), and parts of the South Atlantic (Schneider *et al.*, 1995, 1996; Kirst *et al.*, 1999; Sachs and Lehman, 2001). However, $U^{k'}_{37}$ data indicate that another common pattern was for SST to rise in advance of deglaciation. SST led ice volume temporally in the equatorial Pacific (Lyle *et al.*, 1992) and tropical Indian Ocean (Bard *et al.*, 1997). However, even within one ocean basin, there were strong regional differences in the timing of maximum cooling. Kirst *et al.* (1999) used three cores to form onshore–offshore transect along the Namibian upwelling margin in the South Atlantic. They demonstrated that both the $U^{k'}_{37}$ and the C_{37} total ketones (an index of productivity) varied systematically along the transect in the timing of maxima and minima. Warming began well before the LGM close to the African continental margin. At the same time that warming occurred, the concentration of C_{37} ketones declined steeply in the sediments. Offshore, temperatures followed ice volume closely. Kirst and colleagues ascribe the patterns they see to the impingement of warmer waters from the North along the coastal margin at the LGM, when wind systems were reorganized. The incursion of

this warmer subtropical water coincided with less favorable conditions for upwelling along the Namibian continental margin. The offshore cores stayed distant enough from the front of equatorially derived water that they do not display the early warming, and instead sense the basin-wide cooling that reached its peak at the LGM. My own laboratory has found a similar pattern off the California margin, where core locations near the present-day southern boundary of the cold California Current show only small cooling at the LGM (Herbert *et al*., 2001; Figure 11). As off Benguela, cores along the California margin some distance from the frontal boundaries display the close association between cold SST and the LGM that one would intuitively expect. Alkenone evidence thus suggests that several of the major eastern boundary current systems retracted poleward at the LGM.

A review of the current literature suggests that substantial gaps in coverage of the LGM surface ocean by the alkenone method still exist. Very few records have been obtained from the interior gyres of the major ocean basins. The sediments underlying these regions are less favorable for alkenone analysis, because they tend to have slow deposition rates and low biomarker contents due to low overlying productivity. Nevertheless, the gyres are very broad features in the modern ocean, and their thermal state at the LGM should

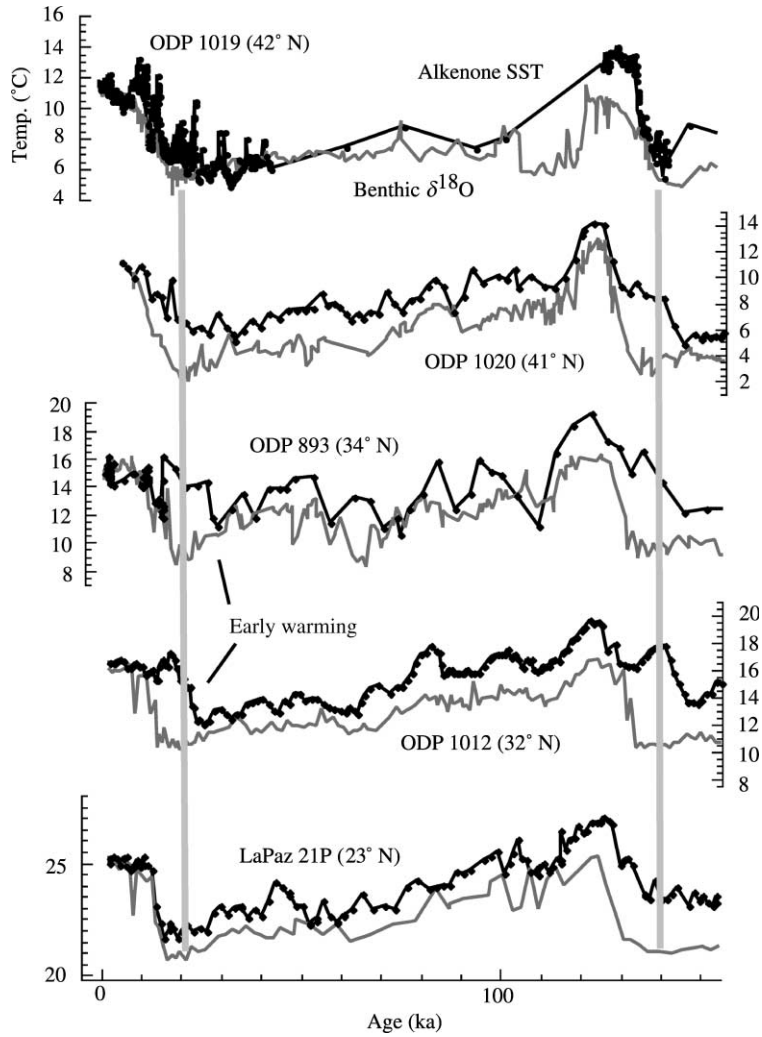

Figure 11 Regional variation in the timing of SST rise at the last two glacial terminations revealed by alkenone determinations along the California margin (Herbert *et al*., 2001). Data are arranged from north to south to demonstrate the regional nature of SST response (dark lines). Benthic δ^{18}O data acquired on the same cores (lighter color) demonstrates unequivocally that SST rose early relative to the global sea level rises at each termination at many sites. The strongest anomalies occur in the southern California borderland region, which today represents the boundary between the cold, equatorward flowing California Current, and subtropical waters that flow northward seasonally (Herbert *et al*., 2001).

not be neglected. In addition, the record of SSTs from the southern hemisphere badly lags the amount of data now available for much of the northern hemisphere. The Bard *et al.* (1997) study demonstrates nicely that SST rose in synchroneity in both hemispheres between 20° N and 20° S in the Indian Ocean beginning at ~15 ka. Such common phasing might indicate that forcing by CO_2 and/or water vapor link the surface ocean of both hemispheres during deglaciation (Bard *et al.*, 1997). More spatial coverage from other parts of the southern hemisphere is still needed. The temperature history of the warm pool of the western equatorial Pacific also awaits more investigation. However, this region is not well suited for the $U^{k'}_{37}$ proxy, as its temperature lies at or above the saturation of the $U^{k'}_{37}$ index at around 28 °C.

6.15.8.4 SST Records of the Late Pleistocene Ice Age Cycles

The rapidity and precision of alkenone analyses make them ideally suited for producing time series of the SST response to the late Pleistocene cycles in glaciation. However, legitimate questions arise about how the proxy will work on long timescales. As with all biologically based proxies, the possibility exists that the response of the alkenone unsaturation could have changed over evolutionary time. That question is sharper in the case of the $U^{k'}_{37}$ proxy, because one of the principal modern producing species, *E. huxleyi*, first appeared in the geological record during marine oxygen isotope stage 8, at ~280 ka (Thierstein *et al.*, 1977). Indeed, micropaleontological examinations show that the rise to dominance of *E. huxleyi* occurred at different times during the last glacial cycle, depending on region (Jordan *et al.*, 1996). Gephyrocapsids dominated the coccolithophorid assemblage until the Holocene in regions such as the Benguela upwelling system (Summerhayes *et al.*, 1995). Several studies that document the sequence of coccolithophorids in late Pleistocene records fail to find any indication that the proportions of alkenone-producing species affect SST reconstructions by the $U^{k'}_{37}$ method. For example, Doose-Rolinski monitored the proportions of *Gephyrocapsa* to *Emiliania* at high resolution in the late Holocene in their Arabian Sea core. High-frequency SST changes did not correspond to changes in the ratio of these species. Jordan *et al.* (1996) also failed to find a relation between reconstructed SST changes and changes in the abundance of *E. huxleyi* in a 130 kyr record from the tropical Atlantic. Other work demonstrates that the proportions of C_{37} ketones to C_{38} ketones do not vary down-core over long time periods, consistent with the evolutionary conservatism of alkenone synthesis (Muller *et al.*, 1997; Rostek *et al.*, 1997, Yamamoto *et al.*, 2000).

Alkenone paleotemperatures appear to give reliable information on orbital-scale changes in SST over the past 500 ka. The 100 kyr cycle of glaciation dominates all long alkenone SST records (Eglinton *et al.*, 1992; Emeis *et al.*, 1995a; Schneider *et al.*, 1995, 1996; Sonzogni *et al.*, 1998; Villanueva *et al.*, 1998; Herbert *et al.*, 2001). There is no indication of significant linear trends in SST over the late Pleistocene, which might warn of systematic diagenetic or evolutionary artifacts. Rather, the results of alkenone work to date show remarkably consistent patterns of SST change in relation to oxygen isotope evidence for glacial–interglacial climate state. Alkenone data suggest that a number of previous interglacial intervals have been warmer by up to 3 °C from the late Holocene. In particular, alkenone estimates for temperatures at the peak of the previous interglacial period (oxygen isotope stage 5e), fall consistently above the late Holocene. This result is consistent with the higher northern hemisphere insolation at 125 ka as compared to the Holocene, and with some evidence for sea level higher than the modern during the last interglacial period. The alkenone results contrast with the CLIMAP reconstruction for isotope stage 5e, which showed no systematic departures in SST from modern-day values (CLIMAP, 1984). The alkenone estimates of a warm stage MIS 5e are consistent, however, with the warm temperatures derived from sparse Mg/Ca data from planktonic foraminifer (Lea *et al.*, 2000; Nuernberg *et al.*, 2000). One should note, however, that the magnitude of the MIS 5e anomaly declines if it is referenced to the Holocene insolation maximum at 9 ka, because many alkenone records show 1–2 °C warming in the early Holocene compared to the modern day.

Alkenone data do show characteristic regional patterns of SST change over the 100 kyr glacial cycles of the late Pleistocene. Records from the North Atlantic tend to show the classical "saw-tooth" pattern of long decline in SST, followed by a rapid rise at glacial terminations (Villanueva *et al.*, 1998; Calvo *et al.*, 2001). Similar asymmetrical cooling and warming also appears in the higher-latitude South Atlantic (Kirst *et al.*, 1999) and South China Sea (Pelejero *et al.*, 1999a). In many places, however, the ocean reached its coldest temperatures well before maximum glaciation. Thus, records from the Indian Ocean consistently show that the coldest temperatures in that region coincided with MIS 4 (Rostek *et al.*, 1993; Emeis *et al.*, 1995a; Bard *et al.*, 1997). Our own data from off the California margin show that the early warming (relative to deglaciation) detected at the end of the last Ice

Age recurred at each of the glacial terminations for the last five glacial cycles (Herbert *et al.*, 2001). In some cases, the positive relation between colder $U^{k'}_{37}$ estimates and increased concentrations of C_{37} ketones in the sediment implicates enhanced upwelling as the cause of cold Ice Age temperatures (Kirst *et al.*, 1999). However, in many locations the pattern of coccolithophorid productivity is completely decoupled from SST, or in inverse relation to the expected increase with colder temperatures if upwelling were the cause. In these cases, the temperature changes must involve changes in ocean heat transport that occur at a larger scale than the regional changes in wind field.

The spectral content of alkenone record has only been assessed in a few records. In one noteworthy example, Schneider *et al.* (1999) provide evidence that tropical Atlantic SST has a strong imprint from the precessional (~21 kyr) cycle of insolation. Precessional variability drives contrasts in summer and winter heating, particularly at low latitudes. An expected result is that precession regulates the monsoonal cycle of the tropics. This result is consistent with the strength of precession and the weakness of obliquity (41 kyr) components in the spectra of equatorial $U^{k'}_{37}$ records. Both Schneider *et al.* (1999) and our own unpublished work off the California margin also show that the 41 kyr component in SST is larger at higher latitudes in late Pleistocene time series than it is in low-latitude records.

One puzzle that remains is the persistent evidence from alkenones that the previous glacial period (MIS 6) was not nearly as cold as the most recent glacial maximum in many locations. Relatively warm estimates for MIS 6 typically come from tropical and subtropical regions (Rostek *et al.*, 1993, 1997; Emeis *et al.*, 1995a; Schneider *et al.*, 1996; Villanueva *et al.*, 1998). However, many other tropical locations provide SST estimates as cold as the most recent cycle for the previous glacial period (Pelejero *et al.*, 1999a; Wang *et al.*, 1999; Sicre *et al.*, 2000). At high latitudes, the temperatures recorded by alkenones for MIS 6 are in line with those of the last glacial period (Schneider *et al.*, 1996; Villanueva *et al.*, 1998; Kirst *et al.*, 1999; Calvo *et al.*, 2001; Herbert *et al.*, 2001 and unpublished). Furthermore, the stage-6 warm anomaly does not repeat itself in previous glacial intervals where $U^{k'}_{37}$ analysis has been performed. There is therefore no obvious reason to dismiss the alkenone result, other than that it does not square with oxygen isotope evidence for a glacial climate as extreme as the most recent episode. If it correctly interpreted, the alkenone data would show that the tropical ocean responded in different ways to glacial maxima over the course of time.

6.15.8.5 SST before the Late Pleistocene

What is the long-term prospect for using alkenones to deduce the large-scale thermal evolution of the oceans in the Cenozoic? There is certainly enormous potential. Unlike the $\delta^{18}O$ proxy, the alkenone unsaturation index depends in theory only on temperature, and thus isolates temperature changes from other influences such as salinity and global ice volume that mingle in the $\delta^{18}O$ record of both benthic and planktonic foraminifera. And unlike micropaleontologically based methods for SST reconstruction, which rely on knowledge of the present-day preferences of extant species, the alkenone paleothermometer may range well back in time, provided that it has behaved in an evolutionarily conservative manner, and provided that diagenesis does not overprint the original SST signal. Although one would clearly prefer that the modern calibration of the $U^{k'}_{37}$ index apply accurately throughout the span of alkenone records, all is not lost if this assumption is not correct. There should still be at a minimum a role for a proxy that can unambiguously record spatial and temporal *variability* of SST in long paleoceanographic time series.

It is one of the ironies of the paleoceanographic record that alkenones are frequently more abundant in sediments before the appearance of *E. huxleyi* than they are in the period in which this coccolithophorid dominates the floral assemblage. Three studies that relate the concentrations of C_{37} ketones to the abundance of *E. huxleyi* found that the ratio of alkenones to total organic carbon actually increased in sediments older than the *E. huxleyi* acme (Muller *et al.*, 1997; Rostek *et al.*, 1997; Sicre *et al.*, 2000). Down-core profiles of alkenone concentration often increase with age, a pattern opposite to what would be expected of long-term diagenetic control on their abundance (Muller *et al.*, 1997). At the same time, time series of alkenone parameters such as the chain length ratio ($\delta C_{37}/\delta C_{37}$ ketones) show no change with time over the past few glacial cycles (Muller *et al.*, 1997; Rostek *et al.*, 1997). Our laboratory has produced longer records that also lead us to conclude that alkenones are very refractory, once incorporated into the sediment. Alkenone data from a 2.8 Myr record off the coast of Southern California (Z. Liu *et al.*, unpublished data) show higher concentrations in the older part of the record than in the late Pleistocene (Figure 3). Furthermore, there is no suggestion of a monotonic increase in SST going backward in time, as might be expected if diagenesis biased the unsaturation index. Changes in the dominant wavelength of the SST oscillations match the spectral evolution of oxygen isotopes from 41 kyr dominance in the early Pleistocene to the later rise of the 100 kyr cycle in the late Pleistocene

(cf. Ruddiman *et al*., 1986). We also note the conservatism of the chain length ratio over this 3 Myr interval.

Although reports of alkenones in sediments of Pliocene, Miocene, Oligocene, and even Eocene age are common (see Lichtfouse *et al*., 1992; Brassell, 1993; van der Smissen and Rulkotter, 1996; Rinna *et al*., 2002), the late Pliocene period provides the only example where data have been generated in enough continuity to see the evolution of SST as recorded by the $U^{k'}_{37}$ index. The alkenone method appears to resolve major cooling in both the North and South Atlantic during the onset of northern hemisphere glaciation (between ~3 Ma and ~2.5 Ma). My laboratory generated a low-resolution record (~50 kyr sampling) of alkenone temperatures from ~6 Ma to ~2.3 Ma in the subtropical North Atlantic (Herbert and Schuffert, 1998). We found warm temperatures before the period of time when sizable ice sheets grew in the northern hemisphere. Furthermore, variability was low (~1 °C). Larger-amplitude SST changes appeared at the time that northern hemisphere ice volume began to grow. The changes presumably record the onset of large, orbitally driven variations in ice volume. An even more substantial change in the pattern of SST over this critical paleoclimatic interval comes from the South Atlantic (Marlow *et al*., 2000). This study followed SST off the Benguela margin from 4.5 Ma to the present, again at 40–50 kyr resolution. According to the alkenone index, a nearly 10 °C cooling occurred between ~3 Ma and ~1.8 Ma. The authors ascribe the cooling to a long-term increase in upwelling along the Benguela margin, but acknowledge that basin-wide changes in heat transport could also be involved. Put together, the two studies of late Pliocene SST demonstrate that the alkenone proxy will play a useful role in understanding the coupling between the growing amplitude of northern hemisphere glacial–interglacial variability and ocean dynamics in the late Pliocene and early Pleistocene.

6.15.8.6 Comparison with other Proxies: $\delta^{18}O$

It should be possible to test the fidelity of alkenone SST reconstructions with an independent paleothermometer such as $\delta^{18}O$. There are a number of reasons why this comparison is not straightforward, however. First, many planktonic foraminifera live below the mixed layer for part or all of their life cycle. Comparing their isotopic temperatures with the unsaturation index of the alkenone producers, which must live in the photic zone, may not yield consistent estimates of past temperature changes. Many foraminifera have seasonal cycles of production far more pronounced than those of *E. huxleyi* and *G. oceanica*, so one may expect offsets in paleotemperatures due to seasonal biases of either foraminiferal or alkenone production. The ideal comparison of foraminiferal isotopic and coccolithophorid $U^{k'}_{37}$ estimates should therefore come from the tropics, where the seasonal amplitude in temperature is small and where some species of planktonic foraminifera spend most of their life in the mixed layer. The ideal foraminiferal species for comparison should be *G. ruber*, which contains algal photosymbionts and consistently shows mixed-layer isotopic temperatures in recent sediments. *G. ruber* dominates many tropical assemblages. It becomes rare in waters colder than ~20 °C. The next best choice should be *G. sacculifer*, also a tropical species. Isotopic depth ranking shows, however, that *G. sacculifer* may often live below the mixed layer. In addition, *G. sacculifer* adds a calcite crust during gametogenesis that apparently forms at greater depth. Its isotopic temperatures are therefore likely to be somewhat cooler than the mixed layer.

Planktonic $\delta^{18}O$ values inherently contain more uncertainty as paleothermometers than do alkenone data. The analytical signal-to-noise ratio favors the $U^{k'}_{37}$ technique by four to five times (e.g., a typical analytical uncertainty of 0.1‰ in $\delta^{18}O$ corresponds to a temperature uncertainty of 0.4–0.05 °C). Planktonic foraminiferal isotopic values also incorporate the effects of changing global ice volume and regional evaporation/precipitation on the isotopic composition of the water in which the foraminifera grow. Indeed, one of the promises of SST proxies such as the $U^{k'}_{37}$ index is to constrain temperatures so that the other components of foraminiferal $\delta^{18}O$ can be studied.

The amplitudes of temperature change at the LGM inferred by both alkenones and planktonic $\delta^{18}O$ seem largely consistent. Broecker (1986) pointed out that the magnitude of tropical sea surface cooling at the LGM was strongly constrained by the modest amount of isotopic enrichment in ice age foraminifera beyond that required by the global ice volume effect. Estimating the ice volume effect precisely has been difficult. The canonical ice volume effect of 1.2‰ comes from a sea-level/$\delta^{18}O$ calibration (Fairbanks and Matthews, 1978). More recent estimates based on pore-water deconvolution put the ice volume effect at 0.9–1‰ (Schrag *et al*., 1996). As discussed previously, alkenone SST estimates support tropical cooling of 1–2 °C in most locations. This cooling is enough to favor the recent smaller estimates for the global ice volume effect, because it would correct the typical glacial isotopic enrichment of 1–1.5‰ by several-tenths of a per mil (see Figure 12). Alternatively, one could infer a relative freshening of many tropical

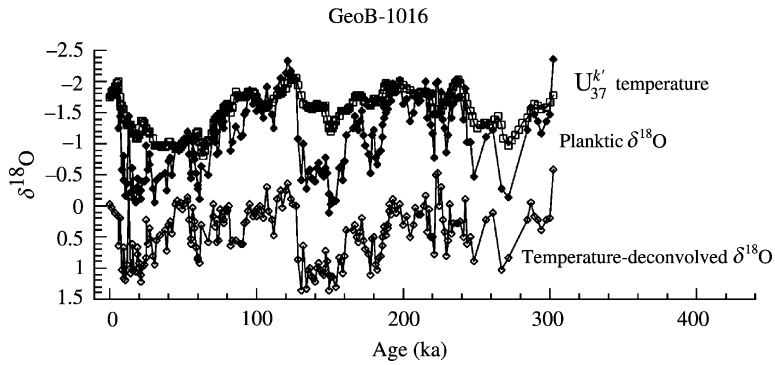

Figure 12 Alkenone data acquired with planktonic foraminiferal $\delta^{18}O$ can be used to remove the temperature effect from oxygen isotopic signals in order to assess global (ice volume) and regional (evaporation/precipitation balance) contributions to isotopic change. Data come from an equatorial Atlantic core studied by Schneider *et al.* (1996); the isotopic deconvolution was made by the present author. Note that the structure and amplitude of the temperature-corrected planktonic $\delta^{18}O$ record are consistent with current thinking on the global ice volume signal for the late Pleistocene 100 kyr cycles.

locations from the comparison of temperature and isotopic change. Pelejero *et al.* provide a regional data set of *G. ruber* isotopic values with corresponding alkenone SST estimates in the South China Sea (Pelejero *et al.*, 1999a). Cores in the northern part of the Sea display amplitudes in $\delta^{18}O$ of 1.4–1.6‰ between the late Holocene and LGM. The corresponding alkenone temperature anomalies are ~3.2–3.5 °C, equivalent to ~0.7‰ in $\delta^{18}O$ by the temperature effect. The lower latitude sites from the South China Sea produce smaller glacial–interglacial differences in $\delta^{18}O$ (1.3–1.4‰) and in $U^{k'}_{37}$ temperatures (2.3–2.6 °C). Cores collected off Hawaii yield glacial/interglacial isotopic differences from *G. ruber* of 1.1–1.3‰ and alkenone-based cooling of 2–3 °C (Lee *et al.*, 2001). However, Muller *et al.* compared isotopic and alkenone data in a tropical (11° S) core from the South Atlantic and found higher isotopic amplitude (1.9‰) accompanied by an ~3.5 °C temperature change deduced from the $U^{k'}_{37}$ index. Such evidence certainly suggests that regional changes in the $\delta^{18}O$ of seawater in the surface ocean at the LGM will have to be considered in addition to the global ice volume effect.

Several studies have in fact attempted to deduce regional changes in salinity by pairing foraminiferal $\delta^{18}O$ data with alkenone paleotemperature estimates. In a seminal paper, Rostek *et al.* (1993) subtracted the isotopic temperature effect from an Indian Ocean $\delta^{18}O$ curve obtained from *G. ruber* using the $U^{k'}_{37}$ index. Their reconstruction put salinity of the tropical Indian Ocean as 1–2 psu more saline than today, and also suggested that the salinities were fresher than modern during the previous interglacial peak at MIS 5e. Regional reconstructions of both $\delta^{18}O$ and $U^{k'}_{37}$ from the Mediterranean also appear to resolve glacial–interglacial shifts in salinity (Emeis *et al.*, 2000; Cacho *et al.*, 2001, 2002). The isotopic shift immediately outside the Mediterranean in the Gulf of Cadiz is modest (1.8‰), as is cooling (~3.5 °C). Glacial age isotopic anomalies grow progressively in the Mediterranean from 2.5‰ in the Alboran Sea to over 3‰ in the eastern Mediterranean (Emeis *et al.*, 2000; Cacho *et al.*, 2001, 2002). Much of the greater isotopic amplitude can be explained by intense surface-ocean cooling in the interior Mediterranean (5–8 °C, depending on location), away from the Atlantic connection. However, the residual isotopic enrichment within the Mediterranean indicates that this region was even more saline than today during the last glacial period, especially in the eastern basin. Another regionally coherent pattern of salinity change comes from the South China Sea (Wang *et al.*, 1999). Surface waters in this region, in contrast to the Mediterranean, apparently freshened during the LGM in comparison to the present day.

One danger, of course, for alkenone deconvolution of planktonic $\delta^{18}O$ records comes from the fact that the proxies originate from two different types of organisms. Some of the differences in amplitude and timing of the two signals may result from ecological changes, rather than changes in the $\delta^{18}O$ of the water the foraminifera grew in. Such ambiguities are present in all multiproxy paleo-environmental work; resolving them is one of the chief challenges of paleoceanography.

6.15.8.7 Comparison with other Proxies: Microfossils

CLIMAP (1976, CLIMAP, 1981) produced its reconstruction of temperatures at the LGM by using the modern-day ecological preferences of

microfossil groups to estimate past SSTs. Since the CLIMAP effort, micropaleontologists have developed new methods of reconstructing SST in addition to the transfer-function method pioneered by CLIMAP investigators. Rather different sets of glacial–interglacial temperature anomalies can result from applying different microfossil calibrations to the same data set (see Mix *et al*., 2001; Waelbroeck and Steinke, 2002). It is therefore simplistic to compare alkenone methods to a particular mode of micropaleontological reconstruction as a general test of either the geochemical or microfossil approach. Furthermore, there are relatively few cores in which the microfossil record (generally from planktonic foraminifera) has been directly compared with the $U^{k'}_{37}$ measurements. Experience shows that spatially sparse data sets can often produce apparent conflicts at the LGM that come simply from extrapolating results from one proxy over too great a distance (Broccoli and Marciniak, 1996).

Temperature estimates produced by alkenone and foraminiferal assemblage methods generally agree quite well for the Holocene (but see Marchal *et al*. (2002) for some discrepancies in the North Atlantic and Mediterranean). Alkenone temperatures usually fall in between the warm and cold season estimates of foraminifera (Chapman *et al*., 1996; Wang *et al*., 1999; Perez-Folgado *et al*., 2003). Since both methods are in some sense optimized for late Holocene conditions, this is perhaps not surprising. Estimates of SST at the LGM more commonly diverge (Chapman *et al*., 1996; Huang *et al*., 1997; Perez-Folgado *et al*., 2003). It is not evident how to reconcile changes in the $U^{k'}_{37}$ index relative to seasonal SST estimates derived from foraminiferal faunas. In one of the best-studied examples, Chapman *et al*. (1996) found that $U^{k'}_{37}$ estimates for glacial temperatures followed summer temperatures estimated from planktonic foraminifera at a subtropical north Atlantic site. Chapman *et al*. (1996) argued that the alkenone producers must have changed their season of production from late winter and spring (present-day) to summer during glacial and early Holocene times. This ecological switch, according to the authors, explains why the alkenone thermometer would underestimate glacial SST cooling at the study location. Chapman *et al*. (1996) do note that the temperatures inferred from alkenones match the isotopic temperatures derived from the planktonic foraminifer *G. bulloides* very well. Precisely the opposite temporal dichotomy between $U^{k'}_{37}$ and foraminiferal estimates was obtained from the South China Sea, where glacial alkenone temperatures are consistently colder than the cold season foraminiferal estimate (Huang *et al*., 1997).

As noted earlier, most alkenone estimates from the tropics support more cooling than inferred by CLIMAP (see Bard *et al*., 1997; Sonzogni *et al*., 1998; Pelejero *et al*., 1999; Lee *et al*., 2001). It is not clear if the differences are larger than overlap of the standard error of the techniques. In most cases, the alkenone method has a clear advantage in signal-noise for resolving smaller temperature changes (see, e.g., Lee *et al*., 2001).

6.15.8.8 Comparison with other Proxies: Mg/Ca

As with the $U^{k'}_{37}$ proxy, Mg/Ca measurements in foraminiferal calcite may yield paleotemperature measurements without the ambiguities of $\delta^{18}O$ or micropaleontological assemblage analyses. In contrast to the alkenone proxy, preservation markedly affects the Mg/Ca ratio in foraminiferal shells, and hence the paleotemperature estimate (Brown and Elderfield, 1996; Lea *et al*., 1999, 2000; Rosenthal *et al*., 2000). The alkenone temperature proxy may also have the advantage in several other aspects. Synthesis of alkenones is tied to the photic zone, unlike that of foraminiferal calcite. The signal-to-noise ratio of alkenone measurements is superior for the paleotemperature range 5–25 °C, where the exponential dependence of Mg/Ca results in a relatively low temperature sensitivity (Lea *et al*., 1999, 2000; Elderfield and Ganssen, 2000). At higher temperatures, the Mg/Ca proxy may become superior because of the same exponential sensitivity to temperature. Furthermore, the Mg/Ca proxy should not lose sensitivity to temperature at the warm end of ocean temperatures, unlike the alkenone proxy. The Mg/Ca proxy should therefore be the tool of choice in determining past changes in SST in warm pool regions of the ocean.

Two direct comparisons of $U^{k'}_{37}$ and Mg/Ca estimates of glacial–interglacial SST changes come from the tropical Atlantic. Elderfield and Ganssen (2000) compared the Mg/Ca and $\delta^{18}O$ of 5 species of planktonic foraminifera at core site BOFS31K, the same core analyzed by Chapman *et al*. (1996) for foraminiferal SST estimates. Elderfield and Ganssen (2000) refer to Mg/Ca temperatures as "calcification temperatures" to account for the observation that many planktonic foraminifera calcify significantly below the mixed layer. Mg/Ca data produced two down-core clusters of species: a cold group (*G. inflata, N. pachyderma*, and *G. menardii*) and a warm group with Mg/Ca temperatures consistently 3–3.5 °C warmer (*G. ruber* and *G. bulloides*). Core-top temperatures estimated from the warm group fell ~2 °C colder than modern SST, while the alkenone estimate falls right at mean annual modern SST (Elderfield and Ganssen, 2000). Temperature changes estimated from *G. ruber* track alkenone temperatures very closely, while maintaining the ~2 °C offset toward colder temperatures. Mg/Ca measurements on *G. bulloides*

show almost no cooling for most of the glacial period. Elderfield and Ganssen conclude that the foraminiferal Mg/Ca temperature estimates at the LGM follow the alkenone estimate (~2 °C) more closely than the foraminiferal transfer function estimate (cooling of ~5 °C). Their work also hints at the ecological uncertainties that enter into interpreting temperature records from different planktonic organisms that may have had diverging depth and seasonal habitats over the course of glacial to interglacial climate change.

Nuernberg *et al*. (2000) compared the Mg/Ca and alkenone approaches over three glacial–interglacial cycles at a cores at 1° S in the central South Atlantic. The foraminifer used was *G. sacculifer*. Core-top temperature estimates differed by ~2 °C. Once again, the Mg/Ca estimate fell consistently cooler than the alkenone record down-core. In most cases, the temperature curves were offset by 2–3 °C. Occasionally, as at the last glacial termination, the two temperature profiles coincided. The authors noted strong qualitative similarities in the two paleotemperature data sets. Both gave similar cooling at the LGM (3.5 °C for the $U^{k'}_{37}$ index, 3.4 °C for Mg/Ca), a warmer-than-Holocene stage 5e, and a warmer previous glacial cycle than the last glacial interval. Both geochemical proxies gave smaller SST changes at the LGM than planktonic foraminiferal transfer function estimates, which gave 9 °C cooling during the cold season and 5 °C cooling for the warm season. They also agreed on the greater warmth of MIS 5e, while the foraminiferal transfer function did not. But the correlation coefficients for the Mg/Ca and $U^{k'}_{37}$ proxies were not strong: 0.49 over the 270 kyr record, and 0.78 over the last 90 ka (Nuernberg *et al*., 2000).

6.15.9 CONCLUSIONS

This review paints an optimistic picture of the ability of alkenone unsaturation indices recorded in sediments to capture past SST change on a wide variety of timescales. I believe this optimism is justified on a number of grounds. First, the analytical precision of the estimate is outstanding. One can anticipate that interlaboratory differences will diminish over time as a result of intercalibration experiments (e.g., Rosell-Mele *et al*., 2001) and the maturation of analytical protocols. The precision of alkenone analyses is meaningful, in the sense that core-top sediments from the same region yield very similar values for $U^{k'}_{37}$, and very similar down-core estimates of cooling at time horizons such as the LGM. Unlike the SST proxies derived from foraminifera, the alkenone index survives extensive degradation in the water columns and sediments. And, it seems unlikely that the calibration of alkenone unsaturation to growth temperature will change with additional data.

The relationship observed in sediments closely mimics the relation measured between unsaturation in photic zone particulates (Conte *et al*. in press) and *in situ* temperature. We should note, however, that the calibration of sedimentary $U^{k'}_{37}$ to mean annual SST represents a statistical relationship and should not be interpreted in too simplistic a manner. We have seen above that this relation holds for sediments because alkenone synthesis generally occurs in the mixed layer, and because alkenone production by selected haptophyte algae is less seasonal than many other planktonic groups. Furthermore, temperatures during the season of maximal alkenone production generally come close to mean annual SST. The index, therefore, is a quite robust *proxy* for mean annual temperature. It should be kept in mind that regional variations in the factors that control the depth and seasonality of alkenone production can cause the index to deviate from mean annual SST.

As is the case for many other paleotemperature proxies, uncertainties grow at the extreme ends of the temperature range sampled by the $U^{k'}_{37}$ index. These come in part from analytical problems, and in part from the lack of a theoretical basis for preferring a linear or curvilinear calibration at very cold and warm temperatures. The behavior of alkenones as fine-grained particles may cause more significant problems for the proxy than does the calibration uncertainty. Recent evidence for advection of alkenones by deep currents (Benthien and Müller, 2000; Ohkouchi *et al*., 2002), suggests that paleoceanographers ignore sedimentology at their peril. In particular, the spectacular evidence from $U^{k'}_{37}$ for rapid SST changes in some drift sediments (Sachs and Lehman, 1999) may need to be reinterpreted as a signal of pulses of input from high latitudes. New tools such as ^{14}C AMS dating of alkenones will lead us to a clearer picture of which sedimentary environments are the most favorable for applying the $U^{k'}_{37}$ index as a measure of past SST. The comforting news is that the very high correlation between sediment core-top $U^{k'}_{37}$ and mean annual SST indicates that advection cannot be a pervasive problem.

Alkenone paleotemperature estimates have already weighed in significantly on the controversy of tropical SST at the LGM. The "modified CLIMAP" view they support seems consistent with tropical cooling of 2–3 °C estimated from Mg/Ca of planktonic foraminifera (Lea *et al*., 2000; Nuernberg *et al*., 2000; Stott *et al*., 2002; Visser *et al*., 2003). SST change over deeper timescales awaits more investigation by the alkenone method. All indications point to the diagenetic stability of alkenones over millions of years. The long evolutionary history and apparent

conservatism of alkenone synthesis suggest that the proxy will play a useful role in solving major paleoclimatic questions over most of the Cenozoic.

REFERENCES

Aksnes D. L., Egge J. K., Rosland R., and Heimdal B. R. (1994) Representation of *Emiliania-huxleyi* in phytoplankton simulation-models—a 1st approach. *Sarsia* **79**, 291–300.

Andruleit H. (1997) Coccolithophore fluxes in the Norwegian-Greenland sea: seasonality and assemblage alterations. *Mar. Micropaleontol.* **31**, 45–64.

Andruleit H., von Rad U., Bruns A., and Ittekkot V. (2000) Coccolithophore fluxes from sediment traps in the northeastern Arabian sea off Pakistan. *Mar. Micropaleontol.* **38**, 285–308.

Antia A. N., Maaßen J., Herman P., Voß M., Scholten J., Groom S., and Miller P. (2001) Spatial and temporal variability of particle flux at the NW European continental margin. *Deep-Sea Res. II* **48**, 3083–3106.

Balch W. M., Holligan P. M., and Kilpatrick K. A. (1992) Calcification, photosynthesis and growth of the bloom-forming coccolithophore, *Emiliania huxleyi*. *Cont. Shelf Res.* **12**, 1353–1374.

Bard E., Rostek F., and Sonzogni C. (1997) Interhemispheric synchrony of the last deglaciation inferred from alkenone paleothermometry. *Nature* **385**, 707–710.

Bard E., Rostek F., Turon J.-L., and Gendreau S. (2000) Hydrological impact of Heinrich events in the subtropical northeast Atlantic. *Science* **289**, 1321–1324.

Beaufort L. and Heussner S. (1999) Coccolithophorids on the continental slope of the Bay of Biscay production, transport and contribution to mass fluxes. *Deep-Sea Res. II* **46**, 2147–2174.

Beaufort L. and Heussner S. (2001) Seasonal dynamics of calcareous nannoplankton on a West European continental margin: the Bay of Biscay. *Mar. Micropaleontol.* **43**, 27–55.

Beck J. W., Edwards R. L., Ito E., Taylor F. W., Recy J., Rougerie F., Joannot P., and Henin C. (1992) Sea-surface temperature from coral skeletal Strontium–Calcium ratios. *Science* **257**, 644–646.

Bell M. V. and Pond D. (1996) Lipid composition during growth of motile and coccolith forms of *Emiliania huxleyi*. *Phytochemistry* **41**, 465–471.

Bentaleb I., Grimalt J. O., Vidussi F., Marty J.-C., Martin V., Denis M., Hatte C., and Fontugne M. (1999) The C_{37} alkenone record of seawater temperatures during seasonal thermocline stratification. *Mar. Chem.* **64**, 301–313.

Bentaleb I., Fontugne M., and Beaufort L. (2002) Long-chain alkenones and $U^{k'}_{37}$ variability along a south–north transect in the western Pacific Ocean. *Global Planet. Change* **34**, 173–183.

Benthien A. and Müller P. J. (2000) Anomalously low alkenone temperatures caused by lateral particle and sediment transport in the Malvinas current region, western Argentine basin. *Deep-Sea Res. I* **47**, 2369–2393.

Bollman J. (1997) Morphology and biogeography of *Gephyrocapsa* coccoliths in Holocene sediments. *Mar. Micropaleontol.* **29**, 319–350.

Bond G. C. and Lotti R. (1995) Iceberg discharges into the North Atlantic on millennial timescales during the last glaciation. *Science* **267**, 1005–1010.

Bond G. C., Broecker W. S., Johnsen S., McManus J., Labeyrie L., Jouzel J., and Bonani G. (1993) Correlations between climate records from North Atlantic sediments and Greenland ice. *Nature* **366**, 552–554.

Boon J. J., van der Meer F. W., Schuyl P. J., de Leeuw J. W., Schenck P. A., and Burlingame A. L. (1978) *Organic Geochemical Analyses of Core Samples from Site 362, Walvis Ridge*. DSDP Leg 40, Initial Reports. DSDP Legs 38, 39, 40, and 41, Suppl., pp. 627–637.

Brand L. E. (1982) Genetic variability and spatial patterns of genetic differentiation in the reproductive rates of the marine coccolithophores *Emiliania huxleyi* and *Gephyrocapsa oceanica*. *Limmnol. Oceanogr.* **27**, 236–245.

Brand L. E. (1984) The salinity tolerance of forty-six marine phytoplankton isolates. *Estuar. Coast. Shelf Sci.* **18**, 543–556.

Brand L. E. (1991) Minimum iron requirements of marine phytoplankton and the implications for the biogeochemical control of new production. *Limnol. Oceanogr.* **36**, 1756–1771.

Brand L. E. (1994) Physiological ecology of marine coccolithophores. In *Coccolithophores* (eds. A. Winter and W. G. Siesser). Cambridge University Press, Cambridge, UK, pp. 39–49.

Brand L. E. and Guillard R. R. L. (1981) The effects of continuous light and light intensity on the reproduction rates of twenty-two species of marine phytoplankton. *J. Exp. Mar. Biol. Ecol.* **50**, 119–132.

Brassell S. C. (1993) Applications of biomarkers for delineating marine paleoclimate fluctuations during the Quaternary. In *Organic Geochemistry* (eds. M. H. Engel and S. A. Macko). Plenum, New York, pp. 669–738.

Brassell S. C., Eglinton G., Marlowe I. T., Pflaumann U., and Sarnthein M. (1986a) Molecular stratigraphy: a new tool for climatic assessment. *Nature* **320**, 129–133.

Brassell S. C., Brereton R. G., Eglinton G., Grimalt J. O., Liebezeit G., Marlowe I. T., Pflaumann U., and Sarnthein M. (1986b) Palaeoclimatic signals recognized by chemometric treatment of molecular stratigraphic data. *Org. Geochem.* **10**, 649–660.

Brassell S. C., Eglinton G., and Howell V. J. (1987) Palaeoenvironmental assessment for marine organic-rich sediments using molecular organic geochemistry. In *Marine Petroleum Source Rocks* (eds. A. J. Fleet and J. Brooks). Blackwell, London, pp. 79–98.

Broccoli A. J. and Marciniak E. P. (1996) Comparing simulated glacial climate and paleodata: a reexamination. *Paleoceanography* **11**, 3–14.

Broecker W. S. (1986) Oxygen isotope constraints on surface ocean temperatures. *Quat. Res.* **26**, 121–134.

Broecker W. S. (1994) Massive iceberg discharges as triggers for global climate change. *Nature* **372**, 421–424.

Broerse A. T. C., Ziveri P., and Honjo S. (2000a) Coccolithophore ($CaCO_3$) flux in the Sea of Okhotsk: seasonality, settling and alteration processes. *Mar. Micropaleontol.* **39**, 179–200.

Broerse A. T. C., Ziveri P., Van Hinte J. E., and Honjo S. (2000b) Coccolithophore export production, species composition, and coccolith-$CaCO_3$ fluxes in the NE Atlantic (34°N 21°W and 48°N 21°W). *Deep-Sea Res. II* **47**, 1877–1905.

Broerse A. T. C., Brummer G.-J. A., and Van Hinte J. E. (2000c) Coccolithophore export production in response to monsoonal upwelling off Somalia (northwestern Indian ocean). *Deep-Sea Res. II* **47**, 2179–2205.

Brown S. and Elderfield H. (1996) Variations in Mg/Ca and Sr/Ca ratios of planktonic foraminifera caused by post-depositional dissolution-evidence of shallow Mg-dependent dissolution. *Paleoceanography* **11**, 543–551.

Brown C. W. and Yoder J. A. (1994) Coccolithophorid blooms in the global ocean. *J. Geophys. Res.* **99**(C), 7467–7482.

Bukry D. (1974) Coccoliths as paleosalinity indicators-evidence from the Black sea. In *The Black Sea, its Geology, Chemistry and Geology* (eds. E. T. Degens and D. A. Ross). Am. Assoc. Petrol. Geol. Mem., Tulsa, OK, vol. 20, pp. 33–363.

Cacho I., Pelejero C., Grimalt J. O., Calfat A. M., and Canals M. (1999) C37 alkenone measurements of sea surface temperature in the Gulf of Lions (NW Mediterranean). *Org. Geochem.* **30**, 557–566.

Cacho I., Grimalt J. O., Canals M., Sbaffi L., Shackleton N. J., Schonfeld J., and Zahn R. (2001) Variability of the western Mediterranean sea surface temperature during the last 25, 000 years and its connection with the Northern Hemisphere climatic changes. *Paleoceanography* **16**, 40–52.

Cacho I., Grimalt J. O., and Canals M. (2002) Response of the western Mediterranean Sea to rapid climatic variability during the last 50,000 years: a molecular biomarker approach. *J. Mar. Sys.* **33–34**(C), 253–272.

Cadee G. C. (1985) Macroaggregates of *Emiliania huxleyi* in sediment traps. *Mar. Ecol. Prog. Ser.* **24**, 193–196.

Calvo E., Villanueva J., Grimalt J. O., Boelaert A., and Labeyrie L. (2001) New insights into the glacial latitudinal temperature gradients in the North Atlantic: results from $U^{k'}_{37}$ sea surface temperatures and terrigenous inputs. *Earth Planet. Sci. Lett.* **188**, 509–519.

Calvo E., Grimalt J., and Jansen E. (2002) High resolution U^{k}_{37} sea surface temperature reconstruction in the Norwegian Sea during the Holocene. *Quat. Sci. Rev.* **21**, 1385–1394.

Cayre O. and Bard E. (1999) Planktonic foraminiferal and alkenone records of the last deglaciation from the eastern Arabian Sea. *Quat. Res.* **52**, 337–342.

Chaler R., Grimalt J. O., Pelejero C., and Calvo E. (2000) Sensitivity effects in $U^{k'}_{37}$ paleotemperature estimation by chemical ionization mass spectrometry. *Anal. Chem.* **72**, 5892–5897.

Chapman M. R., Shackleton N. J., Zhao M., and Eglinton G. (1996) Faunal and alkenone reconstructions of subtropical North Atlantic surface hydrography and paleotemperature over the last 28 kyr. *Paleoceanography* **11**, 343–357.

CLIMAP (1976) The surface of the Ice-age earth. *Science* **191**, 1131–1137.

CLIMAP project members (1981) Seasonal reconstruction of the Earth's surface at the last glacial maximum GSA map and chart series MC-36. Geol. Soc. Amer., Boulder CO.

CLIMAP (1984) The last interglacial ocean. *Quat. Res.* **21**, 123–224.

Conte M., Volkman J. K., and Eglinton G. (1994a) Lipid biomarkers of the Haptophyta. In *The Haptophyte Algae* (eds. J. C. Green and B. S. C. Leadbeater). Clarendon Press, Oxford, pp. 351–377.

Conte M. H. and Eglinton G. (1993) Alkenone and alkenoate distributions within the euphotic zone of the eastern North Atlantic: correlation with production temperature. *Deep-Sea Res.* **40**, 1935–1961.

Conte M. H., Eglinton G., and Madureira L. A. S. (1992) Long-chain alkenones and alkyl alkenoates as palaeotemperature indicators: their production, flux, and early sedimentary diagenesis in the eastern North Atlantic. *Org. Geochem.* **19**, 287–298.

Conte M. H., Thompson A., and Eglinton G. (1994) Primary production of lipid biomarker compounds by *Emiliania huxleyi*: results from an experimental mesocosm study in fjords of southern Norway. *Sarsia* **79**, 319–332.

Conte M. H., Thompson A., Eglinton G., and Green J. C. (1995) Lipid biomarker diversity in the coccolithophorid *Emiliania huxleyi* (Prymniesiophyceae) and the related species *Gephyrocapsa oceanica*. *J. Phycol.* **31**, 272–282.

Conte M. H., Thompson A., Lesley D., and Harris R. P. (1998a) Genetic and physiological influences on the alkenone/alkenoate versus growth temperature relationship in *Emiliania huxleyi* and *Gephyrocapsa oceanica*. *Geochim. Cosmochim. Acta* **62**, 51–68.

Conte M. H., Weber J. C., and Ralph N. (1998b) Episodic particle flux in the deep Sargasso Sea an organic geochemical assessment. *Deep-Sea Res. I.: Ocean. Res.* **45**, 1819–1841.

Conte M. H., Weber J. C., King L. L., and Wakeham S. G. (2001) The alkenone temperature signal in the western North Atlantic surface waters. *Geochim. Cosmochim. Acta* **65**, 4275–4287.

Conte M. H., Sicre M. A., Weber J. C., and Shultz-Bull D. (xxxx) The global temperature calibration of the alkenone unsaturation index ($U^{k'}_{37}$) in surface waters and a comparison of the alkenone production temperature recorded by $U^{k'}_{37}$ in sediments with overlying sea surface temperature. *Paleoceanography* (in press).

Cortés M. Y., Bollmann J., and Thierstein H. R. (2001) Coccolithophore ecology at the HOT station ALOHA, Hawaii. *Deep-Sea Res. II* **48**, 1957–1981.

Cranwell P. A. (1985) Long-chain unsaturated ketones in recent lacustrine sediments. *Geochim. Cosmochim. Acta* **49**, 1545–1551.

Dansgaard W., White J. W. C., and Johnsen S. J. (1989) The abrupt termination of the Younger Dryas climate event. *Nature* **339**, 532–534.

De Leeuw J. W., Meer F. W. V. D., Rijpstra W. I. C., and Schencck P. A. (1980) On the occurrence and structural identification of long chain unsaturated ketones and hydrocarbons in sediments. In *Advances in Organic Geochemistry, 1979*, Phys. Chem. Earth, vol. 12 (eds. A. G. Douglas and J. R. Maxwell). Pergamon, Oxford, 211–217.

Doose H., Prahl F. G., and Lyle M. W. (1997) Biomarker temperature estimates from modern and last glacial surface waters of the California current system between 33° and 42° N. *Paleoceanography* **12**, 615–622.

Doose-Rolinski H., Rogalla U., Scheeder G., Luckge A., and von Rad U. (2001) High-resolution temperature and evaporation changes during the late Holocene in the northeastern Arabian Sea. *Paleoceanography* **16**, 358–367.

Edvardsen B., Eikrem W., Green J. C., Andersen R. A., Moon-van der Staay S. Y., and Medlin L. K. (2000) Phylogenetic reconstructions of the Haptophyta inferred from 18S ribosomal DNA sequences and available morphological data. *Phycologia* **39**, 19–35.

Eglinton G., Bradshaw S. A., Rosell A., Sarnthein M., Pflaumann U., and Tiedemann R. (1992) Molecular record of secular sea surface temperature changes on 100-year timescales for glacial terminations I, II, and IV. *Nature* **356**, 423–426.

Elderfield H. and Ganssen G. (2000) Past temperature and $\delta^{18}O$ of surface ocean waters inferred from foraminiferal Mg/Ca ratios. *Nature* **405**, 442–445.

Emeis K.-C., Anderson D. M., Doose H., Kroon D., and Schulz-Bull D. (1995a) Sea-surface temperatures and the history of monsoon upwelling in the northwest Arabian Sea during the last 500,000 years. *Quat. Res.* **43**, 355–361.

Emeis K.-C., Doose H., Mix A., and Schulz-Bull D. (1995b) Alkenone sea-surface temperatures and carbon burial at Site 846 (eastern equatorial Pacific Ocean): the last 1.3 MY. *Sci. Res. ODP* **138**, 605–613.

Emeis K.-C., Struck U., Schulz H.-M., Rosenberg R., Bernasconi S., Erlenkeuser H., Sakamoto T., and Martinez-Ruiz F. (2000) Temperature and salinity variations of Mediterranean Sea surface waters over the last 16,000 years from records of planktonic stable isotopes and alkenone unsaturation ratios. *Palaeogeogr. Paleaoeclimatol. Palaeoecol.* **158**, 259–280.

Epstein B., D'Hondt S., Quinn J. G., Zhang J., and Hargraves P. E. (1998) An effect of dissolved nutrient concentrations on alkenone-based temperature estimates. *Paleoceanography* **13**, 122–126.

Epstein B. L., D'Hondt S., and Hargraves P. E. (2001) The possible metabolic role of C37 alkenones in *Emiliania huxleyi*. *Org. Geochem.* **32**, 867–875.

Fairbanks R. G. and Matthews R. K. (1978) The marine oxygen isotopic record in Pleistocene coral, Barbados, West Indies. *Quat. Res.* **10**, 181–196.

Farrimond P. G., Eglinton P. G., and Brassell S. C. (1986) Alkenones in cretaceous black shales, Blake-Bahama basin, western North Atlantic. In *Advances in Organic Geochemistry 1985* (eds. D. Leytaheuser and J. Rullkotter). Pergamon, Oxford, vol. 10, pp. 897–903.

Farrington J. W., Davis A. C., Sulanowski J., McCaffrey M. A., McCarthy M., Clifford C. H., Dickinson D., and Volkman J. K. (1988) Biogeochemistry of lipids in surface sediments

of the Peru upwelling area at 15° S. *Org. Geochem.* **19**, 277–285.

Ficken K. J. and Farrimond P. (1995) Sedimentary lipid geochemistry of Framvaren: impacts of a changing environment. *Mar. Chem.* **51**, 31–43.

Fisher N. S. and Honjo S. (1989) Interspecific differences in temperature and salinity responses in the coccolithophore *Emiliania huxleyi*. *Biol. Oceanogr.* **6**, 355–361.

Freeman K. H. and Wakeham S. G. (1992) Variation in the distribution and isotopic composition of alkenones in Black Sea particles and sediments. *Org. Geochem.* **19**, 277–285.

Fujiwara S., Tsuzuki M., Kawchi M., Minaka N., and Inouye I. (2001) Molecular phylogeny of the Haptophyta based on the *rbc* L gene and sequence variation in the spacer region of the rubisco operon. *J. Phycol.* **37**, 121–129.

Giraudeau J., Monteiro M. S., and Nikodemus K. (1993) Distribution and malformation of living coccolithophores in the northern Benguela upwelling system off Namibia. *Mar. Micropaleontol.* **22**, 93–110.

Gong C. and Hollander D. J. (1999) Evidence for differential degradation of alkenones under contrasting bottom water oxygen conditions: implication for paleotemperature reconstruction. *Geochim. Cosmochim. Acta* **63**, 405–411.

Goni M. A., Hartz D. M., Thunell R. C., and Tappa E. (2001) Oceanographic considerations in the application of the alkenone-based paleotemperature $U^{k'}_{37}$ index in the Gulf of California. *Geochim. Cosmochim. Acta* **65**, 545–557.

Grice K., Klein Breteler W. C. M., Schoten S., Grossi V., de Leeuw J. W., and Sinninge Damste J. S. (1998) Effects of zooplankton herbivory on biomarker proxy records. *Paleoceanography* **13**, 686–693.

Grimalt J. O., Rulkotter J., Sicre M.-A., Summons R., Farrington J., Harvey H. R., Goni M., and Sawada K. (2000) Modifications of the C_{37} alkenone and alkenoate composition in the water column and sediment: possible implications for sea surface temperature estimates in Paleoceanography. *Geochem. Geophys. Geosys. 1* (paper number 2000GC000053).

Grimalt J. O., Calvo E., and Pelejero C. (2001) Sea surface paleotemperature errors in $U^{k'}_{37}$ estimation due to alkenone measurements near the limit of detection. *Paleoceanography* **16**, 226–232.

Grootes P. M., Stuiver M., White J. W. C., Johnsen S., and Jouzel J. (1993) Comparison of oxygen isotope records from the GISP2 and GRIP Greenland ice cores. *Nature* **366**, 552–554.

Grossi V., Rapel D., Auber C., and Rontani J.-F. (2000) The effect of growth temperature on the long-chain alkenes composition in the marine coccolithophorid *Emiliania huxleyi*. *Phytochemistry* **54**, 393–399.

Guilderson T. P., Fairbanks R. G., and Rubenstone J. L. (1994) Tropical temperature variations since 20,000 years ago: modulating interhemispheric climate change. *Science* **263**, 663–665.

Haidar A. T. and Thierstein H. R. (2001) Coccolithophore dynamics off Bermuda (N. Atlantic). *Deep-Sea Res. II* **48**, 1925–1956.

Hamanaka J., Sawada K., and Tanoue E. (2000) Production rates of C37 alkenones determined by ^{13}C-labeling technique in the euphotic zone of Sagami Bay, Japan. *Org. Geochem.* **31**, 1095–1102.

Harada N., Handa N., Harada K., and Matsuoka H. (2001) Alkenones and particulate fluxes in sediment traps from the central equatorial Pacific. *Deep-Sea Res. I: Oceanogr. Res. Pap.* **48**, 891–907.

Herbert T. D. (2000) Review of alkenone calibrations (culture, water column, and sediments). *Geochem. Geophys. Geosys.* **1** [Paper no. 2000GC000055].

Herbert T. D. and Schuffert J. (1998) Alkenone unsaturation estimates of late Miocene through late Pliocene sea surface temperature changes, ODP Site 958. *Proc. Ocean Drill. Prog.: Sci. Results* **159T**, 17–22.

Herbert T. D., Schuffert J. D., Thomas D., Lange K., Weinheimer A., and Herguera J.-C. (1998) Depth and seasonality of alkenone production along the California margin inferred from a core-top transect. *Paleoceanography* **13**, 263–271.

Herbert T. D., Schuffert J. D., Andreasen D., Heusser L., Lyle M., Mix A., Ravelo A. C., Stott L. D., and Herguera J. C. (2001) Collapse of the California current during glacial maxima linked to climate change on land. *Science* **293**, 71–76.

Hoefs M. J. L., Versteegh G. J. M., Ripstra W. I. C., de Leeuw J. W., and Sinninghe Damste J. S. (1998) Postdepositional oxic degradational of alkenones: implications for the measurement of palaeo sea surface temperatures. *Paleoceanography* **13**, 42–59.

Houghton S. D. and Guptha M. V. S. (1991) Monsoonal and fertility controls on recent marginal sea and continental shelf coccolith assemblages from the western Pacific and the northern Indian oceans. *Mar. Geol.* **97**, 251–259.

Huang C. Y., Wu S. F., Zhao M., Chen M. T., Wang C. H., Tu X., and Yuan P. B. (1997) Surface ocean and monsoon climate variability in the South China sea since the last glaciation. *Mar. Micropaleontol.* **32**, 71–94.

Jasper J. and Gagosian R. B. (1989) Alkenone molecular stratigraphy in an oceanic environment affected by glacial freshwater events. *Paleoceanography* **4**, 603–614.

Jiang M. J. and Gartner S. (1984) Neogene and quaternary calcareous nannofossil biostratigraphy of the Walvis ridge. In *Init Rep. DSDP 74* (eds. T. C. Moore and E. Rabinowitz). US Govt. Printing Office, Washington, DC, pp. 561–595.

Johnsen S. J., Clausen H. B., Dansgaard W., Fuhrer K., Gundestrup N., Hammer C. U., Iversen P., Jouzel J., Stauffer B., and Steffensen J. P. (1992) Irregular glacial interstadials recorded in a new Greenland ice core. *Nature* **359**, 311–313.

Jordan R. W., Zhao M., Eglinton G., and Weaver P. P. E. (1996) Coccolith and alkenone stratigraphy at a NW African upwelling site (ODP 658C) over the last 130,000 years. In *Microfossils and Oceanic Environments*, British Micropaleontol. Soc. Series (eds. A. L. Moguilevsky and R. Whateley), pp. 111–130.

Kennedy J. and Brassell S. C. (1992) Molecular records of twentieth century El Nino events in laminated sediments from Santa Barbara basin. *Nature* **357**, 62–64.

Kienast S. and McKay J. L. (2001) Sea surface temperatures in the subarctic northeast Pacific reflect millennial-scale climate oscillations during the last 16 kyr. *Geophys. Res. Lett.* **28**, 1563–1566.

Kienast M., Steinke S., Stattegger K., and Calvert S. E. (2001) Synchronous tropical South China Sea SST change and Greenland warming during deglaciation. *Science* **291**, 2132–2134.

Kim J. H., Schneider R. R., Müller P. J., and Wefer G. (2002) Interhemispheric comparison of deglacial sea-surface temperature patterns in Atlantic eastern boundary currents. *Earth Planet. Sci. Lett.* **194**, 383–393.

Kirst G., Schneider R. R., Muller P. J., von Storch I., and Wefer G. (1999) Late quaternary temperature variability in the Benguela current system derived from Alkenones. *Quat. Res.* **52**, 92–103.

Koopmans M. P., Schaeffer-Reiss C., DeLeeuw J. W., Lean M. D., Maxwell J. R., Schaeffer P., and Sinninghe Damste J. S. (1997) Sulphur and oxygen sequestration of n-C37 and n-C38 unsaturated ketones in an immature kerogen and the release of their carbon skeletons during early stages of thermal maturation. *Geochim. Cosmochim. Acta* **61**, 2397–2408.

Lea D. W., Mashiotta T. A., and Spero H. J. (1999) Controls on magnesium and strontium uptake in planktonic foraminifera determined by live culturing. *Geochim. Cosmochim. Acta* **63**, 2369–2379.

Lea D. W., Pak D. K., and Spero H. J. (2000) Climate impact of late quaternary Equatorial Pacific sea surface temperature variations. *Science* **289**, 1719–1724.

Lee K. Y., Slowey N., and Herbert T. D. (2001) Glacial sea surface temperatures in the subtropical North Pacific: a comparison of $U^{k'}_{37}$, $\delta^{18}O$, and foraminiferal assemblage temperature estimates. *Paleoceanography* **16**, 268–279.

Levitus S. (1994) *Climatological Atlas of the World Ocean*, NOAA Prof. Pa.13. US Govt. Print. Off., Washington, DC, 173pp.

Li J., Philp R. P., Pu F., and Allen J. (1996) Long-chain alkenones in Qighai lake sediments. *Geochem. Cosmochim. Acta* **60**, 235–241.

Lichtfouse E., Littke R., Disko U., Willshc H., Ruldotter J., and Stein R. (1992) Geochemistry and petrology of organic matter in Miocene to quaternary deep sea sediments from the Japan Sea (Sites 798 and 799). *Sci. Res. ODP* **127/128**, 667–675.

Lyle M., Prahl F. G., and Sparrow M. A. (1992) Upwelling and productivity changes inferred from a temperature record in the central equatorial Pacific. *Nature* **355**, 812–815.

Madureira L. A. S., Conte M. H., and Eglinton G. (1995) The early diagenesis of lipid biomarker compounds in North Atlantic sediments. *Paleoceangraphy* **10**, 627–642.

Marchal O., Cacho I., Stocker T. F., Grimalt J. O., Calvo E., Martrat B., Shackleton N., Vautravers M., Cortijo E., van Kreveld S., Andersson C., Koc N., Chapman M., Sbaffi L., Duplessy J. C., Sarnthein M., Turon J. L., Duprat J., and Jansen E. (2002) Apparent long-term cooling of the sea surface in the northeast Atlantic and Mediterranean during the Holocene. *Quat. Sci. Rev.* **21**, 455–483.

Marlow J. R., Lange C. B., Wefer G., and Rosell-Mele A. (2000) Upwelling intensification as part of the Pliocene-pleistocene climate transition. *Science* **290**, 2288–2291.

Marlowe I. T., Green J. C., Neal A. C., Brassell S. C., Eglinton G., and Course P. A. (1984a) Long chain (n-C37–C39) alkenones in the prymnesiophyceae: distribution of alkenones and other lipids and their taxonomic significance. *British Phycol. J.* **19**, 203–216.

Marlowe I. T., Brassell S. C., Eglinton G., and Green J. C. (1984b) Long chain unsaturated ketones and esters in living algae and marine sediments. *Org. Geochem.* **6**, 135–141.

Marlowe I. T., Brassell S. C., Eglinton G., and Green J. C. (1990) Long-chain alkenones and alkyl alkenoates and the fossil coccolith record of marine sediments. *Chem. Geol.* **88**, 349–375.

Mayer B. and Schwark L. (1999) A 15,000-year stable isotope record from sediments of lake Steisslingen, southwest Germany. *Chem. Geol.* **161**, 315–337.

Mazaud A., Sicre M. A., Ezat U., Pichon J. J., Duprat J., Laj C., Kissel C., Beaufort L., Michel E., and Turon J. L. (2002) Geomagnetic-assisted stratigraphy and sea surface temperature changes in core MD94-103 (southern Indian ocean): possible implications for North-South climatic relationships around H4. *Earth Planet. Sci. Lett.* **201**, 159–170.

McCaffrey M. A., Farrington J. W., and Repeta D. J. (1990) The organic geochemistry of Peru margin surface sediments: 1. A comparison of the C37 alkenone and historical El Nino records. *Geochim. Cosmochim. Acta* **54**, 1671–1682.

McIntyre A. (1970) *Gephyrocapsa protohuxleyi* sp. n. as possible phyletic link and index fossil for the Pleistocene. *Deep-Sea Res.* **17**, 187–190.

Medlin L. K., Barker G. L. A., Campbell L., Green J. C., Hayes P. K., Marie D., Wrieden S., and Vaulot G. (1996) Genetic characterization of *Emiliania huxleyi* (Haptophyta). *J. Mar. Sys.* **9**, 13–31.

Mercer J. L., Zhao M., and Coleman S. M. (1999) Alkenone evidence of sudden changes in Chesapeake Bay conditions ca. 300 years ago. *EOS 80 Suppl.* S185.

Mix A. C., Morey A. E., Pisias N. G., and Hostetler S. W. (1999) Foraminiferal faunal estimates of paleotemperature: circumventing the no-analog problem yields cool ice age tropics. *Paleoceanography* **14**, 350–359.

Mix A. C., Bard E., and Schneider R. (2001) Environmental processes of the Ice age: land, ocean, glaciers (EPILOG). *Quat. Sci. Rev.* **20**, 627–657.

Mouzdahir A. v., Grossi Bakkas S., and Rontani J.-F. (2001) Visible light-dependent degradation of long-chained alkenes in killed cells of *Emiliania huxleyi* and *Nannocchlorpsis salina*. *Phytochemistry* **56**, 677–684.

Muller P. J. and Fischer G. (2001) A 4-year sediment trap record of alkenones from the filamentous upwelling region off Cape Blanc, NW: Africa and a comparison with distributions in underlying sediments. *Deep-Sea Res.* **48**, 1877–1903.

Muller P. J., Cepek M., Ruhland G., and Schneider R. R. (1997) Alkenone and coccolithophorid species changes in late quaternary sediments from the Walvis ridge: implications for the alkenone paleotemperature method. *Palaeogeogr. Palaeoclimatol. Palaeoecol.* **135**, 71–96.

Muller P. J., Kirst G., Ruhland G., von Storch I., and Rosell-Mele A. (1998) Calibration of the alkenone paleotemperature index $U^{k'}_{37}$ based on core-tops from the eastern South Atlantic and the global ocean (60° N–60° S). *Geochim. Cosmochim. Acta* **62**, 1757–1772.

Nanninga H. J. and Tyrell T. (1996) The importance of light for the formation of algal blooms by *Emiliania huxleyi*. *Mar. Ecol. Prog. Ser.* **136**, 195–203.

Nishida S. (1986) Nannoplankton flora in the southern Ocean, with special reference to siliceous varieties. *Mem. Nat. Inst. Polar. Res.* (spec. issue) **40**, 56–68.

Nuernberg D., Muller A., and Schneider R. R. (2000) Paleo-sea surface temperature calculations in the equatorial East Atlantic from Mg/Ca ratios in planktic foraminifera: a comparison to sea surface temperature estimates from $U^{k'}_{37}$, oxygen isotopes, and foraminiferal transfer functions. *Paleoceanography* **15**, 124–134.

Ohkouchi N., Kawamua K., Nakamura T., and Taira A. (1994) Small changes in the sea surface temperature during the last 20,000 years: molecular evidence from the western tropical Pacific. *Geophys. Res. Lett.* **21**, 2207–2210.

Ohkouchi N., Kawamura K., Kawahata H., and Okada H. (1999) Depth ranges of alkenone production in the central Pacific Ocean. *Global Biogeochem. Cycles* **13**, 695–704.

Ohkouchi N., Eglinton T. I., Keigwin L. D., and Hayes J. M. (2002) Spatial and temporal offsets between proxy records in a sediment drift. *Science* **298**, 1224–1227.

Okada H. and Honjo S. (1973) The distribution of oceanic coccolithophorids in the Pacific. *Deep-Sea Res.* **26**, 355–374.

Okada H. and McIntyre A. (1979) Seasonal distribution of modern coccolithophores in the western North Atlantic Ocean. *Mar. Biol.* **54**, 319–328.

Paasche E. (2002) A review of the coccolithophorid *Emiliania huxleyi* (Prymnesiophyceae) with particular reference to growth, coccolith formation, and calcification-photosynthesis interactions. *Phycologia* **40**, 503–529.

Pelejero C. and Grimalt J. O. (1997) The correlation between the $U^{k'}_{37}$ index and sea surface temperatures in the warm boundary: the South China Sea. *Geochim. Cosmochim. Acta* **61**, 4789–4797.

Pelejero C., Grimalt J. O., Heilig S., Kienast M., and Wang L. (1999a) High-resolution $U^{k'}_{37}$ temperature reconstructions in the South China Sea over the past 220 kyr. *Paleoceanography* **14**, 224–231.

Pelejero C., Kienast M., Wang L., and Grimalt J. O. (1999b) The flooding of Sundaland during the last deglaciation: imprints in hemipelagic sediments from the southern South China Sea. *Earth Planet. Sci. Lett.* **171**, 661–671.

Pelejero C. and Calvo E. (2003) The upper end of the $U^{k'}_{37}$ temperature calibration revisited. *Geochem. Geophys. Geosyst.* **4**, article 1014.

Perez-Folgado M., Sierro F. J., Flores J. A., Cacho I., Grimalt J. O., Zahn R., and Shackleton N. (2003) Western Mediterranean planktonic foraminifera events and millennial climatic variability during the last 70 kyr. *Mar. Micropaleontol.* **48**, 49–70.

Popp B. N., Kenig F., Wakeham S. G., and Bidigare R. R. (1998) Does growth rate affect ketone unsaturation

and intracellular carbon isotopic variability in *Emiliania huxleyi*? *Paleoceanography* **13**, 35–41.

Prahl F. G. and Wakeham S. G. (1987) Calibration of unsaturation patterns in long-chain ketone compositions for paleotemperature assessment. *Nature* **330**, 367–369.

Prahl F. G., Muelhausen L. A., and Zahnle D. L. (1988) Further evaluation of long-chain alkenones as indicators of paleoceanography conditions. *Geochim. Cosmochim. Acta* **52**, 2303–2310.

Prahl F. G., de Lange G. J., Lyle M., and Sparrow M. A. (1989a) Post-depositional stability of long-chain alkenones under contrasting redox conditions. *Nature* **341**, 434–437.

Prahl F. G., Muelhausen L. A., and Lyle M. (1989b) An organic geochemical assessment of oceanographic conditions at MANOP site C over the past 26,000 years. *Paleoceanography* **5**, 495–510.

Prahl F. G., Collier R. B., Dymond J., Lyle M., and Sparrow M. A. (1993) A biomarker perspective on prymnesiophyte productivity in the northeast Pacific Ocean. *Deep-Sea Res.* **40**, 2061–2076.

Prahl F. G., Pisias N., Sparrow M. A., and Sabin A. (1995) Assessment of sea-surface temperature at 42°N in the California current over the last 30,000 years. *Paleoceanography* **10**, 763–773.

Prahl F. G., Dymond J., and Sparrow M. A. (2000) Annual biomarker record for export production in the central Arabian Sea. *Deep-Sea Res II* **47**, 1581–1604.

Prahl F. G., Pilskaln C. H., and Sparrow M. A. (2001) Seasonal record for alkenones in sedimentary particles from the Gulf of Maine. *Deep-Sea Res. I* **48**, 515–528.

Pujos A. (1987) Late Eocene to Pleistocene medium-sized and small-sized 'Reticulofenestrids'. *Abh. Geol. Bund. A* **39**, 239–277.

Rinna J., Warning B., Meyers P. A., Brumsack H.-J., and Rullkötter J. (2002) Combined organic and inorganic geochemical reconstruction of paleodepositional conditions of a Pliocene sapropel from the eastern Mediterranean Sea. *Geochim. Cosmochim. Acta* **66**, 1969–1986.

Rio D. (1982) The fossil distribution of coccolithophore genus gephyrocapsa kamptner and related plio-pleistocene chronostratigraphic problems. In *Init. Rep. DSDP* 68 (eds. W. L. Prell and J. V. Gardner). US Govt. Printing Office, Washington, DC, pp. 325–343.

Rontani F.-F., Cuny P., Gossi V., and Beker B. (1997) Stability of long-chain alkenones in senescing cells of *Emiliania huxleyi*: effect of photochemical and aerobic microbial degradation on the alkenone unsaturation ratio ($U^{k'}_{37}$). *Org. Geochem.* **26**, 503–509.

Rosell-Mele A. (1998) Interhemispheric appraisal of the value of alkenone indices as temperature and salinity proxies in high-latitude locations. *Paleoceanography* **13**, 694–703.

Rosell-Mele A., Carter J., and Eglinton G. (1994) Distribution of long-chain alkenones and alkyl alkenoates in marine surface sediments from the North East Atlantic. *Org. Geochem.* **22**, 501–509.

Rosell-Mele A., Carter J., Parry A. T., and Eglinton G. (1995a) Determination of the U^{k}_{37} index in geological samples. *Anal. Chem.* **67**, 1283–1289.

Rosell-Mele A., Eglinton G., Pflaumann U., and Sarnthein M. (1995b) Atlantic core top calibration of the U^{k}_{37} index as a sea-surface temperature indicator. *Geochim. Cosmochim. Acta* **59**, 3099–3107.

Rosell-Mele A., Maslin M. A., Maxwell J. R., and Schaeffer P. (1997) Biomarker evidence for Heinrich events. *Geochim. Cosmochim. Acta* **61**, 1671–1678.

Rosell-Mele A., Bard E., Emeis E.-C., Grimalt J. O., Muller P., Schneider R., Bouloubassi I., Epstein B., Fahl K., Fluegge A., Freeman K., Goni M., Guntner U., Hrtz D., Hellebust S., Herbert T., Ikehara M., Ishiwatari R., Kawamura K., Kenig F., de Leeuw J., Lehman S., Mejanelle L., Ohkouchi N., Pancost R. D., Pelejero C., Prahl F., Quinn J., Rontani J. F., Rostek F., Rulkotter J., Sachs J., Blanz T., Sawada K., Schulz-Bull D., Sikes E., Sonzogni C., Ternois Y., Versteegh G., Volkman J. K., and Wakeham S. (2001) Precision of the current methods to measure the alkenone proxy $U^{k'}_{37}$ and absolute alkenone abundance in sediments: results of an interlaboratory comparison study. *Geochem. Geophys. Geosys.* **2**, paper 2000GC000141.

Rosell-Mele A., Jansen E., and Weinelt M. (2002) Appraisal of a molecular approach to infer variations in surface ocean freshwater inputs into the North Atlantic during the last glacial. *Global Planet. Change* **34**, 143–152.

Rosenthal Y., Lohmann G. P., Lohmann K. C., and Sherrell R. M. (2000) Incorporation and preservation of Mg in *Globigerinoides sacculifer*: implications for reconstructing the temperature and $^{18}O/^{16}O$ of seawater. *Paleoceanography* **15**, 135–145.

Rostek F., Ruhland G., Bassinot F. C., Muller P. J., Labeyrie L. D., Lancelot Y., and Bard E. (1993) Reconstructing sea surface temperature using $\delta^{18}O$ and alkenone records. *Nature* **364**, 319–321.

Rostek F., Bard E., Beaufort L., Sonzogni C., and Ganssen G. (1997) Sea surface temperature and productivity records for the past 240 kyr in the Arabian Sea. *Deep-Sea Res.* **44**, 1461–1480.

Roth P. H. (1994) Distribution of coccoliths in oceanic sediments. In *Coccolithophores* (eds. A. Winter and W. G. Siesser). Cambridge University Press, Cambridge, UK, pp. 199–218.

Ruddiman W. F., Raymo M., and McIntyre A. (1986) Matuyama 41000 year cycles: North Atlantic Ocean and northern hemisphere ice sheets. *Earth Planet. Sci. Lett.* **80**, 117–129.

Ruhlemann C., Mulitza S., Muller P. J., Wefer G., and Zahn R. (1999) Warming of the tropical Atlantic Ocean and slowdown of thermohaline circulation during the last deglaciation. *Nature* **402**, 511–514.

Sachs J. P. and Lehman S. J. (1999) Subtropical North Atlantic temperatures 60,000 to 30,000 years ago. *Science* **286**, 756–759.

Sachs J. and Lehman S. J. (2001) Glacial surface temperatures of the southeast Atlantic Ocean. *Science* **293**, 2077–2079.

Samtleben C. and Bickert T. (1990) Coccoliths in sediment traps from the Norwegian Sea. *Mar. Micropaleontol.* **16**, 39–64.

Sawada K., Handa N., Shiraiwa Y., Danbara A., and Montani S. (1996) Long-chain alkenones and alkyl alkenoates in the coastal and pelagic sediments of the northwest North Pacific, with special reference to the reconstruction of *Emiliania huxleyi* and *Geophyrocapsa oceanica* ratios. *Org. Geochem.* **24**, 751–764.

Sawada K., Handa N., and Nakatsuka T. (1998) Production and transport of long-chain alkenones and alkyl alkenoates in a sea water column in the northwestern Pacific off central Japan. *Mar. Chem.* **59**, 219–234.

Schneider R. R., Muller P. J., and Ruhland G. (1995) Late quaternary surface circulation in the east-equatorial Atlantic: evidence from alkenone sea surface temperatures. *Paleoceanography* **10**, 197–220.

Schneider R. R., Muller P. J., Ruhland G., Meinecke G., Schmidt H., and Wefer G. (1996) Late quaternary surface temperatures and productivity in the east-equatorial South Atlantic: response to changes in trade/monsoon wind forcing and surface water advection. In *The South Atlantic: Present and Past Circulation* (eds. G. Wefer, W. H. Berger, G. Siedler, and D. J. Webb). Springer, Berlin, pp. 527–551.

Schneider R. R., Muller P. J., and Acheson R. (1999) Atlantic alkenone sea surface temperature records. In *Reconstructing Ocean History: A Window into the Past* (eds. Abrantes and A. C. Mix). Academic Press, New York, pp. 33–55.

Schrag D. P., Hampt G., and Murray D. W. (1996) Pore fluid constraints on the temperature and oxygen isotopic composition of the Glacial Ocean. *Science* **272**, 1930–1932.

Schulte S. and Müller P. J. (2001) Variations in sea-surface temperature and primary productivity during Heinrich and

Dansgaard-Oeschger events in the northeastern Arabian Sea. *Geo-Mar. Lett.* **21**, 168–175.

Schulte S., Rostek F., Bard E., Rulkotter J., and Marchal O. (1999) Variations of oxygen-minimum and primary productivity recorded in sediments of the Arabian Sea. *Earth Planet. Sci. Lett.* **173**, 205–221.

Schulz H.-H., Schoener A., and Emeis K.-C. (2000) Long-chain alkenone patterns in the Baltic Sea an ocean-freshwater transition. *Geochim. Cosmochim. Acta* **64**, 469–477.

Seki O., Ishiwatari R., and Matsumoto K. (2002) Millennial climate oscillations in NE Pacific surface waters over the last 82 kyr: new evidence from alkenones. *Geophys. Res. Lett.* **29** 101029/2002GL015200.

Sicre M.-A., Ternois Y., Miquel J.-C., and Marty J.-C. (1999) Alkenones in the Mediterranean Sea: interannual variability and vertical transfer. *Geophys. Res. Lett.* **26**(12), 1735–1738.

Sicre M.-A., Ternois Y., Paterne M., Boireau P., Beaufort L., Martinez P., and Betrand P. (2000) Biomarker stratigraphic records over the last 150 Kyrs off the NW African coast at 25° N. *Org. Geochem.* **31**, 577–588.

Sicre M.-A., Bard E., Ezat U., and Rostek F. (2002) Alkenone distributions in the North Atlantic and Nordic Sea surface waters. *Geochem. Geophys. Geosys.* **3**, paper 2001GC000159.

Sikes C. S. and Fabry V. J. (1994) Photosynthesis, $CaCO_3$ deposition, coccolithophorids and the global carbon cycle. In *Regulation of Atmospheric CO_2 and O_2 by Photosynthetic Carbon Metabolism* (eds. N. E. Tolbert and J. Preiss). Oxford University Press, New York, pp. 217–233.

Sikes E. L. and Keigwin L. D. (1994) Equatorial Atlantic sea surface temperatures for the last 16 kyr: a comparison of U^k_{37}, $\delta^{18}O$, and foraminiferal assemblage temperature estimates. *Paleoceanography* **9**, 31–45.

Sikes E. L. and Volkman J. K. (1993) Calibration of alkenone unsaturation ratios (U^k_{37}) for paleotemperature estimation in cold polar waters. *Geochim. Cosmochim. Acta* **57**, 1883–1889.

Sikes E. L., Farrington J. W., and Keigwin L. D. (1991) Use of the alkenone unsaturation ratio U^k_{37} to determine past sea surface temperatures: core-top SST calibrations and methodology considerations. *Earth Planet. Sci. Lett.* **104**, 36–47.

Sikes E. L., Volkman J. K., Robertson L. G., and Pichon J.-J. (1997) Alkenones and alkenes in surface waters and sediments of the Southern Ocean: implications for paleotemperature estimation in polar regions. *Geochim. Cosmochim. Acta* **61**, 1495–1505.

Simoneit B. R. T., Prahl F. G., Leif R. N., and Mao S.-Z. (1994) Alkenones in sediments of middle valley. *Sci. Res. ODP* **139**, 479–484.

Sinninghe-Damsté J. S., Rijpstra W. I. C., and Reichart G.-J. (2002) The influence of oxic degradation on the sedimentary biomarker record: II. Evidence from Arabian Sea sediments. *Geochim. Cosmochim. Acta* **66**, 2737–2754.

Sonzogni C., Bard E., Rostek F., Dollfus D., Rosell-Mele A., and Eglinton G. (1997) Temperature and salinity effects on alkenone ratios measured in surface sediments from the Indian Ocean. *Quat. Res.* **47**, 344–355.

Sonzogni C., Bard E., and Rostek F. (1998) Tropical sea surface temperatures during the last glacial period: a view based on alkenones in Indian Ocean sediments. *Quat. Sci. Rev.* **17**, 1185–1201.

Sprengel C., Baumann K. H., and Neuer S. (2000) Seasonal and interannual variation of coccolithophore fluxes and species composition in sediment traps north of Gran Canaria (29 degrees N 15 degrees W). *Mar. Micropaleontol.* **39**, 157–178.

Sprengel C., Baumann K. H., Henderiks J., Henrich R., and Neuer S. (2002) Modern coccolithophore and carbonate sedimentation along a productivity gradient in the Canary Islands region: seasonal export production and surface accumulation rates. *Deep-Sea Res. II* **49**, 3577–3598.

Steinke S., Kienast M., Pflaumann U., Weinelt M., and Stattegger K. (2001) A high-resolution sea-surface temperature record from the tropical South China Sea (16,500–3,000 yr BP). *Quat. Res.* **55**, 352–362.

Stott L., Poulsen C., Lund S., and Thunell R. (2002) Super ENSO and global climate oscillations at millennial timescales. *Science* **297**, 222–226.

Stute M., Forster M., Frischkorn H., Serejo A., Clark J. F., Schlosser P., Broecker W. S., and Bonani G. (1995) Cooling of tropical Brazil (5°C) during the last glacial maximum. *Science* **269**, 379–383.

Summerhayes C. P., Kroon D., Rosell-Mele A., Jordan R. W., Schrader H.-J., Hearn R., Villanueva J., Grimalt J. O., and Eglinton G. (1995) Variability in the benguela current upwelling system over the past 70,000 years. *Prog. Oceanogr.* **35**, 207–251.

Sun M.-Y. and Wakeham S. G. (1994) Molecular evidence for degradation and preservation of organic matter in the anoxic Black Sea basin. *Geochim. Cosmochim. Acta* **58**, 3395–3406.

Teece M. A., Getliff J. M., Leftley J. W., Parkes R. J., and Maxwell J. R. (1998) Microbial degradation of the marine prymnesiophyte *Emiliania huxleyi* under oxic and anoxic conditions as a model for early diagenesis: long chain alkadienes, alkenones, and alkyl alkenoates. *Org. Geochem.* **29**, 863–880.

Ternois Y., Sicre M.-A., Boireau A., Marty J.-C., and Miquel J.-C. (1996) Production pattern of alkenones in the Mediterranean Sea. *Geophys. Res. Lett.* **23**, 3171–3174.

Ternois Y., Sicre M.-A., Boireau A., Conte M. H., and Eglinton G. (1997) Evaluation of long-chain alkenones as paleotemperature indicators in the Mediterranean Sea. *Deep-Sea Res.* **44**, 271–286.

Ternois Y., Sicre M.-A., Boireau A., Beaufort L., Migquel J.-C., and Jeandel C. (1998) Hydrocarbons, sterols, and alkenones in sinking particles in the Indian Ocean sector of the Southern Ocean. *Org. Geochem.* **28**, 489–501.

Thiel V., Jenisch A., Landmann G., Reimer A., and Michaelis W. (1997) Unusual distributions of long-chain alkenones and tetrahymanol from the highly alkaline Lake Van, Turkey. *Geochim. Cosmochim. Acta* **61**, 2053–2064.

Thierstein H. R., Geitzenauer K. R., Molfino B., and Shackleton N. J. (1977) Global synchroneity of late Quaternary coccolith datum levels: validation by oxygen isotopes. *Geology* **5**, 400–404.

Thomsen C., Schulz-Bull D. E., Petrick G., and Duinker J. C. (1998) Seasonal variability of the long-chain alkenone flux and the effect on the $U^{k'}_{37}$ index in the Norwegian Sea. *Org. Geochem.* **28**, 311–323.

Thomsen H. A., Buck K. R., and Chavez F. P. (1994) Haptophytes as components of marine phytoplankton. In *The Haptophyte Algae* (eds. J. C. Green and B. S. C. Leadbeater). Clarendon Press, Oxford, pp. 187–208.

van der Smissen J. H. and Rulkotter J. (1996) Organofacies variations in sediments from the continental slope and rise of the New Jersey continental margin (Sites 903 and 905). *Proc. ODP Sci. Res.* **150**, 329–344.

Versteegh G. J. M., Riegman R., de Leew J. W., and Jansen J. H. F. (2001) $U^{k'}_{37}$ values for Isochrysis galbana as a function of culture temperature, light intensity and nutrient concentrations. *Org. Geochem.* **32**, 785–794.

Villanueva J. and Grimalt J. O. (1996) Pitfalls in the chromatographic determination of the alkenone $U^{k'}_{37}$ index for paleotemperature estimation. *J. Chromatogr. A* **723**, 285–291.

Villanueva J. and Grimalt J. O. (1997) Gas chromatographic tuning of the $U^{k'}_{37}$ paleothermometer. *Anal. Chem.* **69**, 3329–3332.

Villanueva J., Pelejero C., and Grimalt J. O. (1997) Clean-up procedures for the unbiased estimation of C_{37} alkenone sea

surface temperatures and terrigenous n-alkane inputs in Paleoceanographyapy. *J. Chromatogr. A* **757**, 145–151.

Villanueva J., Grimalt J. O., Cortijo E., Vidal L., and Labeyrie L. (1998) Assessment of sea surface temperature variations in the central North Atlantic using the alkenone unsaturation index ($U^{k'}_{37}$). *Geochim. Cosmochim. Acta* **62**, 2421–2427.

Visser K., Thunell R., and Stott L. (2003) Magnitude and timing of temperature change in the Indo-Pacific warm pool during deglaciation. *Nature* **421**, 152–155.

Volkman J. K., Eglinton G., Corner E. D. S., and Sargent J. R. (1980a) Novel unsaturated straight-chain C37–C39 methyl and ethyl ketones in marine sediments and a coccolithophore *Emiliania huxleyi*. In *Advances in Organic Geochemistry 1979, Physics and Chemistry of the Earth* (eds. A. G. Douglas and J. R. Maxwell). Pergamon, Oxford, vol. 12, pp. 219–227.

Volkman J. K., Eglinton G., Corner E. D. S., and Forsberg T. E. V. (1980b) Long-chain alkenes and alkenones in the marine coccolithophorid *Emiliania huxleyi*. *Phytochemistry* **19**, 2619–2622.

Volkman J. K., Burton H. R., Everitt D. A., and Allen D. I. (1988) Pigment and lipid compositions of algal and bacterial communities in Ace Lake, Vestfold Hills, Antarctica. *Hydrobiologia* **165**, 41–57.

Volkman J. K., Jeffer S. W., Nichols P. D., Rogers G. I., and Garland C. D. (1989) Fatty acid and lipid composition of 10 species of microalgae used in mariculture. *J. Exp. Mar. Biol. Ecol.* **128**, 219–240.

Volkman J. K., Barrett S. M., Blackburn S. I., and Sikes E. L. (1995) Alkenones in *Gephyrocapsa oceanica*: implications for studies of paleoclimate. *Geochim. Cosmochim. Acta* **59**, 513–520.

Waelbroeck C. and Steinke S. (2002) Comment on Steinke *et al*. (2001). *Quat. Res.* **57**, 432–433.

Wang L., Sarnthein M., Erlenkeuser H., Grimalt J., Grootes P., Heilig S., Ivanova E., Kienast M., Pelejero C., and Pflaumann U. (1999) East Asian monsoon climate during the Late Pleistocene: high-resolution sediment records from the South China Sea. *Mar. Geol.* **156**, 245–284.

Weaver P. P. E., Chapman M. R., Eglinton G., Zhao M., Rutledge D., and Read G. (1999) Combined coccolith, foraminiferal, and biomarker reconstruction of paleoceanography conditions over the past 120 kyr in the northern North Atlantic (59° N, 23° W). *Paleoceanography* **14**, 336–349.

Wei W. C. (1993) Calibration of upper pliocene-lower pleistocene nannofossil events with oxygen isotope stratigraphy. *Paleoceanography* **8**, 85–99.

Winter A., Jordan R., and Roth P. (1994) Biogeography of living coccolithophores in ocean waters. In *Coccolithophores* (eds. A. Winter and W. G. Siesser). Cambridge University Press, Cambridge, UK, pp. 161–177.

Xu L., Reddy C. M., Farrington J. W., Frysinger G. S., Gaines R. B., Johnson C. G., Nelson R. K., and Eglinton T. I. (2001) Identification of a novel alkenone in Black Sea sediments. *Org. Geochem.* **32**, 633–645.

Yamamoto M., Ficken K., Baas M., Bosch H.-J., and de Leuw J. W. (1996) Molecular paleontology of the earliest danian at geulhemmerberg (the Netherlands). *Egol. en Mijnbouw* **75**, 255–267.

Yamamoto M., Shiraiwa Y., and Inouye I. (2000) Physiological responses of lipids in *Emiliania huxleyi* and *Gephyrocapsa oceanica* (Haptophyceae) to growth status and their implications for alkenone paleothermometry. *Org. Geochem.* **31**, 799–811.

Young J. R. and Westbroek P. (1991) Genotypic variation in the coccolithophorid species *Emiliania huxleyi*. *Mar. Micropaleontol.* **18**, 5–23.

Zhao M., Rosell A., and Eglinton G. (1993) Comparison of two U^{k}_{37} sea surface temperature records for the last climatic cycle at ODP site 658 from the sub-tropical Northeast Atlantic. *Palaeogeogr. Palaeoclimat. Palaeoecol.* **103**, 57–65.

Zhao M., Beveridge N. A. S., Shackleton N. J., Sarnthein M., and Eglinton G. (1995) Molecular stratigraphy of cores off northwest Africa: sea surface temperature history over the last 80 ka. *Paleoceanography* **10**, 661–675.

Zhao M., Eglinton, Read G. G., and Schimmelmann A. (2000) An alkenone ($U^{k'}_{37}$) quasi-annual sea surface temperature record (AD 1440 to 1940) using varved sediments from the Santa Barbara basin. *Org. Geochem.* **31**, 903–917.

Zink K. G., Leythaeuser D., Melkonian M., and Schwark L. (2001) Temperature dependency of long-chain alkenone distributions in recent to fossil limnic sediments and in lake waters. *Geochim. Cosmochim. Acta* **65**, 253–265.

Ziveri P. and Thunell R. (2000) Cocolithophore export in Guaymas Basin, Gulf of California: response to climate forcing. *Deep-Sea Res. II* **47**, 2073–2100.

Ziveri P., Thunell R., and Rio D. (1995) Export production of coccolithophore in an upwelling region: results from San Pedro basin, Southern California bight. *Mar. Micropaleontol.* **24**, 335–358.

Ziveri P., Broerse A. T. C., van Hinte J. E., Westbroek P., and Honjo S. (2000) The fate of coccoliths at 48° N 21° W, northeastern Atlantic. *Deep-Sea Res. II* **47**, 1853–1875.

Treatise on Geochemistry
ISBN (set): 0-08-043751-6
Volume 6; (ISBN: 0-08-044341-9); pp. 391–432